

Manuscript version: Author's Accepted Manuscript

The version presented in WRAP is the author's accepted manuscript and may differ from the published version or Version of Record.

Persistent WRAP URL:

<http://wrap.warwick.ac.uk/163864>

How to cite:

Please refer to published version for the most recent bibliographic citation information.

Copyright and reuse:

The Warwick Research Archive Portal (WRAP) makes this work by researchers of the University of Warwick available open access under the following conditions.

Copyright © and all moral rights to the version of the paper presented here belong to the individual author(s) and/or other copyright owners. To the extent reasonable and practicable the material made available in WRAP has been checked for eligibility before being made available.

Copies of full items can be used for personal research or study, educational, or not-for-profit purposes without prior permission or charge. Provided that the authors, title and full bibliographic details are credited, a hyperlink and/or URL is given for the original metadata page and the content is not changed in any way.

Publisher's statement:

Please refer to the repository item page, publisher's statement section, for further information.

For more information, please contact the WRAP Team at: wrap@warwick.ac.uk.



Oxidative stress-induced autophagy compromises stem cell viability via the ROS-p38-Erk1/2-MAPK pathways

Journal:	<i>Stem Cells</i>
Manuscript ID	SC-21-0266
Manuscript Type:	Original Research
Date Submitted by the Author:	26-Oct-2021
Complete List of Authors:	Prakash, Ravi; Era's Lucknow Medical College and Hospital, Biotechnology Fauzia, Eram; Biology Centre Czech Academy of Sciences, Biotechnology Siddiqui, Abu ; Era's Lucknow Medical College and Hospital, Biotechnology Yadav, Santosh; Era's Lucknow Medical College and Hospital, Biotechnology Kumari, Neha; Era's Lucknow Medical College and Hospital, Biotechnology Shams, Mohammad; Era's Lucknow Medical College and Hospital, Biotechnology Naeem, Abdul; Era's Lucknow Medical College and Hospital, Biotechnology Praharaaj, Parkash; National Institute of Technology Rourkela Khan, Mohsin; Era's Lucknow Medical College and Hospital, Biotechnology Bhutia, Sujit; National Institute of Technology Rourkela Janowski, Mirosław; University of Maryland School of Medicine Boltze, Johannes; University of Warwick School of Life Sciences Raza, Syed; Era's Lucknow Medical College and Hospital, Biotechnology
Keywords:	Mesenchymal stem cells (MSCs), Stem cell transplantation, Adult stem cells, Cell biology
Journal Section:	Regenerative Medicine
Cell Types:	Cord / Cord Blood Stem Cells (WJ-MSCs), Dental Pulp Stem Cells
Diseases/Processes/Areas:	Stroke / Traumatic Brain Injury

SCHOLARONE™
Manuscripts

1
2
3 1 **Oxidative stress-induced autophagy compromises stem cell viability via the ROS-p38-**
4 2 **Erk1/2-MAPK pathways**
5
6 3 Ravi Prakash^a, Eram Fauzia^{b#}, Abu Junaid Siddiqui^{a#}, Santosh Kumar Yadav^{a#}, Neha
7 4 Kumari^a, Mohammad Tayyab Shams^a, Abdul Naeem^a, Prakash P Praharaj^c, Mohsin Ali
8 5 Khan^d, Sujit Kumar Bhutia^c, Mirosław Janowski^e, Johannes Boltze^f, Syed Shadab Raza^{*a,g}
9 6
10 7 ^aLaboratory for Stem Cell & Restorative Neurology, Department of Biotechnology, Era's
11 8 Lucknow Medical College Hospital, Era University, Sarfarazganj, Lucknow–226003, India
12 9 ^bInstitute of Parasitology, Biology Center Czech Academy of Science, Czech Republic
13 10 ^cDepartment of Life Science, National Institute of Technology, Rourkela–769008, India
14 11 ^dEra University, Sarfarazganj, Lucknow–226003, India
15 12 ^eCenter for Advanced Imaging Research, Department of Diagnostic Radiology and Nuclear
16 13 Medicine University of Maryland, University of Maryland Baltimore, MD 21201-1595, USA
17 14 ^fSchool of Life Sciences, University of Warwick, Coventry, UK
18 15 ^gDepartment of Stem Cell Biology and Regenerative Medicine, Era's Lucknow Medical
19 16 College Hospital, Era University, Sarfarazganj, Lucknow–226003, India
20 17
21 18
22 19 EF[#], AJS[#], and SKY[#] contributed equally to this work
23 20
24 21
25 22
26 23 Correspondence:
27 24 **Dr. Syed Shadab Raza**
28 25 drshadab@erauniversity.in
29 26 Lab: +91–0522–66600777 Extn: 119
30 27 Fax: +91–0522–2407824
31 28
32 29 **Running title:** O₂^{•-} or H₂O₂ mediated autophagy regulation in hDPSCs and hMSCs' fate
33 30 determination
34 31
35 32

Abstract

Mesenchymal derived stem cell therapies have emerged as a promising treatment strategy for various degenerative ischemic-reperfusion diseases, such as ischemic stroke. However, human dental pulp (hDP) and human mesenchymal stem cells (hMSCs) survival after transplantation remains a critical issue. Autophagy appears to play a critical role in hDPSCs and hMSCs fate, particularly under oxidative stress, which is typically present in ischemia-challenged tissue. We used oxygen-glucose deprivation (OGD) to induce oxidative stress in hDPSCs and hMSCs. OGD-induced abrupt generation of $O_2^{\bullet-}$ or H_2O_2 enhanced autophagy by inducing the expression of Activating Molecule In BECN1-Regulated Autophagy Protein 1 (Ambra1) and Beclin1 in both cell types. However, hDPSCs and hMSCs pre-conditioning with reactive oxygen species (ROS) scavengers significantly repressed the expression of Ambra1 and Beclin1 and inactivated autophagy. $O_2^{\bullet-}$ or H_2O_2 acted upstream of autophagy and the mechanism was unidirectional. Further, our findings revealed ROS-p38-Erk1/2 involvement. Pre-treatment with selective inhibitors of p38 and Erk1/2 pathways (SB202190 and PD98059) reversed OGD effects on the expression of Ambra1 and Beclin1, suggesting that these pathways induced oxidative stress-mediated autophagy. Global ROS inhibition by NAC or a combination of Polyethylene glycol-superoxide dismutase (PEG-SOD) and Polyethylene glycol-catalase (PEG-catalase) indicated that the participation of both $O_2^{\bullet-}$ or H_2O_2 or a combination of ROS impacts stems cells' viability. Further, autophagy inhibition by 3-Methyladenine (3-MA) significantly improved hDPSCs viability, indicating the autophagy involvement in stem cell death. These findings contribute to understanding low post-transplantation mesenchymal derived stem cells survival and may assist in strategies to minimize therapeutic cell loss in ischemic brains.

Keywords: oxygen-glucose deprivation, human dental pulp stem cells, human mesenchymal stem cells, autophagy, stem cell survival, Ambra1, Beclin1

1
2
3
4
5
6
7
8
9
10
11
12
13
14
15
16
17
18
19
20
21
22
23
24
25
26
27
28
29
30
31
32
33
34
35
36
37
38
39
40
41
42
43
44
45
46
47
48
49
50
51
52
53
54
55
56
57
58
59
60

Introduction

Oxidative stress is an unbalanced redox state characterized by an excessive accumulation of reactive oxygen species (ROS) or insufficient antioxidant mechanisms. Oxidative stress contributes to the pathogenesis of acute ischemic cardiovascular (e.g., myocardial infarction) and cerebrovascular diseases (e.g., stroke), Alzheimer’s disease, Parkinsonism, immune disorders, and cancer [1-4]. According to the World Health Organization, cardiovascular diseases are the leading cause of death worldwide, particularly in low- and middle-income countries, accounting for 85 percent of total deaths [5]. There are only few effective treatments, though limited by relatively narrow time windows, accessibility, and a number of contraindications. Thus, patients would benefit significantly from novel treatments that could mitigate or even reverse ischemic damage. Therapeutic approaches using stem cells are a promising option and the first clinical trials are currently underway. Transplanted stem cells, on the other hand, are typically short-lived [6], and the reasons for their poor survival are still unknown. There is preliminary evidence that a hostile microenvironment, characterized by oxidative and mechanical stress, may contribute to stem cell loss after transplantation. Other considerations include a lack of trophic support impeding incorporation into the host organ, and of structural support, which reduces stem cell efficacy and numbers [7]. Therefore, understanding the short survival of stem cells following transplantation is essential to improve stem cell-based clinical applications.

ROS are chemically reactive molecules or ions formed as by-products of oxygen metabolism. They comprise superoxide ($O_2^{\cdot-}$), hydrogen peroxide (H_2O_2), hydroxyl radical ($\cdot OH$), and singlet oxygen (1O_2). Mitochondria are the primary sources of intracellular oxidant activity in most cell types. NADPH oxidases, nitric oxide synthase, xanthine oxidase, cyclooxygenases, cytochrome P450 enzymes, and cell organelles such as the peroxisomes and the endoplasmic reticulum are all involved in intracellular ROS production [8]. Redox status is essential for cell functioning and maintenance, including in stem and progenitor cells [9]. The balance between ROS-generating and antioxidant systems precisely regulates these processes. ROS at low levels function as signalling molecules mediating cell proliferation, migration, differentiation, and gene expression. Hence, like any other cell type, it is important to understand ROS' impact on stem cells, especially during oxidative stress.

Autophagy is an intracellular process that maintains homeostasis by degrading and recycling cytosolic proteins and organelles. Since autophagy has both protective and destructive effects, it may represent a treatment target with interventions aiming to mitigate its adverse or improve its protective effects. Defects in autophagy are associated with a wide range of diseases [10-12]. A growing body of evidence suggests that ROS is involved in autophagy under various pathological conditions. However, the molecular pathways governing ROS-induced autophagy are still unclear.

In the present study, we focused on stem cell viability and dysfunction under oxidative stress with a particular focus on autophagy. We investigated the effect of dysregulated autophagy on human dental pulp stem cell (hDPSC) and human mesenchymal stem cell (hMSC) survival and function using oxygen-glucose deprivation (OGD) with subsequent reoxygenation. This model is considered as one of the most relevant *in vitro* models of ischemia-reperfusion injury [13]. We particularly examined the roles of $O_2^{\bullet-}$ and H_2O_2 in autophagy activation under oxidative stress (schematic presentation in Fig S1).

Materials and Methods

The supporting information section has a full discussion of the materials and methodology parts.

Results

Determination of optimal OGD time

We investigated the effects of oxidative stress during OGD on hDPSCs and hMSCs. The 12h time point showed best results indicated by minimal cell loss (Fig. 1A) and significantly unregulated expression levels of $O_2^{\bullet-}$ through flow cytometry and H_2O_2 through spectrophotometry in hDPSCs (Fig.1B and C) and fluorescent microscopy and spectrophotometry for hMSCs (Fig.S2A and S2B). In contrast to OGD-treated hDPSCs and hMSCs, those treated with PEG-SOD ($O_2^{\bullet-}$ -quencher) and PEG-catalase (H_2O_2 decomposer) had lower levels of $O_2^{\bullet-}$ and H_2O_2 . Rotenone, known to increase mitochondrial superoxide release, and exogenous supplementation of H_2O_2 served as positive controls for the experiments involving $O_2^{\bullet-}$ and H_2O_2 respectively.

OGD promotes autophagy activation in stem cells

1
2
3 124 We investigated the autophagy response to OGD by assessing changes in the expression of
4 125 microtubule-associated protein 1 light chain 3 (MAP1LC3) in hDPSCs and hMSCs. LC3-I, a
5 126 cytosolic protein, undergoes lipidation to form LC3II, which is involved in forming
6 127 autophagosomes. The ratio of LC3II to LC3I is a critical indicator of autophagic activation.
7 128 Western blotting showed that LC3II and the LC3II/I ratio was increased after 12h of OGD in
8 129 hDPSCs (Fig. 1D). EGFP-LC3-transfected hDPSCs subjected to OGD displayed a
9 130 remarkable increase in cytoplasmic EGFP-LC3 puncta formation (Fig. 1E) that was
10 131 confirmed by electron microscopy for autophagosomes (Fig. 1F). 3-MA inhibited the
11 132 conversion of LC3II and significantly reduced the LC3II/I ratio (Fig. 1G). The addition of
12 133 rapamycin served as positive control for autophagy, and we observed a high expression of
13 134 EGFP-LC3 puncta formation (Fig. 1E) as well as a high expression of LC3II and LC3II/I
14 135 band ratio (Fig. 1G). It should be noted that the amount of LC3-II present at a given time
15 136 point does not always correspond to autophagic activity, as both activations of autophagy and
16 137 inhibition of autophagosome degradation significantly increase the amount of LC3-II. Thus,
17 138 it is critical to determine the amount of LC3-II degraded in a lysosome-dependent manner
18 139 during a given time to quantify autophagic flux. Because p62 binds directly to LC3 and is
19 140 selectively degraded by autophagy, degradation of p62 is a widely used marker for
20 141 autophagic activity. Hence, using p62, we investigated autophagic flux, which is a measure of
21 142 degradation activity. Our findings showed low p62 levels along with an induced LC3II
22 143 deposition and LC3II/I ratio in hDPSCs after OGD, again suggesting autophagy activation
23 144 (Fig. 1H). The increase in LC3II was an indication of induction of autophagy, which co-
24 145 related well with the degradation of p62, indicating the degradation of forming
25 146 autophagosomes.

26 147
27 148 Next, we confirmed autophagy in hMSC after OGD (Fig. S2C-E). Similar findings were
28 149 evident, as in hDPSCs. Rapamycin treatment significantly increased autophagy, while 3-MA
29 150 treatment significantly reduced the expression of LC3II/I in hMSCs too. Similar to hDPSCs,
30 151 hMSCs' autophagic flux examination showed a low p62 and a high LC3II deposition and
31 152 LC3II/I ratio (Fig. S2F).

32 153
33 154 **Autophagy activation in hDPSCs and hMSCs in the presence of $O_2^{\cdot-}$ and H_2O_2**
34 155 We then determined the role of OGD-generated $O_2^{\cdot-}$ and H_2O_2 in hDPSCs. A significant
35 156 increase in autophagy was found. Treatment with PEG-SOD and PEG-catalase significantly
36 157 decreased the accumulation of EGFP-LC3 puncta in hDPSCs after OGD. Expectedly, EGFP-

LC3 puncta increased under rotenone (Fig. 2A) and exogenous H₂O₂ (Fig. 2B) exposure was evident through microscopy. Similar results were observed in hMSCs (Fig. S3A and Fig. S3B) by western blotting. In total, these results suggested that OGD activates autophagy in hDPSCs and hMSCs by the participation of O₂^{•-} and H₂O₂.

OGD activates Ambra1 and Beclin1 through the participation of O₂^{•-} and H₂O₂

Previous studies have reported that Ambra1 and Beclin1 can control autophagy via several regulatory mechanisms [14]. In these lines, we observed an elevated expression of Ambra1 (Fig. 2C) and Beclin1 (Fig. 2D) after 12 h of OGD followed by 24 h of normoxia in hDPSCs. We further investigated the function of Ambra1 and Beclin1 in mediating dysregulated autophagy using siRNAs targeting Ambra1 and Beclin1. Expectedly, siRNA treatment decreased the expression of Ambra1 and Beclin1 at both mRNA (Fig. 2E and Fig. 2F) and protein levels (Fig. 2G for Ambra1 and Fig. 2H for Beclin1) in OGD-exposed hDPSCs. We obtained similar results in hMSCs for Ambra1- and Beclin1-mediated autophagy after OGD (Fig. S3C-S3F).

O₂^{•-} and H₂O₂ activate Ambra1 and Beclin1

Next, we were interested in assessing the expression of Ambra1 and Beclin1 in response to O₂^{•-} and H₂O₂-induced oxidative stress. Hence, we investigated the hDPSCs' response to OGD in the presence and absence of PEG-SOD and PEG-catalase, for Ambra1 (Fig. 3A and Fig. 3B) and Beclin1 (Fig. 3C and Fig. 3D). Treatment with PEG-SOD and PEG-catalase down-regulated the expression of Ambra1 and Beclin1. Similar to hDPSCs, in response to O₂^{•-} and H₂O₂ generation, the expression of Ambra1 and Beclin1 increased in hMSCs. However, employing PEG-SOD and PEG-catalase, for Ambra1 (Fig. S4A and S4B) and Beclin1 (Fig. S4C and S4D), diminished the expression. Altogether, the data suggests that Ambra1 and Beclin1 are regulated in the presence of O₂^{•-} and H₂O₂.

Ambra1 and Beclin1 activate autophagy

We next examined the effect of up-regulated expression of Ambra1 and Beclin1 on autophagy. Consistent with the previous reports [15,16], our results confirmed the involvement of Ambra1 and Beclin1 in autophagy activation by EGFP-LC3 puncta counting in hDPSCs (Fig. 3E and 3F) and hMSCs (Fig. S4E and S4F) subjected to OGD.

OGD triggers ROS-dependent autophagy via p38 and Erk1/2 pathways

1
2
3
4 192 Given that OGD activates the mitogen-activated protein kinases (MAPKs) signalling
5 193 pathways [17,18], we mapped the expression of c-jun NH2-terminal kinase (JNKs), p38 and
6
7 194 growth factor-regulated extracellular signal-related kinase 1/2 (ERK1/2) after OGD in
8
9 195 hDPSCs. There was a high expression of p38 and Erk1/2, suggesting an association between
10 196 OGD and MAPKs (p38; Fig. 4A, and Erk1/2; Fig. 4B). The results were confirmed by the
11
12 197 addition of respective inhibitors of these two pathways (Fig. 4C and 4D). Based on these
13
14 198 results, we decided to assess the effect of $O_2^{\bullet-}$ and H_2O_2 production on p38 (Fig. 4E and 4F)
15 199 and Erk1/2 (Fig. 4G and 4H) pathways. We observed a decrease in p-p38 and p-Erk1/2 with
16
17 200 the supplementation of PEG-SOD and PEG-catalase respectively. These results suggest the
18
19 201 involvement of $O_2^{\bullet-}$ and H_2O_2 in both p38 and Erk1/2 activation
20
21 202 We further examined the effect of p38 and Erk1/2 MAPKs activation on autophagy in
22
23 203 hDPSCs. The involvement of both pathways was confirmed by a decreased LC3II/I ratio
24 204 when supplementing the respective inhibitors, SB202190 (Fig. S5A) and PD98059 (Fig.
25
26 205 S5B). Moreover, western blot analysis showed that the levels of Ambra1 (Fig. S5C and S5D)
27 206 and Beclin1 (Fig. S5E and S5F) were decreased when applying these inhibitors. This
28
29 207 suggests that MAPKs controlled Ambra1 and Beclin1 during OGD. The participation of p38
30
31 208 and Erk1/2 on autophagy regulation was further confirmed by simultaneous supplementation
32
33 209 of respective inhibitors, SB202190 and PD98059, on autophagy (Fig. S5G and S5H).
34
35 210 Notably, we did not discover a significant impact on the JNK pathway (Fig. S6).

36 211
37
38 212 **Total ROS, $O_2^{\bullet-}$, and H_2O_2 in OGD-induced stem cell death in hDPSCs**
39
40 213 Exposure of hDPSCs to 0 to 72h of OGD resulted in a gradual loss of hDPSC viability (Fig.
41 214 1A). To confirm that an increase in autophagy decreased cell survival, we examined the cell
42
43 215 viability through MTT assay of hDPSCs after OGD in the presence of 3-MA. Expectedly,
44
45 216 OGD reduced hDPSC viability but 3-MA exerted protective effects (Fig. 5A). Rapamycin, a
46
47 217 positive regulator of autophagy, also decreased hDPSC viability. Next, we examined the
48
49 218 impact of $O_2^{\bullet-}$ and H_2O_2 in the presence of PEG-SOD and PEG-catalase, respectively. The
50
51 219 results indicated that the supplementation of PEG-SOD (Fig. 5B) or PEG-catalase (Fig. 5C)
52
53 220 alone did not significantly increase hDPSC viability. However, simultaneous application of
54
55 221 both had a protective effect (Fig. 5D). We further blocked the production of total ROS using
56
57 222 N-acetyl-L-cysteine (NAC). This significantly reduced autophagy (Fig. S7) and increased
58
59 223 hDPSC viability after OGD (Fig. 5E). An assessment of hMSC viability, at 12h of OGD
60
224 followed by 24h of normoxia, by the Trypan blue-based viability assay revealed a similar
225 finding (Fig. S8A-S8E). Taken together, these findings indicate the increased hMSC viability

observed under combined PEG-SOD and PEG-catalase or NAC exposure during OGD was due to either a selective or cumulative effect of ROS.

$O_2^{\bullet-}$ and H_2O_2 generation is an upstream event in stem cells subjected to OGD

Dysregulation of autophagy results in excessive ROS production [19]. To investigate a similar phenomenon in our case we inhibited the generation of $O_2^{\bullet-}$ and H_2O_2 in hDPSCs via 3-MA (Fig. 6A and 6B), Ambra1-siRNA (Fig. 6C and 6D), and Beclin1-siRNA (Fig. 6E and 6F) and mapped $O_2^{\bullet-}$ and H_2O_2 generation through fluorescent microscopy and spectrophotometry. The inhibition of $O_2^{\bullet-}$ and H_2O_2 -related autophagy did not significantly change $O_2^{\bullet-}$ and H_2O_2 levels, indicating that $O_2^{\bullet-}$ and H_2O_2 act upstream of autophagy in a unidirectional manner.

Discussion

Regenerative therapies using hDPSCs and hMSCs are of increasing interest. In the present study, we hypothesized that hDPSCs and hMSCs undergo autophagy in response to OGD-induced oxidative stress, and that dysregulation of autophagy may cause hDPSCs and hMSCs death. To test this hypothesis, we exposed hDPSCs and hMSCs to OGD. We monitored autophagy in the presence and absence of both ROS and autophagy modulators. The results demonstrated that 1) OGD induced oxidative stress mediated autophagy in hDPSCs and hMSCs; 2) $O_2^{\bullet-}$ and H_2O_2 were the primary mediators of dysregulated autophagy; 4) OGD activated the pro-autophagic proteins Ambra1 and Beclin1 in both hDPSCs and hMSCs; 5) $O_2^{\bullet-}$ and H_2O_2 induced autophagy via p38 and Erk1/2 pathways, and 6) the above cascade affected cell viability.

The pathological process of oxidative stress induces irregular changes in tissue metabolism, function, and morphological structure. In response to low tissue oxygenation, we detected $O_2^{\bullet-}$ and H_2O_2 after 12h of OGD in hDPSCs and hMSCs. By contrast, other studies have identified ROS at earlier time points, which might be attributed to cell line variations, differences in the procedures or quantification methods of different ROS species. Nonetheless, the relationship between ROS production and autophagy induction was consistent across all studies, and excessive $O_2^{\bullet-}$ and H_2O_2 production was also a key finding in our study.

1
2
3
4
5
6
7
8
9
10
11
12
13
14
15
16
17
18
19
20
21
22
23
24
25
26
27
28
29
30
31
32
33
34
35
36
37
38
39
40
41
42
43
44
45
46
47
48
49
50
51
52
53
54
55
56
57
58
59
60

259 Next, we looked at autophagy induction in hDPSCs and hMSCs during OGD. To determine
260 autophagy induction, we confirmed the presence of autophagosomes using EGFP-LC3 puncta
261 quantification. As expected, hDPSCs and hMSCs subjected to OGD exhibited increased
262 numbers of EGFP-LC3 puncta. The accesement of p62 along with the LC3II/I ratio
263 confirmed the autophagy induction in both hDPSCs and hMSCs. Further findings revealed
264 increased Ambra1 and Beclin1 mRNA and protein levels. Ambra1 and Beclin1 activation
265 induced autophagy even further, which is another key finding in our study. Interestingly,
266 these two pro-autophagic proteins have been linked to autophagy dysfunction *in vivo* [20,21].
267 Our findings indicate that Ambra1 and Beclin1 play an important role in autophagy activation
268 via $O_2^{\bullet-}$ and H_2O_2 during OGD. Of note, our results indicated that autophagy is induced
269 downstream of $O_2^{\bullet-}$ and H_2O_2 formation. These findings indicate that targeting Ambra1 and
270 Beclin1 could help reverse adverse OGD effects.

271
272 Recent reports have provided evidence for MAPK involvement in oxidative stress-mediated
273 autophagy [22,23]. MAPKs are protein kinases that regulate the transmission of cellular
274 signals from the cell membrane to the nucleus. We investigated the effect of ROS generation
275 on MAPKs in hDPSCs and hMSCs. We observed activated p38 and Erk1/2 in both hDPSCs
276 and hMSCs. Furthermore, our results indicated that p38 and Erk1/2 MAPKs are involved in
277 autophagy activation, resulting in autophagy and cell death. Based on these findings, we
278 conclude that inhibiting these pathways decreases ROS levels and thus autophagy, improving
279 cell survival. However, since these signalling pathways are not directly involved in
280 autophagy, it is unclear how exactly MAPKs affect autophagy during oxidative stress.
281 Interestingly, a few studies have shown that MAPKs are involved in the early stages of
282 autophagosome formation [24,25], which may be the first evidence of a mechanistic link. To
283 summarize, we demonstrated that $O_2^{\bullet-}$ and H_2O_2 up-regulated autophagy via Ambra1 and
284 Beclin1, and activating the p38 and Erk1/2 pathways in hDPSCs and hMSCs subjected to
285 OGD.

286
287 While autophagy is a cell survival mechanism, it can also result in cell death under specific
288 circumstances. We suggest that reduced viability in cells subjected to OGD is due to ROS-
289 mediated autophagy. Our findings indicated that neither $O_2^{\bullet-}$ nor H_2O_2 alone can induce cell
290 death, suggesting that either a combination of both, participation of other ROS or a
291 considerably higher ROS concentration is required to trigger cell death. Based on these

results, we conclude that autophagy is a critical factor that can influence hDPSC and hMSC survival during oxidative stress.

Conclusion

We demonstrated that OGD initiates $O_2^{\bullet-}$ and H_2O_2 production, in turn inducing autophagy via p38 and Erk1/2 pathways in hDPSCs and hMSCs. We further showed that the pharmacological inhibition of either ROS production or autophagy revoked the harmful effects of OGD. One limitation of our study is the overall small number of biological replicates. This was partly related to limited accessibility of cell batches, but effects observed were consistent across the batches assessed. Moreover, a relatively large number of independent technical replicates were performed for each cell batch, giving us some confidence that the observed effects are real and not due to differences in individual cells or cell batches. Nevertheless, our observations should be verified in a larger, confirmative study. The modulation of either oxidative stress, autophagy, or both may provide a novel strategy to increase hDPSC and hMSC survival in hostile environments. Future studies should investigate pathophysiological links and ways to counter those in more detail, and confirm both *in vivo*.

Statement on Data Availability

The datasets that support the findings of this study are available from the corresponding author upon reasonable request.

Author Contributions

SSR: experiment planning, conception, design, and drafting. RP, EF, AJS, and AN: acquisition of data, results preparation. SSR, SKB, MJ, and JB visualization and revision. SSR, RP, EF, NK, PPP, and SKB: analysis and interpretation of data. MAK: Resources. SKY: qRT-PCR experiments. SKY: electron microscopy sample preparation.

Acknowledgements

We are grateful to Mr. Hari Shankar, Mr. Sishant Rav Divya, and Mr. Mohammad. Danish Siddiqui for technical support.

Funding

We are thankful to SERB, Department of Science and Technology, Government of India, for the hypoxia chamber purchased from grant no. YSS/2015/001731.

References

1. Raza SS, Khan MM, Ahmad A et al. Neuroprotective effect of naringenin is mediated through suppression of NF-κB signaling pathway in experimental stroke. *Neuroscience* 2013;230:157-71.
2. Tsutsui H, Kinugawa S, Matsushima S et al. Oxidative stress and heart failure. *Am J Physiol Heart Circ Physiol* 2011;301(6):H2181-90.
3. Gaillard H, Garcia-Muse T, Aguilera A et al. Replication stress and cancer. *Nat Rev Cancer* 2015;15(5):276-89.
4. Butterfield DA, Halliwell B. Oxidative stress, dysfunctional glucose metabolism and Alzheimer disease. *Nat Rev Neurosci* 2019;20(3):148-160.
5. https://www.who.int/health-topics/cardiovascular-diseases/#tab=tab_1
6. Jablonska A, Drela K, Wojcik-Stanaszek L et al. Short-Lived Human Umbilical Cord-Blood-Derived Neural Stem Cells Influence the Endogenous Secretome and Increase the Number of Endogenous Neural Progenitors in a Rat Model of Lacunar Stroke. *Mol Neurobiol* 2016;53(9):6413-25.
7. Li L, Chen X, Wang WE et al. How to improve the survival of transplanted mesenchymal stem cells in ischemic heart? *Stem Cells Int* 2016;9682757.
8. Holmstrom KM, Finke T. Cellular mechanisms and physiological consequences of redox-dependent signalling. *Nat Rev Mol Cell Biol* 2014;15(6):411-21.
9. Tan DQ, Suda T. Reactive Oxygen Species and Mitochondrial Homeostasis as Regulators of Stem Cell Fate and Function. *Antioxid Redox Signal* 2018;29(2):149-168.
10. Ichimiya T, Yamakawa T, Hirano T et al. Autophagy and Autophagy-Related Diseases: A Review. *Int J Mol Sci* 2020;21(23):8974.
11. Jin M, Zhang Y. Autophagy and Immune-Related Diseases. *Adv Exp Med Biol* 2020;1207:401-403.
12. Guo F, Liu X, Cai H et al. Autophagy in neurodegenerative diseases: pathogenesis and therapy. *Brain Pathol* 2018;28(1):3-13.
13. Chiang MH, Liang CJ, Liu CW et al. Aliskiren Improves Ischemia- and Oxygen Glucose Deprivation-Induced Cardiac Injury through Activation of Autophagy and AMP-Activated Protein Kinase. *Front Pharmacol* 2017;14:8:819.
14. Cianfanelli V, D’Orazio M, Cecconi F et al. AMBRA1 and BECLIN 1 interplay in the crosstalk between autophagy and cell proliferation. *Cell Cycle* 2015;14(7):959–63.
15. Antonioli M, Albiero F, Fimia GM et al. AMBRA1-regulated autophagy invertebrate development. *Int J Dev Biol* 2015;59(1–3):109–17.
16. Kang R, Zeh HJ, Lotze MT et al. The Beclin 1 network regulates autophagy and apoptosis. *Cell Death Differ* 2011;18(4):571–80.

17. Runden-Pran E, Tanso R, Haug FM et al. Neuroprotective effects of inhibiting N-methyl-D-aspartate receptors, P2X receptors and the mitogen-activated protein kinase cascade: a quantitative analysis in organotypical hippocampal slice cultures subjected to oxygen and glucose deprivation. *Neurosci* 2005;136(3):795–810.
18. Qi H, Soto-Gonzalez L, Krychtiuk KA et al. Pretreatment With Argon Protects Human Cardiac Myocyte-Like Progenitor Cells from Oxygen Glucose Deprivation-Induced Cell Death by Activation of AKT and Differential Regulation of Mapkinases. *Shock* 2018;49(5):556–563.
19. Mitter SK, Song C, Qi X et al. Dysregulated autophagy in the RPE is associated with increased susceptibility to oxidative stress and AMD. *Autophagy* 2014;10(11):1989–2005.
20. Li H, Ham A, Ma TC et al. Mitochondrial dysfunction and mitophagy defect triggered by heterozygous GBA mutations. *Autophagy* 2019;15(1):113-130.
21. Salminen A, Kaarniranta K, Kauppinen A et al. Impaired autophagy and APP processing in Alzheimer's disease: The potential role of Beclin 1 interactome. *Prog Neurobiol* 2013;106-107:33-54.
22. Mi Y, Xiao C, Du Q et al. Momordin Ic couples apoptosis with autophagy in human hepatoblastoma cancer cells by reactive oxygen species (ROS)-mediated PI3K/Akt and MAPK signaling pathways. *Free Radic Biol Med* 2016;90:230–42.
23. Niu NK, Wang ZL, Pan ST et al. Pro-apoptotic and pro-autophagic effects of the Aurorakinase A inhibitor alisertib (MLN8237) on human osteosarcoma U-2 OS and MG-63 cells through the activation of mitochondria-mediated pathway and inhibition of p38 MAPK/PI3K/Akt/mTOR signaling pathway. *Drug Des Devel Ther* 2015;9:1555–84.
24. Thapalia BA, Zhou Z, Lin X et al. Sauchinone augments cardiomyocyte viability by enhancing autophagy proteins -PI3K, ERK(1/2), AMPK and Beclin-1 during early ischemia-reperfusioninjury *in vitro*. *Am J Transl Res* 2016;8(7):3251–65.
25. Diomedede F, Tripodi D, Trubiani O et al. HEMA Effects on Autophagy Mechanism in Human Dental Pulp Stem Cells. *Materials (Basel)* 2019;12(14):2285.

Legends

Fig. 1: OGD induces $O_2^{\cdot-}$ and H_2O_2 generation and activates autophagy in hDPSCs. Fig (A) revealed changes in viability which were evident from 3h onwards, but a significant reduction was observed only after 12h of OGD treatment, n=6. Figure (B) depicts an example

of flow cytometry data for $O_2^{\cdot-}$. A high production of $O_2^{\cdot-}$ in hDPSCs subjected to OGD compared to controls; however, addition of PEG-SOD reversed the effect. Rotenone induced the generation of $O_2^{\cdot-}$, $n=5$. (C) shows the spectrophotometric analysis of H_2O_2 staining. An abrupt generation of $O_2^{\cdot-}$ in OGD treated hDPSCs compared to the control was observed, which was diminished by the addition of PEG-catalase. The group receiving exogenous H_2O_2 has documented a high generation of H_2O_2 , $n=4$. (D) The expression level of LC3II and the LC3II/I ratio was significantly enhanced after 12h of OGD in hDPSC, $n=9$. (E) hDPSCs transfected with EGFP-LC3 showed enhanced EGFP-LC3 puncta formation. Rapamycin treatment induced a similar effect, which was strongly mitigated by 3-MA ($n=12$; cells=at least 50/group); scale bar: 20 μ M. Fig. (F) documents transmission electron microscopical images; OGD and rapamycin exposure resulted in the formation of autophagic vacuoles. AP stands for autophagosomes, AL stands for autolysosomes, AM stands for autophagosomes engulfing mitochondria, PP stands for phagophore; scale bar: 20 μ M. Fig. (G) shows western blot analysis of rapamycin and 3-MA treatment in hDPSCs, $n=6$. Fig. (H) shows lowered expression of p62 under OGD in hDPSCs and increased LC3II band and LC3II/I ratio, $n=4$. GAPDH was used as an internal control for figs (G and H), while β -actin was used as an internal control for fig. (D). The maroon arrow in Fig D shows the band which was quantified. Error bars represent the mean \pm SD.

Fig. 2: $O_2^{\cdot-}$ and H_2O_2 activate autophagy in hDPSCs through activating Ambra1 and Beclin1. Fig (A) depicts a microscopic representation of $O_2^{\cdot-}$ generation in hDPSCs during OGD treatment. The group receiving PEG-SOD along with OGD showed a decrease in the EGFP-LC3 puncta staining compared to the OGD alone treated group. Rotenone showed a high EGFP-LC3 puncta staining as compared to the control treatment, $n=12$; Scale bar: 20 μ M. Fig. (B) represents the effect of H_2O_2 generation in OGD treatment in hDPSCs. The group receiving PEG-catalase along with OGD showed a decrease in the EGFP-LC3 puncta staining compared to the OGD alone treated group. Exogenous H_2O_2 treatment showed a high EGFP-LC3 puncta staining as compared to the control treatment. Pictures were taken at 40X by an inverted fluorescent microscope, ($n=12$; cells=at least 50/group). (C) Ambra1 expression peaked in hDPSC after 12 hours of OGD, $n=10$. (D) The same pattern was observed for Beclin1, $n=9$. Expression of Ambra1-siRNA (E, 15 pmole for 48h prior to OGD) $n=5$, and si-Beclin1 (F, 12.5 pmol for 48h prior to OGD) was measured by quantitative real-time PCR, $n=5$. The activated Ambra1 and Beclin1 were found to be reduced with the supplementation of the siRNAs (Ambra1 and Beclin1 respectively). Figs (G and H) show

increased Ambra1-(n=4, at least) and Beclin1-(n=4, at least) protein expression, which was reversed by siRNA application. GAPDH was used as an internal control for all the experiments. The maroon arrow in Fig **H** shows the band which was quantified. Error bars represent the mean±SD.

Fig. 3: Ambra1 and Beclin1 activated by to $O_2^{\cdot-}$ and H_2O_2 induce autophagy in hDPSCs. The cellular response of hDPSCs during 12h of OGD treatment was mapped and linked to $O_2^{\cdot-}$ and H_2O_2 . Figs. (**A and B**) represent the mitigation of the effect of $O_2^{\cdot-}$ and H_2O_2 on Ambra1. In brief, $O_2^{\cdot-}$ and H_2O_2 enhanced Ambra1 expression during OGD, but the supplementation of PEG-SOD (n=4) and PEG-catalase (n=4) counteracted this effect. Likewise, Figs. (**C and D**) represent the mitigation of the effect of $O_2^{\cdot-}$ and H_2O_2 on Beclin1. In short, $O_2^{\cdot-}$ and H_2O_2 increased Beclin1 expression during OGD, and both PEG-SOD (n=4) and PEG-catalase (n=5) mitigated the effect. GAPDH was used as an internal control. Figs. (**E and F**) represent the role of Ambra1 and Beclin1 in activating autophagy in hDPSCs (n=12; cells=at least 50/group); scale bar: 20μM. Error bars represent the mean±SD.

Fig. 4: OGD produces $O_2^{\cdot-}$ and H_2O_2 through the involvement of P38 and Erk1/2 MAPKs in hDPSCs. Fig. (**A**) shows the expression of p-P38 increased after OGD, n=4. Fig. (**B**) shows the expression of p-Erk1/2 enhanced after OGD, n=4. Fig. (**C**) shows the application of the P38 inhibitor SB202190 in suppressing the P38 pathway during OGD, n=4. (**D**) Application of the Erk1/2 inhibitor PD98059 inhibited the pathway during OGD, n=4. The application of PEG-SOD (**E**, n=4) and PEG-catalase (**F**, n=4) confirmed the participation of ROS in inhibiting the p-P38, and p-Erk1/2 pathways during OGD (**G**, n=4; **H**, n=4). GAPDH was used as an internal control. The maroon arrow in Figs. **A**, **C**, **D**, **F**, and **G** shows the band which was quantified. Error bars represent the mean±SD.

Fig. 5 Prevention of ROS-mediated hDPSCs death. Fig. (**A**) depict OGD and rapamycin reduced hDPSC viability. Though, the OGD-induced decrease of hDPSC viability was partially prevented by 3-MA, n=5. Fig. (**B**). The results showed a low cell survival in the OGD group cells, while the supplementation of PEG-SOD was unable to suppress cell death at a significant level, n=5. Fig. (**C**). PEG-catalase alone failed to improve hDPSC survival, n=5. Fig. (**D**). Combined PEG-SOD/PEG-catalase exposure during OGD improved hDPSC viability, n=5. (**E**) Similar effects were observed for NAC, n=5. The pre-treatment of OGD-

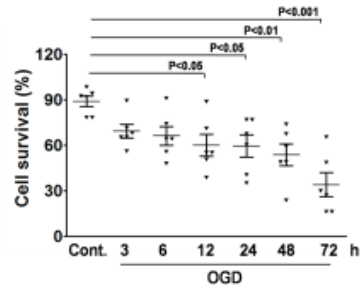
1
2
3
4
5
6
7
8
9
10
11
12
13
14
15
16
17
18
19
20
21
22
23
24
25
26
27
28
29
30
31
32
33
34
35
36
37
38
39
40
41
42
43
44
45
46
47
48
49
50
51
52
53
54
55
56
57
58
59
60

465 treated hDPSCs with NAC, a pan-inhibitor of ROS, mitigate the effect observed in OGD
466 group. Error bars represent the mean±SD.

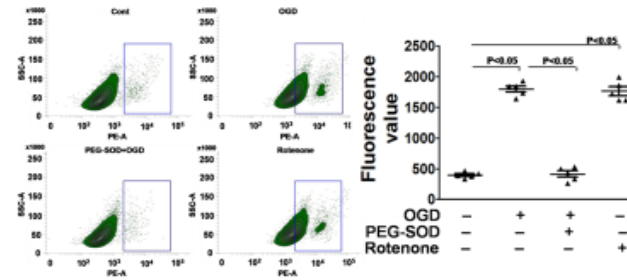
467
468 **Fig. 6: O₂^{•-} and H₂O₂ are unidirectional inducers of autophagy in hDPSCs.** The
469 autophagic machinery was inhibited either by exposing hDPSCs to 3-MA or by silencing
470 Ambra1 and Beclin1 during OGD, followed by ROS estimation via DHE and Amplex Red
471 staining. (A) O₂^{•-} (n=9, cells=atleast 50/group), and (B) H₂O₂ (n=4) production were
472 significantly increased during OGD, but autophagy inhibition via 3-MA did not reduce the
473 respective production levels. (C) O₂^{•-} (n=9, cells=atleast 50/group), and (D) H₂O₂ (n=4)
474 production was also not efficiently reduced by Ambra1 silencing during OGD. (E) O₂^{•-} (n=9,
475 cells=atleast 50/group), and (F) H₂O₂ (n=4) production was further unaffected by Beclin1
476 silencing. Taken together, this indicates that ROS production is an upstream event in
477 autophagy. Scale bar: 50µM. Error bars represent the mean±SD.

478
479 **Graphical abstract:** Schematic diagram of a summary scheme of the current findings,
480 including pharmacological treatments and genetic manipulations. In brief, OGD treatment to
481 human DPSC and human MSC induces hypoxia and oxidative stress in these cells. Further,
482 OGD regulates cell fate by activating autophagy via the generation of O₂^{•-} and H₂O₂. The
483 excessive O₂^{•-} and H₂O₂ production, in turn, activates Ambra1-Beclin1. The activation of
484 Ambra1-Beclin1 enhanced autophagy in the cells. Further, the production of O₂^{•-} and H₂O₂
485 activates the Erk-p38 pathway, which also contributes to cell impairment. The participation
486 of ROS, O₂^{•-}, H₂O₂, Erk1/2, and p38 were confirmed by NAC, PEG-SOD, PEG-Catalase,
487 PD98059, and SB202190, while the use of the respective siRNAs confirmed the Ambra1 and
488 Beclin1 involvement. Our results also suggest that O₂^{•-} and H₂O₂ are the inducers of
489 autophagy, and the process is unidirectional. Finally, the results revealed that OGD induces
490 oxidative stress and cell death through the participation of O₂^{•-} and H₂O₂ Erk1/2 and p38
491 pathways.

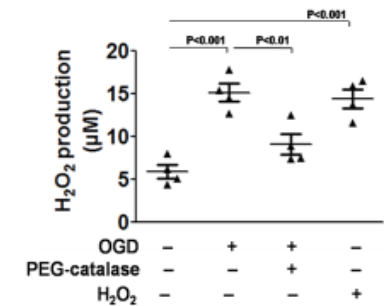
A



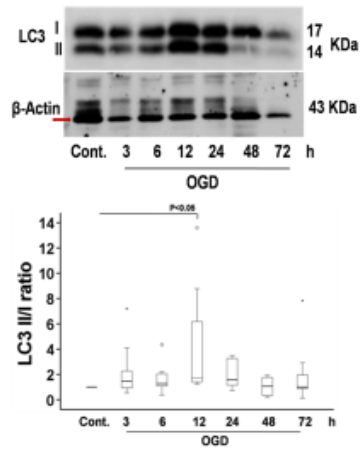
B



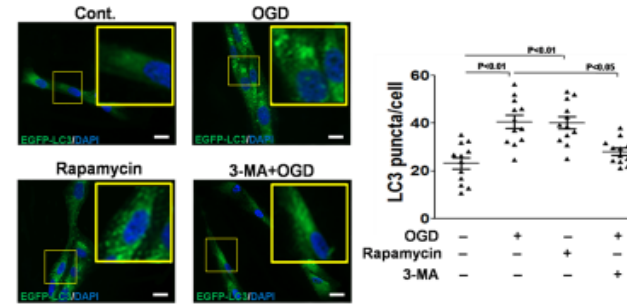
C



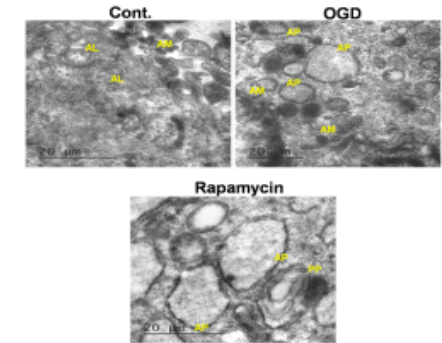
D



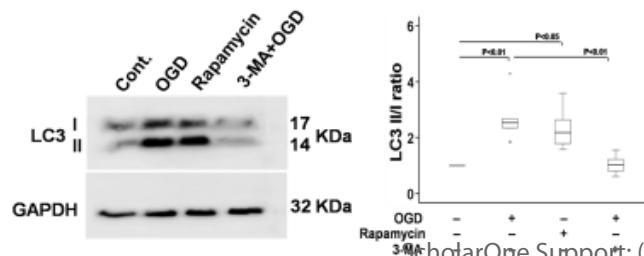
E



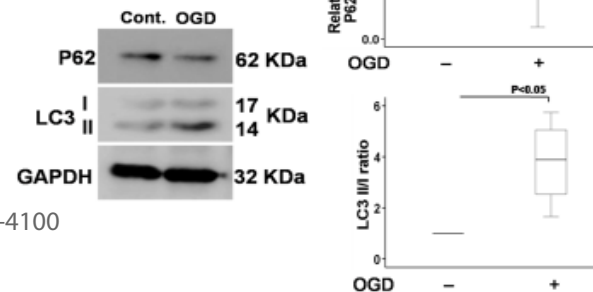
F



G



H



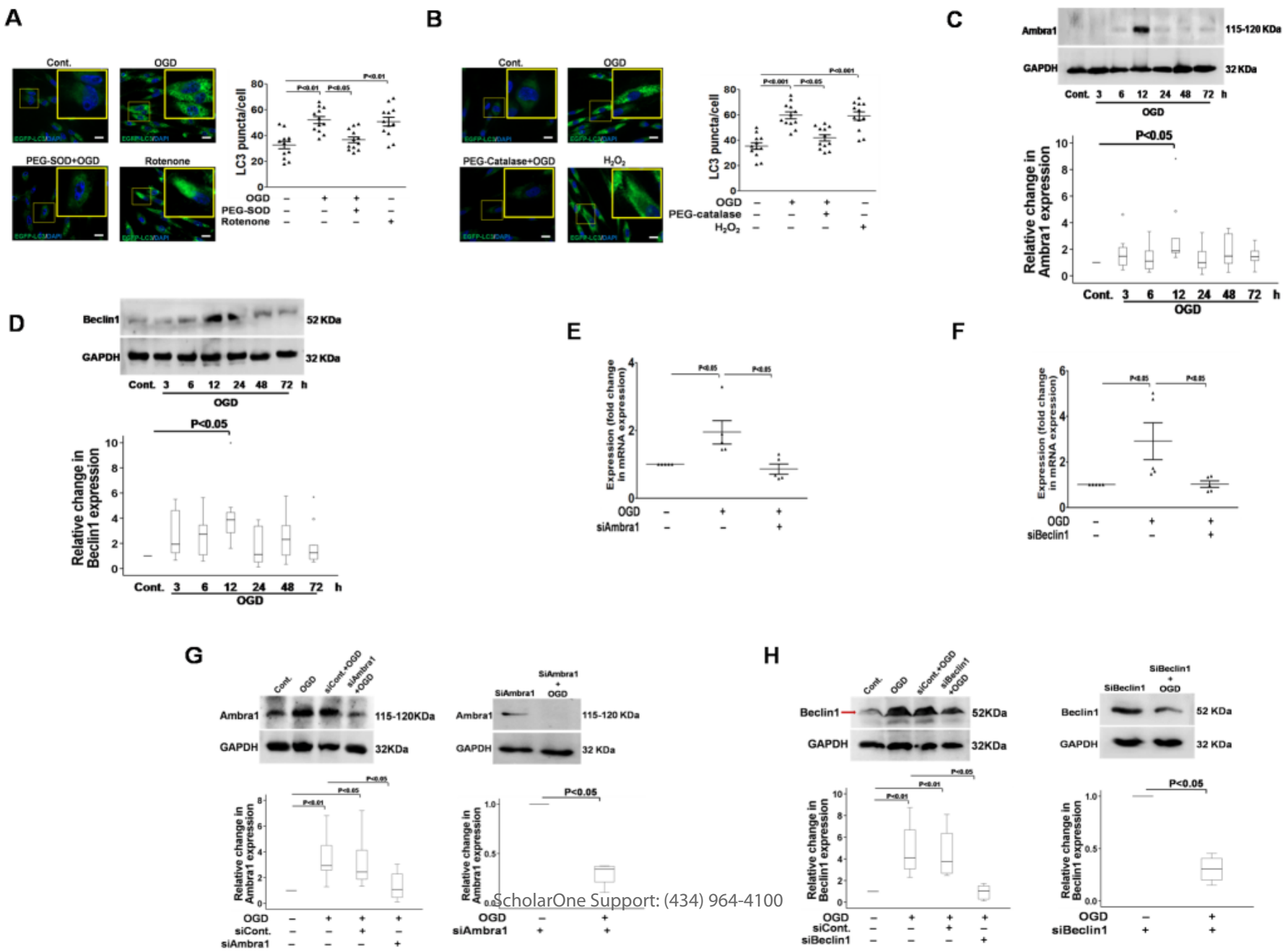
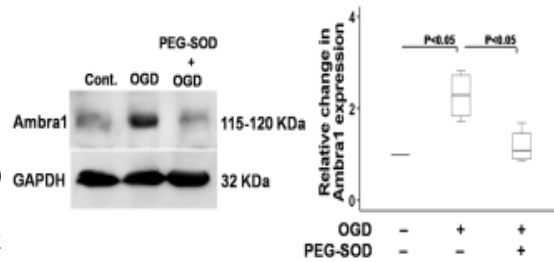
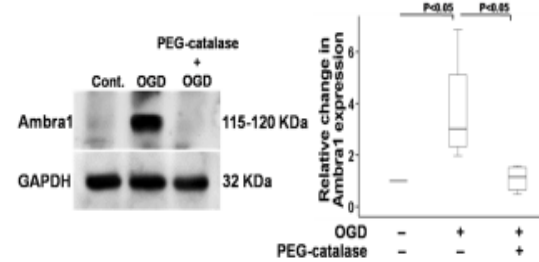
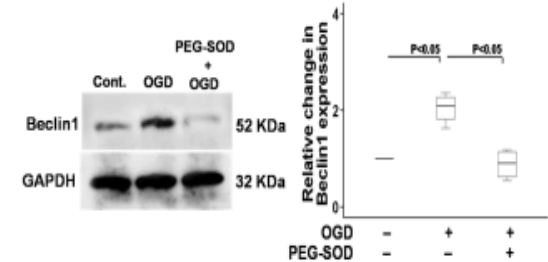
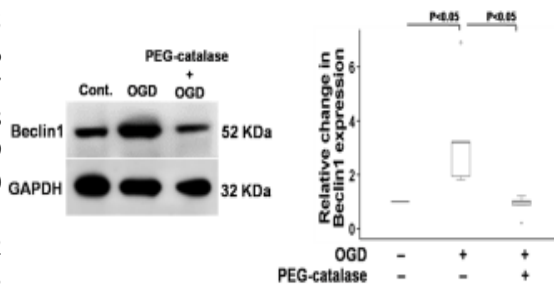
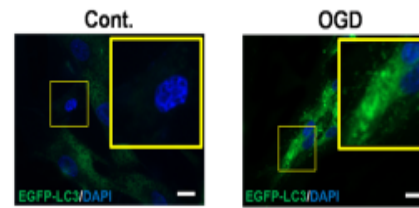
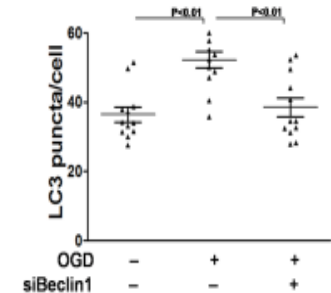
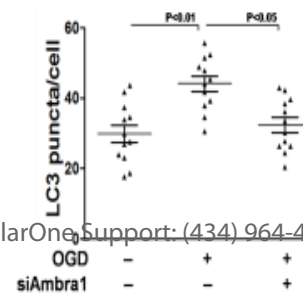
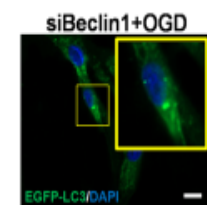
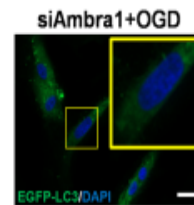
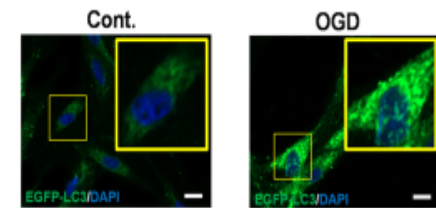


Fig. 3**A****B****C****D****E****F**

1
2
3
4
5
6
7
8
9
10
11
12
13
14
15
16
17
18
19
20
21
22
23
24
25
26
27
28
29
30
31
32
33
34
35
36
37
38
39
40
41

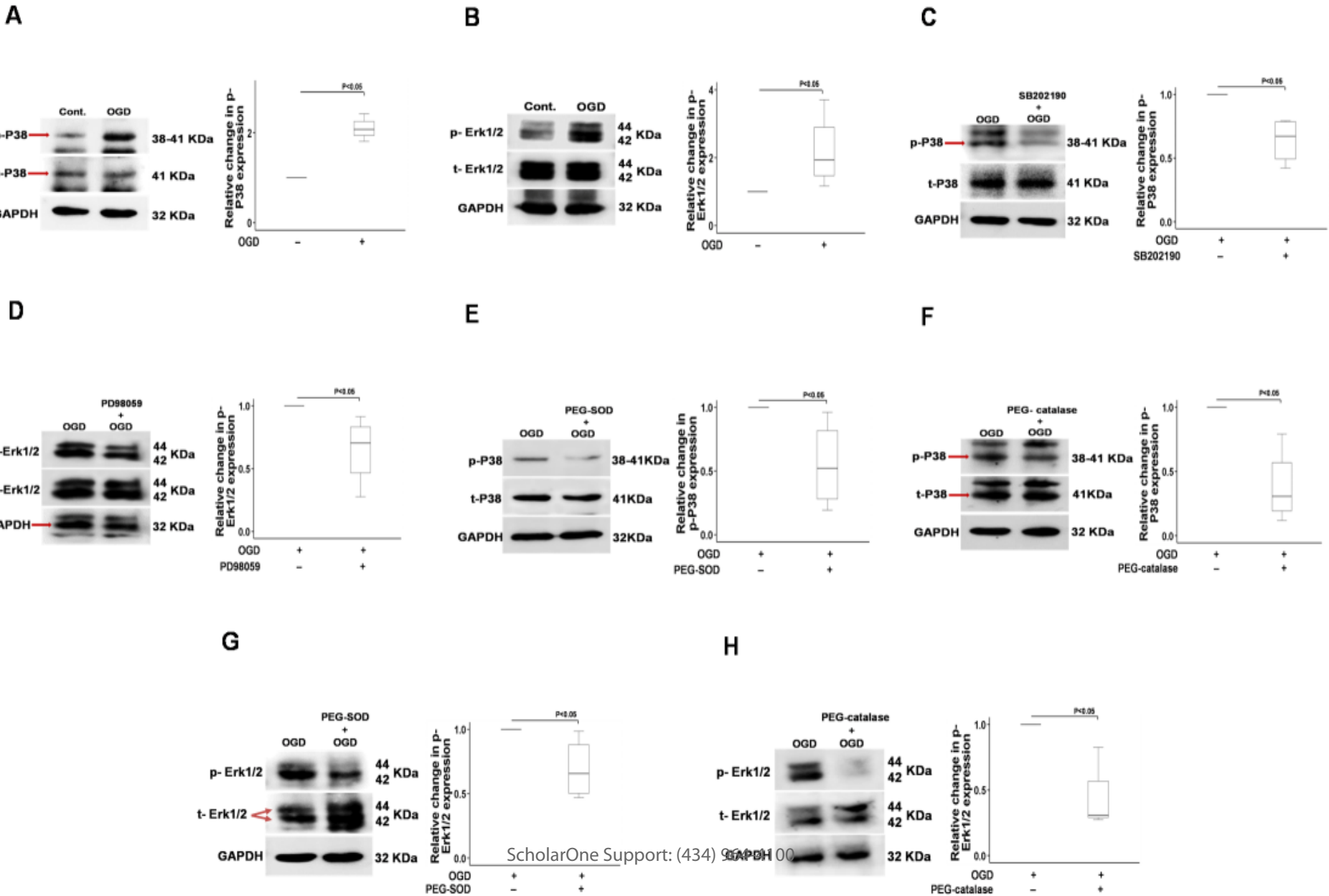
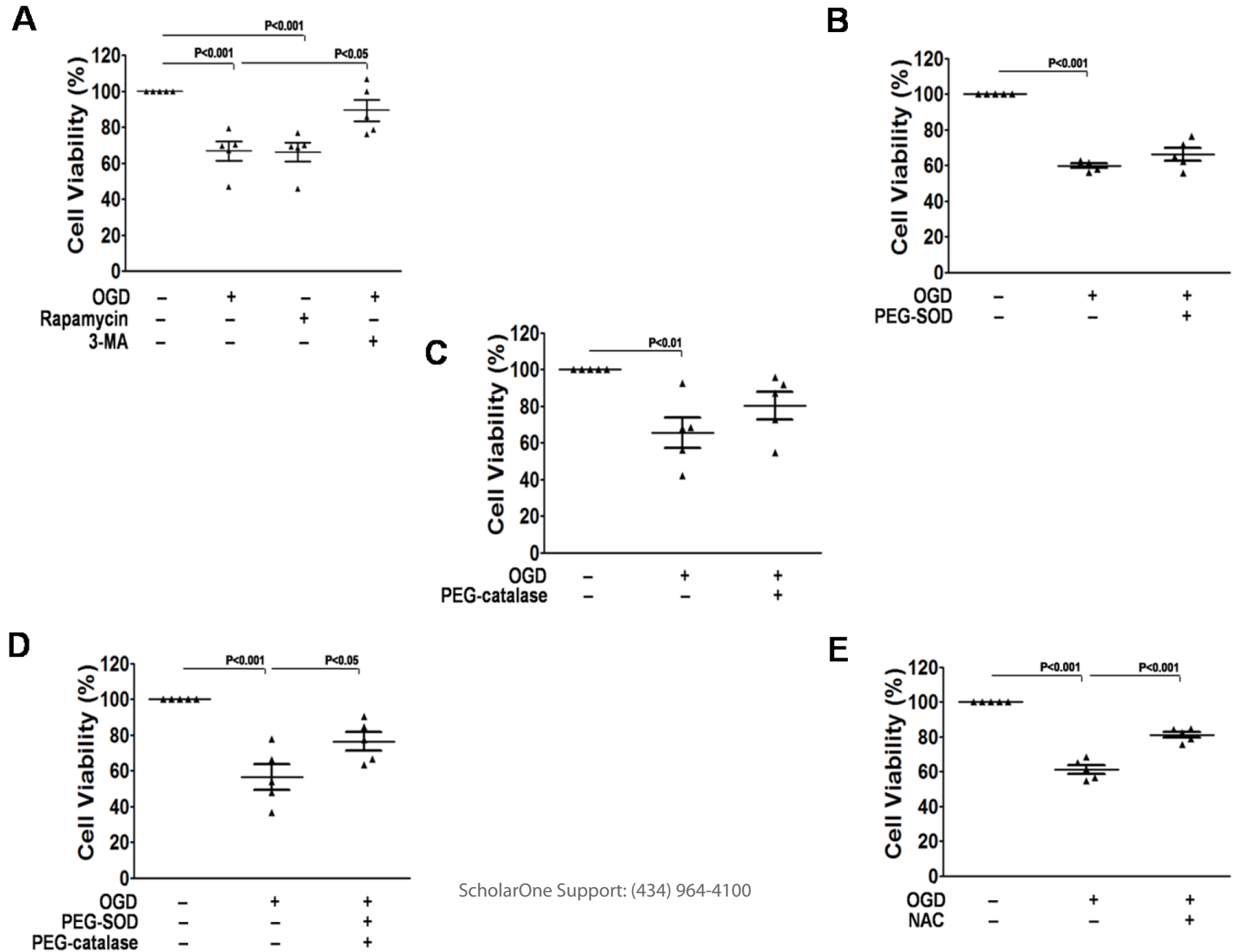
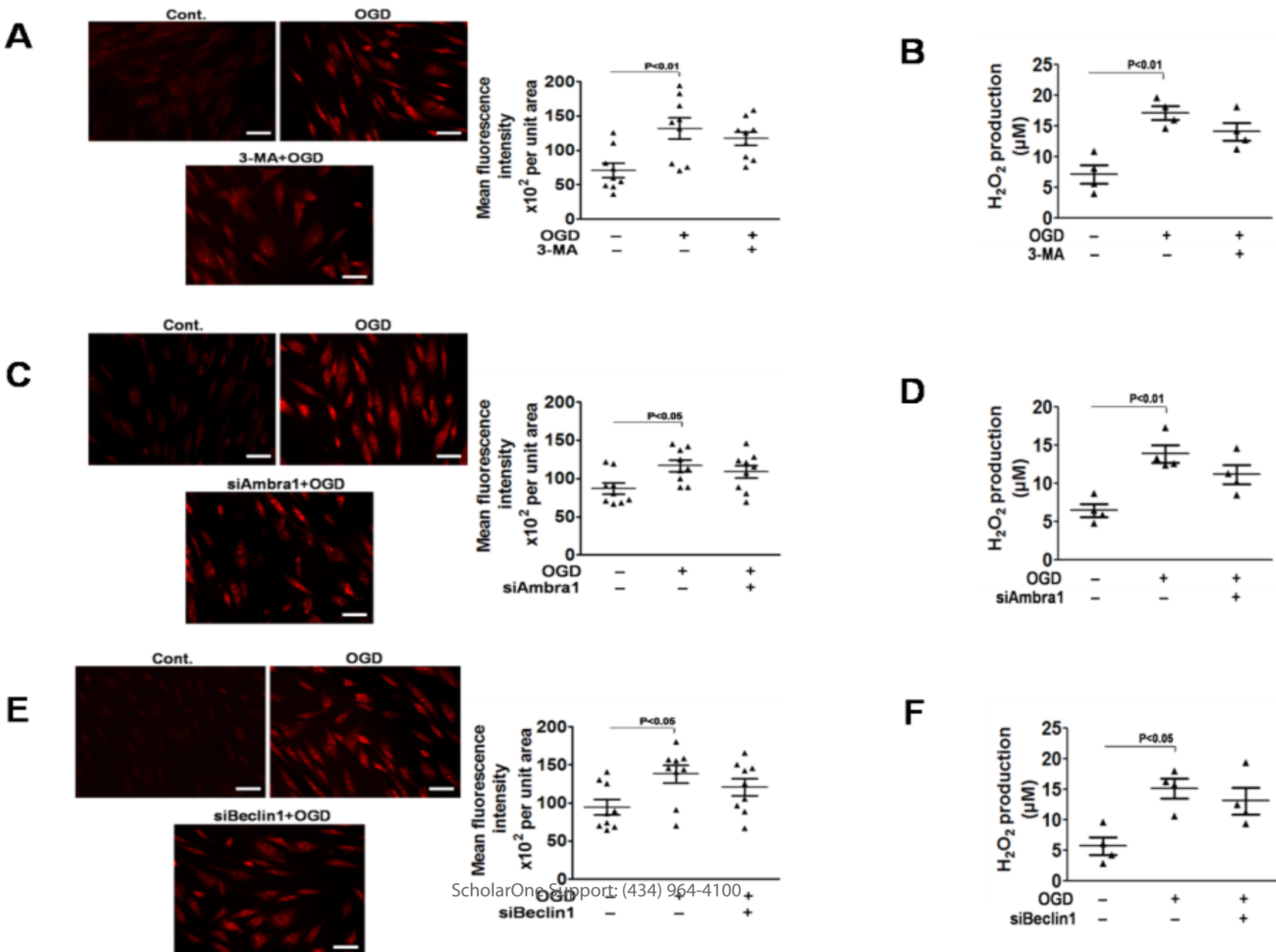


Fig. 5



Supplementary data

Materials and Methods

Chemicals

Chemical information has been included in Table ST1. Supplementary Table ST2 provides the concentration, dilution, and treatment period of the activators and inhibitors used in this study.

Antibodies, primers, and small interfering RNAs

Supplementary Tables ST3 and ST4 provide details on primary and secondary antibodies used. Ambra1 and Beclin1 small interfering RNAs (siRNAs) were used for knockdown studies. Glyceraldehyde 3-phosphate dehydrogenase (GAPDH) or β -actin was used as the internal controls, and scrambled siRNA was used as the negative control. The TaqMan gene expression assay was used for Ambra1, Beclin1, and GAPDH.

hDPSCs and hMSCs culture and treatment paradigm

hDPSCs and hMSCs were purchased from HiMedia Laboratories (Appendix-I and Appendix-II) and maintained in a humidified CO₂ incubator (5% CO₂, 37°C) in low glucose Dulbecco's Modified Eagle Medium (DMEM) supplemented with 10% heat-inactivated fetal bovine serum, 100U/mL penicillin, and 100mg/mL streptomycin. For OGD treatment, hDPSCs and hMSCs were seeded at 1×10^6 cells per well and grown to 65-70% confluency. Next, the culture medium was replaced with OGD medium (DMEM) without serum, glucose, and sodium pyruvate, and cells were incubated for 30min. The impact of OGD times from 0 to 72h (Fig. S1A) was first determined. hDPSCs were cultured in 1% O₂, 5% CO₂, and 94% N₂ in a hypoxia chamber (Stem Cell Technologies; Cambridge, MA, USA). An oxygen meter (Lutron Electronics; Taipei, Taiwan, PO2-250) was placed in the hypoxia chamber during OGD to monitor O₂ levels. Based on the above results, OGD time was set to 12h followed by 24h of normoxia for subsequent experiments (Fig.S1B).

Trypan blue cell viability assay

Cells were detached from culture dishes by 0.25% Trypsin-EDTA incubation for 3min at 37°C and then centrifuged at 300×g for 5min. Stem cell viability was determined using

1
2
3 33 Trypan blue under an inverted fluorescent microscope (Zeiss, Oberkochen
4 34 Germany) according to standard protocol.
5
6
7 35

8 36 **MTT cell viability assay**

9
10 37 For cell viability assays, each well was treated with a 5mg/mL MTT solution in phosphate-
11 38 buffered saline (PBS), pH 7.4, and the cells were incubated for another 3h under culture
12 39 conditions. Formazan crystals formed inside viable cells were solubilized in dimethyl
13 40 sulfoxide (DMSO), and the absorbance was measured at 595nm using a microplate reader
14 41 (BioRad, Hercules, California, USA).
15
16
17
18
19 42

20 43 **EGFP-LC3 transfection and detection through immunostaining**

21
22 44 After reaching 60-70% confluency, hDPSCs or hMSC were transiently transfected using
23 45 Lipofectamine 3000 as per the manufacturer's instructions. In brief, the hDPSCs were
24 46 transfected with 1µg of total DNA (enhanced green fluorescent protein (EGFP)-LC3
25 47 expression construct) in a T25 flask. Subsequently, hDPSCs were seeded in 35mm Petri
26 48 dishes containing normoxia or OGD medium and incubated for 12h. Rapamycin was used as
27 49 a positive control to observe the pattern of EGFP-LC3 puncta. After fixation with 4%
28 50 formaldehyde for 10min, hDPSCs were washed three times in ice-cold PBS. Fluorescence
29 51 microscopy (Axio ObserverZ1, Zeiss) was used to observe the EGFP-LC3 puncta.
30 52 Autophagy was quantified by counting the percentage of hDPSCs and hMSCs containing
31 53 EGFP-LC3 puncta in 200 cells/group by ImageJ software using the "Analyze particles"
32 54 plugin. Results are presented as EGFP-LC3 puncta count/cells.
33
34
35
36
37
38
39
40
41
42

43 56 **siRNA silencing of Ambra1 and Beclin1**

44 57 hDPSCs or hMSCs were seeded in 35mm Petri dishes and incubated at 37°C and 5% CO₂.
45 58 After reaching 50-70% confluency, cells were transfected with siRNAs (siRNA for Beclin1,
46 59 Ambra1, and scrambled siRNA). Two days later, cells were subjected to 12h OGD followed
47 60 by 24h of normoxia. Afterwards, hDPSCs and hMSCs were analyzed by Western blotting or
48 61 immune cytochemistry. Control hDPSCs and hMSCs were incubated at 37°C with 5% CO₂ in
49 62 a regular medium for 36h. siRNA transfection was performed using the manufacturer's
50 63 protocol. Regular medium without the Lipofectamine reagent and siRNAs was added to non-
51 64 siRNA hDPSCs and hMSCs. hDPSCs and hMSCs transfected with scrambled siRNA
52 65 underwent similar treatment.
53
54
55
56
57
58
59
60

Measurement of intracellular $O_2^{\cdot-}$ generation

Intracellular generation of $O_2^{\cdot-}$ was detected by dihydroethidium staining (DHE) [1]. After OGD, the hDPSCs and hMSCs were harvested by trypsinization and washed with a serum-free medium. Subsequently, hDPSCs were stained with 10 μ M DHE in a serum-free medium followed by incubation at 37°C for 30min in the dark. After incubation, hDPSCs were collected by centrifugation (300×g, 5min), washed once with PBS, resuspended in 300 μ L PBS, and analyzed using a flow cytometer (BD Lyric; Becton-Dickinson, New Jersey, USA). hMSCs were accessed by fluorescent imaging. PEG-SOD (Sigma-Aldrich, S9549) was used as the $O_2^{\cdot-}$ quencher. Rotenone was used as a positive control for superoxide estimation [2].

Measurement of intracellular H_2O_2 generation through a spectrophotometer

Intracellular H_2O_2 was estimated using Amplex Red according to the manufacturer's protocol. Exogenous H_2O_2 was used as a positive control [3]. Briefly, hDPSCs and hMSCs were subjected to OGD in the presence or absence of PEG-catalase (100U/mL for 24h). Thereafter, hDPSCs and hMSCs were scraped in RIPA buffer and incubated on ice for 30min. Next, hDPSCs and hMSCs were centrifuged at 20,000×g for 30min at 4°C. The supernatant was recovered and used for H_2O_2 estimation. Afterwards, 50 μ L of supernatant was mixed with 50 μ L of the reaction mixture (Amplex Red-100 μ M, HRP-0.2U/mL in sodium phosphate buffer, pH 7.4) and incubated at room temperature for 30min. The absorbance was read at 560nm, and the concentration of H_2O_2 was calculated by extrapolating the absorbance against the standard curve of H_2O_2 (1-5 μ M).

Analysis of ROS production

hDPSCs were seeded in 12 well plates containing sterile coverslips at a density of 2×10^4 hDPSCs/well and allowed to grow overnight under standard culture conditions. After achieving 65-70% confluency, the hDPSCs were given respective treatments, i.e., 12h/24h OGD followed by normoxia. The NAC+OGD group received NAC (10mM for 45min) before 12h/24h OGD, followed by normoxia. Subsequently, hDPSCs were washed with 1X-PBS and stained with DCFDA (10 μ M) in the serum-free medium by incubating at 37°C for 30min in the dark. After incubation, the DCFDA solution was replaced with fresh PBS (pre-warmed), and hDPSCs were analyzed under the inverted fluorescent microscope.

Western blotting

1
2
3 100 hDPSCs and hMSCs were lysed with ice-cold RIPA buffer containing protease and
4 101 phosphatase inhibitors and centrifuged at 20,000×g for 30min at 4°C. The Pierce BCA
5 102 protein assay kit was used to measure protein concentration. In brief, proteins were
6 103 fractionated by SDS-PAGE and transferred onto PVDF membranes. The membranes were
7 104 blocked with 5% non-fat dry milk for 1h at room temperature (RT), probed with primary
8 105 antibodies overnight at 4°C, and incubated with HRP-conjugated secondary antibodies at RT
9 106 for 1h. Immunoblot bands were developed using Clarity™ Western ECL substrate (peroxide
10 107 solution) and quantified through densitometry using ImageJ software. Densities were
11 108 normalized to control treatment, and relative fold changes normalized to β-actin or GAPDH.
12
13
14
15
16
17
18
19

20
21 **Immunocytochemistry with fluorescence imaging**

22 111 hDPSCs and hMSCs were rinsed thrice in 1×PBS and fixed in 4% paraformaldehyde for
23 112 10min at RT, followed by three rinses in 1×PBS. hDPSCs were blocked with 1% BSA in
24 113 1×PBS for 1h at RT. After blocking, hDPSCs and hMCSs were incubated overnight at 4°C
25 114 with primary antibodies against Beclin1 and Ambra1. The samples were then rinsed three
26 115 times in 1×PBS (10min/rinse) and incubated with secondary antibodies for 1h at RT. Finally,
27 116 the samples were washed and mounted using a ProLong antifade fluoroshield mounting
28 117 medium containing DAPI.
29
30
31
32
33
34
35

36 119 **qRT-PCR analysis**

37 120 Total RNA was extracted from hDPSCs using Trizol according to the manufacturer's
38 121 protocol. An equal amount of RNA (approximately 1μg) was reverse-transcribed into cDNA
39 122 using the Revert Aid First Strand cDNA Synthesis Kit in each experiment. Subsequently, 1
40 123 μL of diluted cDNA was used as a template for RT-PCR analyses using TaqMan Universal
41 124 Master Mix II with UNG. PCR was performed with TaqMan gene assays for Beclin1,
42 125 Ambra1, and GAPDH as follows: 10min at 50°C, then 2min of initial denaturation (1 cycle),
43 126 followed by 40 cycles of denaturation; 94°C for 20sec, and annealing and extension at 60°C
44 127 for 60sec. Supplementary Table ST5 lists the chemical dilutions.
45
46
47
48
49
50
51
52

53 129 **Electron microscopy**

54 130 hDPSCs were fixed with 2% glutaraldehyde–paraformaldehyde in 0.1M PBS, pH 7.4, for 2h,
55 131 and post-fixed with 1% OsO4 for 1h at 4°C. Cells were then dehydrated in 70% acetone, and
56 132 infiltrated with epoxy-embedding medium using an epoxy-embedding medium kit. After
57 133 embedding the specimens in pure fresh resin, 70nm thick sections on a microtome
58
59
60

(Leica Biosystems, Heidelberg, Germany) were cut and stained with toluidine blue for viewing under a light microscope. Thin sections were double-stained with 7% (20min) uranyl acetate and lead citrate for contrast staining. A transmission electron microscope (Tecnai G2 20 S-TWIN, Amsterdam, The Netherlands) was used to visualize the thin sections at an acceleration voltage of 80kV.

Fluorescence intensity per unit area

The fluorescence generated is presented in the form of “Mean Fluorescence intensity $\times 10^2/\text{unit area (mm}^2\text{)}$ ”, which was calculated using ImageJ. First, we set the scale in the software by using the scale bar of the image (number of pixels per mm distance) and calculated the area of interest and mean intensity using the “polygonal selection” tool. Subsequently, the fluorescence intensity per unit area of all the cells was calculated and presented.

Evaluation of fluorescent autophagic puncta

The hDPSCs were seeded in 35mm discs (containing sterile, gelatin-coated coverslips) at a concentration of 20,000 cells/ well and allowed to attain a confluence of ~60%–70%. The cells were transiently transfected using Lipofectamine 3000, following the manufacturer’s instructions. Subsequently, the discs dedicated to the OGD group were cultured in hypoxia medium without glucose for 12h followed by incubation under normoxic conditions for 24 h. The control discs were incubated under normoxic conditions throughout the experiment. The cells treated with Rapamycin were used as a positive control to observe the pattern of EGFP-LC3 puncta. Finally, the cells were fixed with 4% formaldehyde for 10min followed by washing thrice in ice-cold PBS. All the specimens were mounted with Antifade reagent containing DAPI. The cells were observed under a fluorescence microscope (ObserverZ1, Zeiss, Germany) to detect autophagy induction. The number of EGFP-LC3 puncta in autophagic cells was counted by ImageJ software using the "Analyze particles" plugin. For each group, LC3 puncta were counted in 200 cells and represented as LC3 Puncta/cell. The results are the outcome of three independent repeats.

Statistical analysis

In all experiments, "n" represents the number of independent experiments. At least four independent experiments (n=4) were conducted to collect data. For imaging data sets, we used at least 50 cells per group per experiment. Data distribution was checked by the Shapiro-Wilk test of normality. One way analysis of variance (ANOVA) with Newman-Keuls test (for normally distributed data); Mann-Whitney test was used to compare the differences between two groups, and Kruskal-Wallis test followed by Dunn's test for multiple comparisons (for non-normally distributed data) were used to test statistical differences using SPSS Statistics 28.0 software (IBM). 0.05 was considered statistically significant (*#P<0.05, **/##P<0.01, and ***/###P<0.001 compared to the control/OGD/Rotenone-treated group).

Supplementary figures' legends

Fig. S1: Figs. (A) and (B) are representative sketches of the experimental design.

Fig. S2: OGD induces O₂^{•-} and H₂O₂ generation and activates autophagy in hMSCs.

Figs. (A and B) depict the generation of O₂^{•-} and H₂O₂. DHE staining analysis of OGD-induced O₂^{•-} generation in hMSC, n=9; scale bar: 50μM (A). H₂O₂ estimation using Amplex Red shows an abrupt generation of endogenous H₂O₂ after OGD, n=4 (B). The group receiving rotenone (Fig. A) or exogenous H₂O₂ (Fig. B) has documented a high generation of O₂^{•-} and H₂O₂ compared to the control. Fig. (C) represents the effect of OGD on autophagy in hMSCs. Measurement of autophagy by EGFP-LC3 punctate formation in the presence and absence of 3-MA, n=12 (cells=at least 50/group); scale bar: 20μM. Figure (D) depicts the effect of OGD on LC3II conversion and the LC3II/I ratio. LC3II/I expression was evident at 12h of OGD, n=4. Fig (E). is the representative picture of the effect of Rapamycin and 3-MA on hMSCs. In summary, OGD and rapamycin increased the LC3II/I ratio whereas 3-MA attenuated the effect of OGD, n=8 (E). Fig (F) represents a lower expression of p62 under OGD in hMSCs and an increased LC3II/I ratio, n=4. Pictures were taken at 40X by an inverted fluorescent microscope. GAPDH was used as internal control for Figs. D-F. Error bars represent the mean±SD.

Fig. S3: OGD mediated activation of autophagy is mediated through O₂^{•-} and H₂O₂ in hMSCs.

Fig. (A) represents the effect of O₂^{•-} generation in the presence and absence of PEG-SOD on autophagy, n=5, and Fig. (B) represents the effect of H₂O₂ generation in the presence

and absence of PEG-catalase on autophagy, n=4. Figs (C and D) represent activation of Ambra1 and Beclin1. In brief, the data represents OGD for 12h increases Ambra1 (C, n=4) and Beclin1 (D, n=4) levels. Fig (E) represents a significant increase in Ambra1 expression post-OGD, though applying Ambra1-siRNA reduced this effect (n=7). The same pattern was observed for Beclin1 (n=6) (F). GAPDH was used as internal control for Fig (A, C-F) and β -actin for Fig (B), respectively. The maroon arrow in Fig C shows the band which was quantified. Error bars represent the mean \pm SD.

Fig. S4: $O_2^{\bullet-}$ and H_2O_2 in Ambra1 and Beclin1 activation, and activated Ambra1 and Beclin1 enhance autophagy in hMSCs. Figs (A and B) represent the effect of $O_2^{\bullet-}$ and H_2O_2 on Ambra1 expression post-OGD. Notably, the supplementation of PEG-SOD (n=4) and PEG-catalase (n=4) mitigated the activation of Ambra1 significantly. Figs. (C and D) show a similar effect for Beclin1 as observed for the expression of Ambra1 with PEG-SOD (n=5) and PEG-catalase (n=4). Figs. (E and F) show the quantification of autophagy induction through Ambra1 and Beclin1. In brief, OGD treatment significantly increased the EGFP-LC3 puncta in hMSCs. However, silencing of Ambra1 (E, n=12, cells=at least 50/group) and Beclin1 (F, n=12, cells=at least 50/group) resulted in reduced puncta numbers. Pictures were taken at 40X by an inverted fluorescent microscope; scale bar: 20 μ M. GAPDH was used as an internal control for all experiments. Error bars represent the mean \pm SD.

Fig S5: $O_2^{\bullet-}$ and H_2O_2 trigger autophagy through P38 and Erk1/2 MAPKs in hDPSCs. Fig. (A) represents downregulation of the LC3II/I ratio by SB202190 during OGD, n=4. Fig. (B) represents the LC3II/I ratio by PD98059 during OGD, n=4. A similar pattern of Ambra1 inhibition was observed in the presence of SB202190 (C, n=4) and PD98059 (D, n=4) during OGD. Likewise, inhibition of Beclin1 expression by SB202190 (E, n=4) and PD98059 (F, n=4) during OGD had a similar effect. Interestingly, with the supplementation of both SB202190 and PD98059 in combination, the expression of Ambra1 was depleted significantly (G, n=4). Similarly, with the supplementation of both SB202190 and PD98059 in combination, the expression of LC3II band and Beclin1 depleted significantly (H, n=4). β -actin was used as an internal control for figs. (A-C, E) and GAPDH was used for figs. (D, F-H). The maroon arrow in Figs. C, D, E, F, and G shows the band which was quantified. Error bars represent the mean \pm SD.

1
2
3
4
5
6
7
8
9
10
11
12
13
14
15
16
17
18
19
20
21
22
23
24
25
26
27
28
29
30
31
32
33
34
35
36
37
38
39
40
41
42
43
44
45
46
47
48
49
50
51
52
53
54
55
56
57
58
59
60

Fig. S6: p-cJNK MAPK is not activated in hDPSCs during OGD. This figure represents that the expression of p-cJNK did not alter after 12h OGD, n=4. GAPDH was used as an internal control. Error bars represent the mean±SD.

Fig. S7: ROS activates autophagy in hDPSCs. Increased autophagy, as indicated by increased numbers of EGFP-LC3 puncta after OGD in hDPSCs were observed, which was reduced to a significant level by NAC, indicating the participation of cumulative ROS in autophagy induction (n=12, cells=at least 50/group); scale bar: 20μM. Error bars represent the mean±SD.

Fig. S8: ROS-mediated decrease in hMSCs viability. Fig (A) depicts OGD and rapamycin both reduce hMSC viability, but 3-MA partially rescues hMSCs during OGD (n=6). Fig. (B and C) depict the roles of O₂^{•-} and H₂O₂ in cell viability. The results showed that either PEG-SOD (B, n=6) or PEG-catalase (C, n=6) alone failed to improve survival. Fig. (D) represents the effect of O₂^{•-} and H₂O₂ together on cell viability, n=6. Fig. (E) represents that NAC efficiently enhanced the viability, n=6. Error bars represent the mean±SD.

Appendix-I: hDPSCs characterization sheet

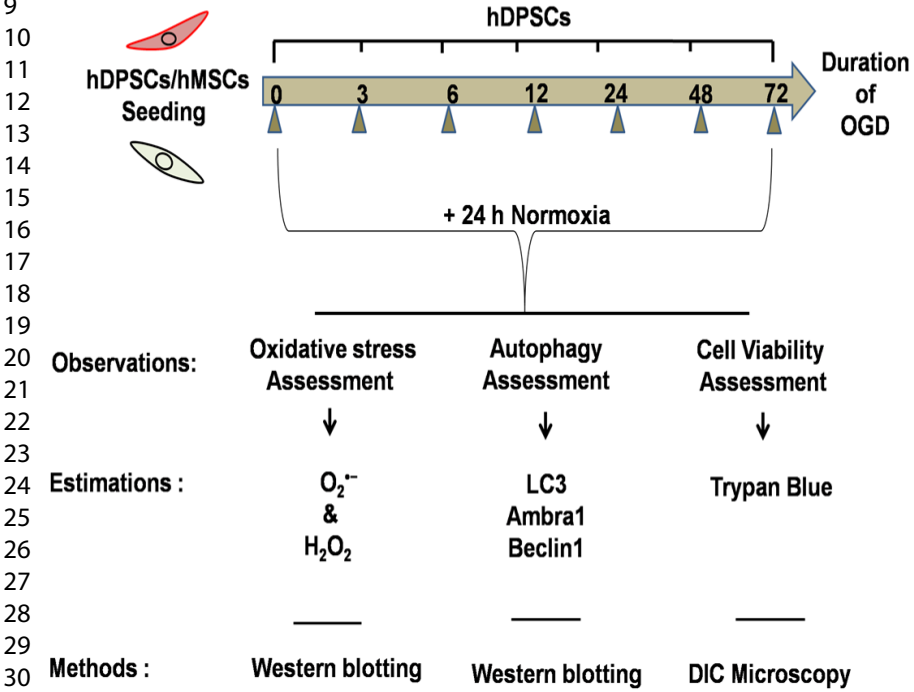
Appendix-II: hMSCs characterization sheet

References

1. Chen Y, Azad MB, Gibson SB et al. Superoxide is the major reactive oxygen species regulating autophagy. Cell Death and Differ 2009;16(7):1040-52.
2. MacKenzie EL, Ray PD, Tsuji Y et al. Role and regulation of ferritin H, in rotenone mediated mitochondrial oxidative stress. Free Radic Biol Med 2008;44(9):1762–71.
3. Byun YJ, Lee SB, Kim DJ et al. Protective effects of vacuolar H⁺-ATPase c on hydrogen peroxide-induced cell death in C6 glioma cells. Neurosci Lett 2007;425(3):183-7.

Fig. S1

A



B

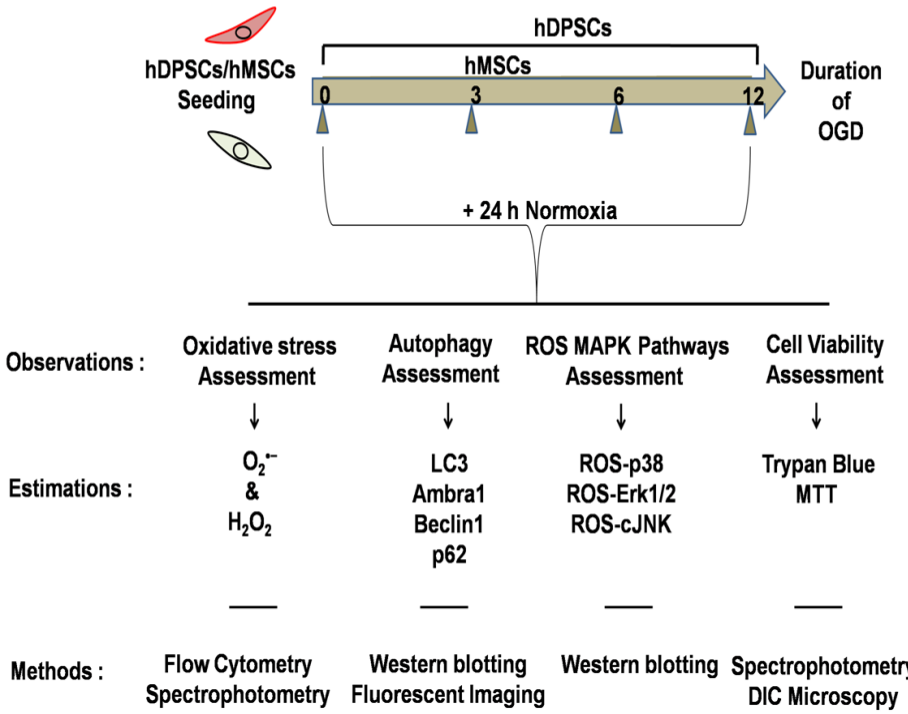
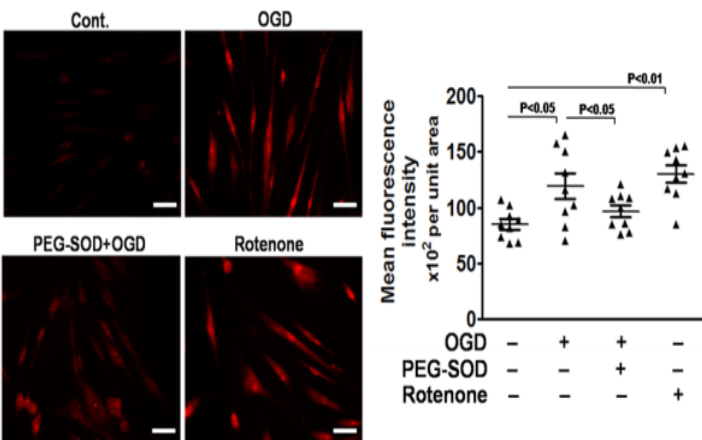
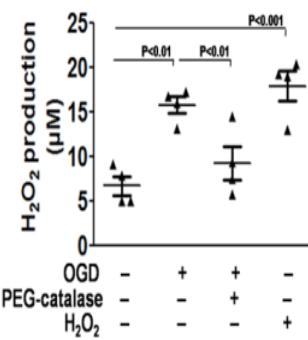


Fig. S2

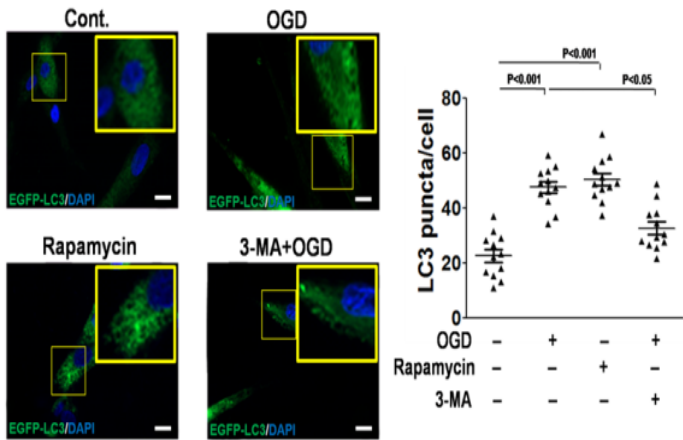
1
2 **A**
3
4
5
6
7
8
9
10
11
12
13
14
15
16
17



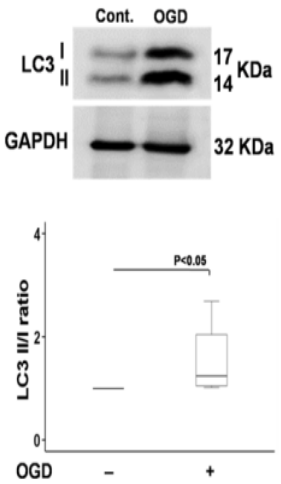
B



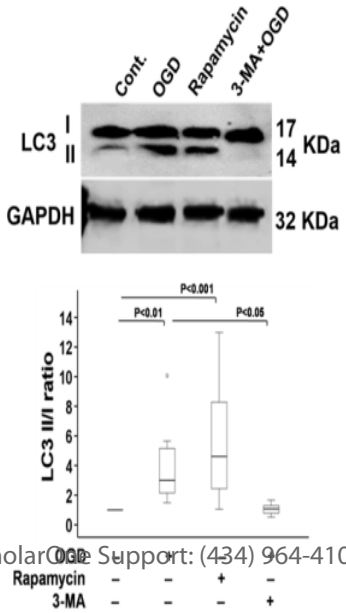
C



18
19
20 **D**
21
22
23
24
25
26
27
28
29
30
31
32
33
34
35
36
37
38
39
40
41



E



F

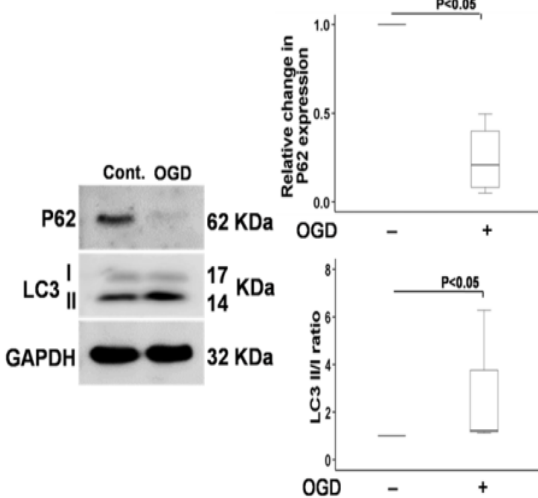
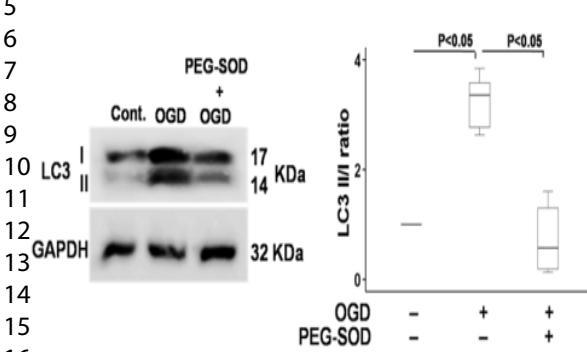
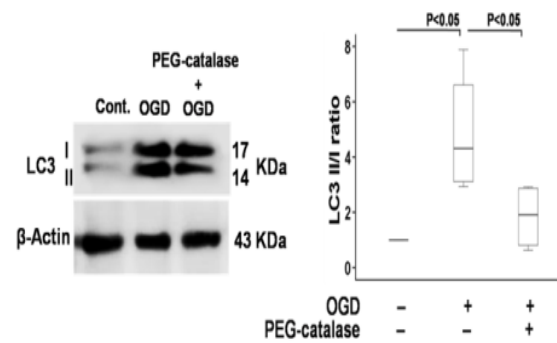
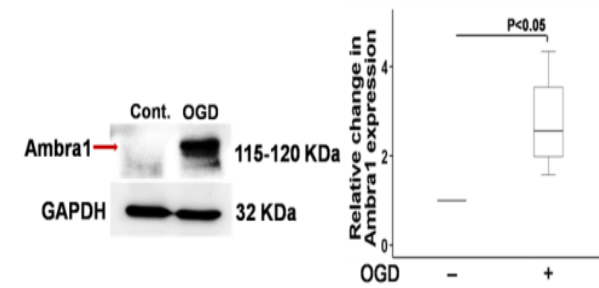
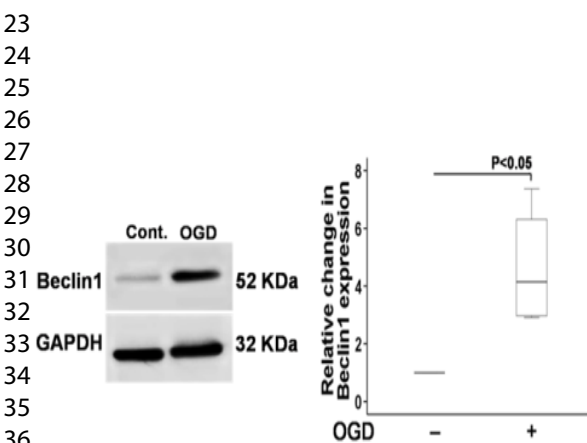
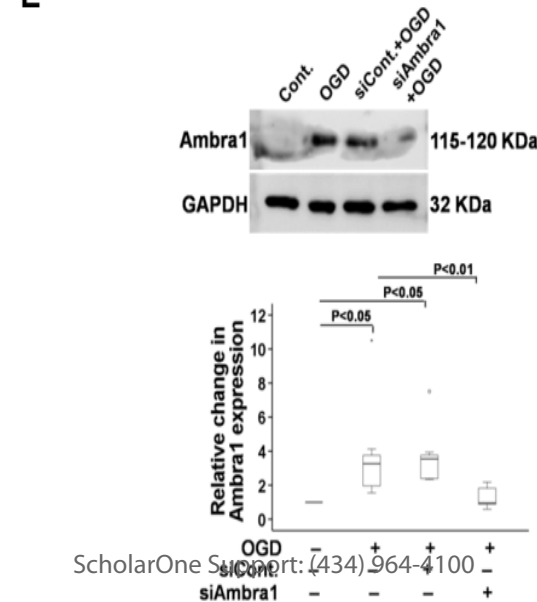
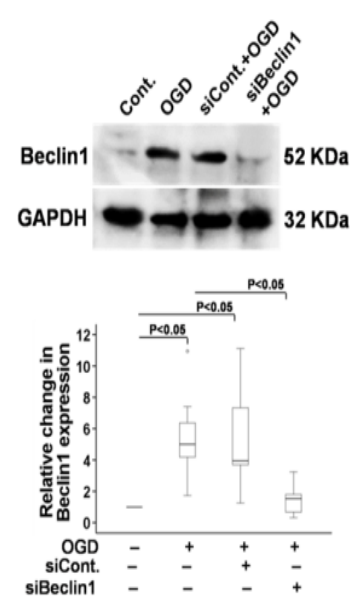
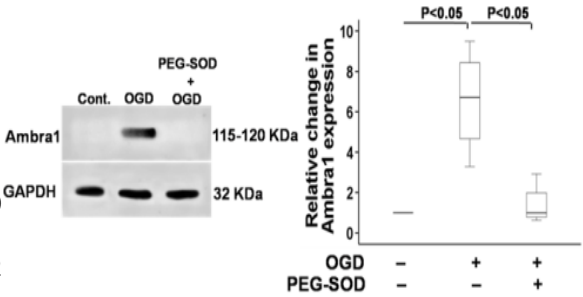


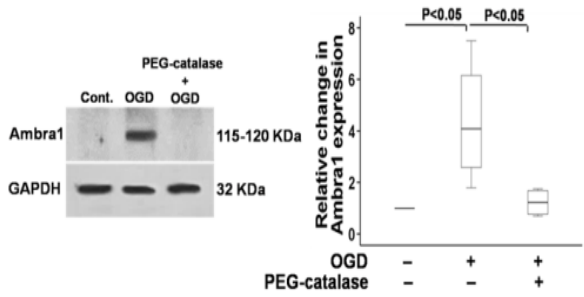
Fig. S3**A****B****C****D****E****F**

1
2
3
4
5
6
7
8
9
10
11
12
13
14
15
16
17
18
19
20
21
22
23
24
25
26
27
28
29
30
31
32
33
34
35
36
37
38
39
40
41

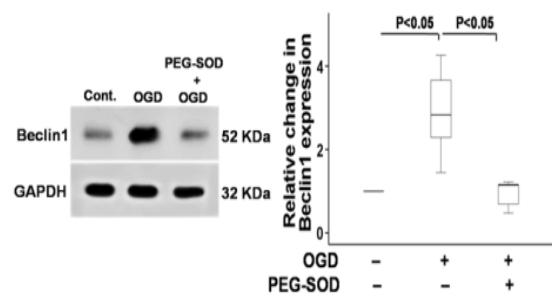
A



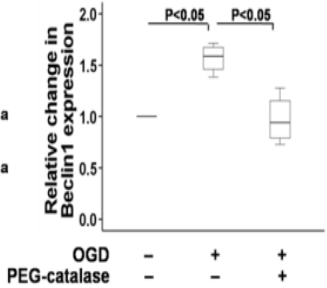
B



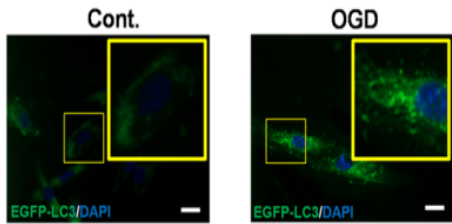
C



D



E



F

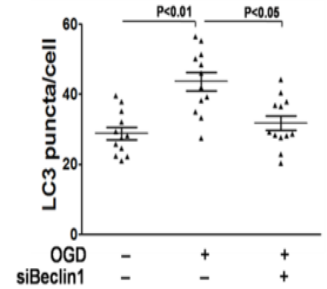
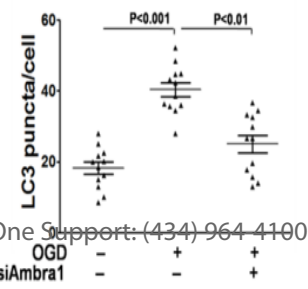
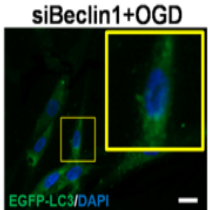
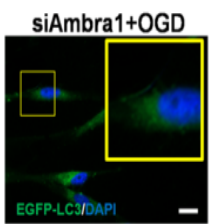
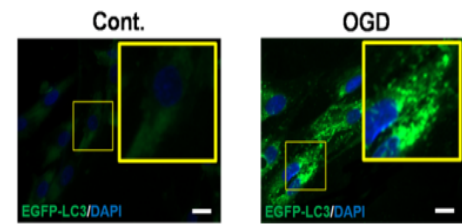
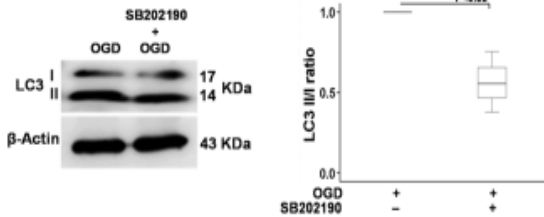
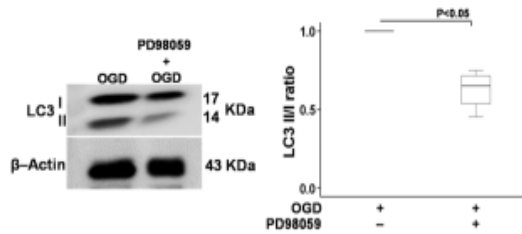


Fig. S5

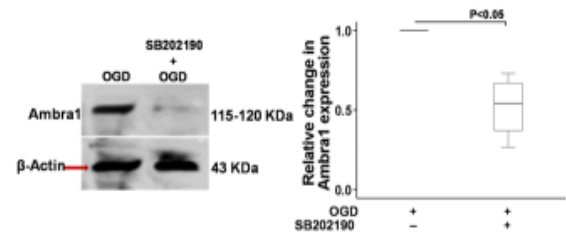
A



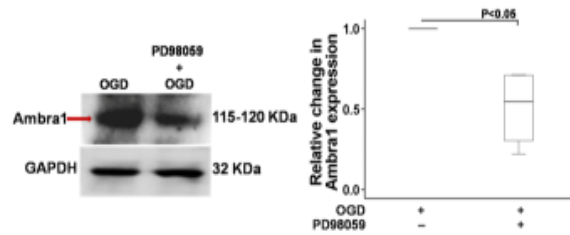
B



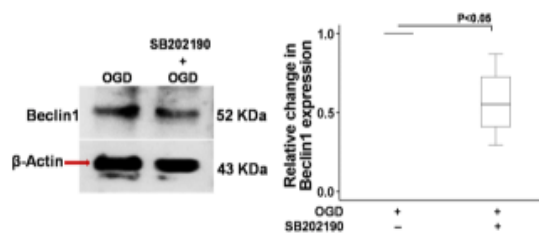
C



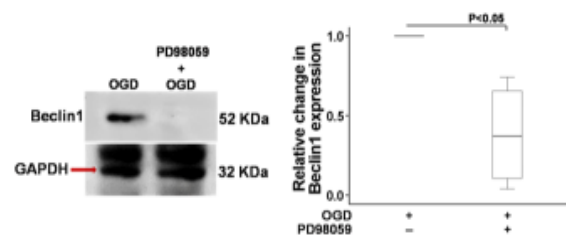
D



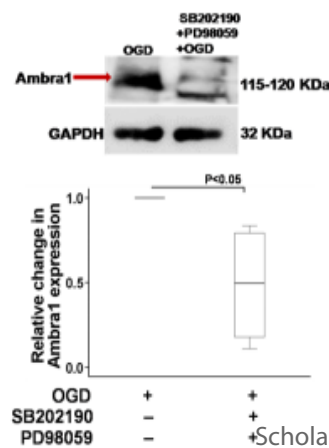
E



F



G



H

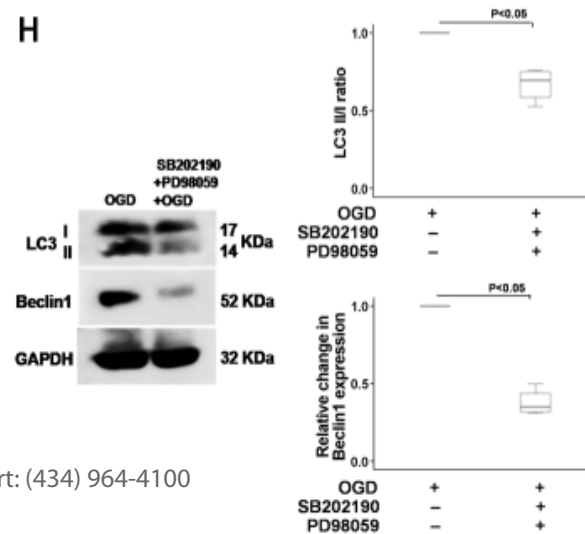


Fig. S6

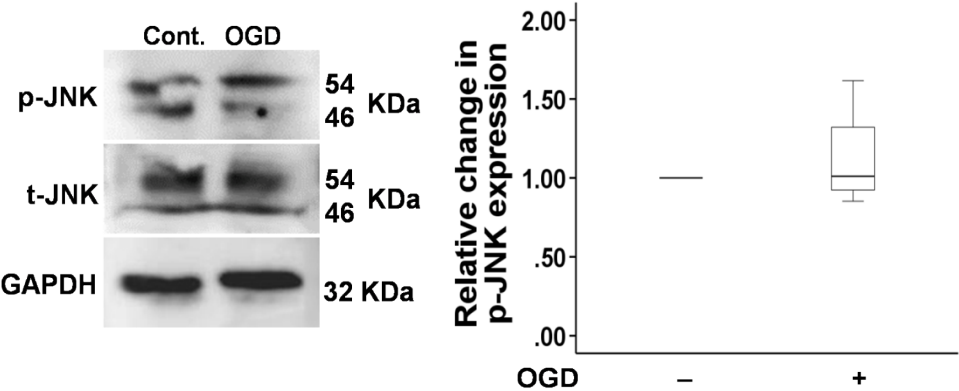
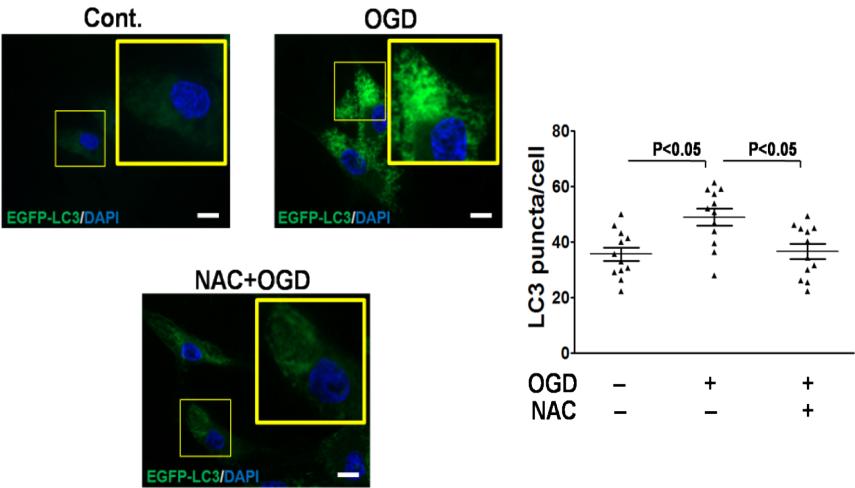
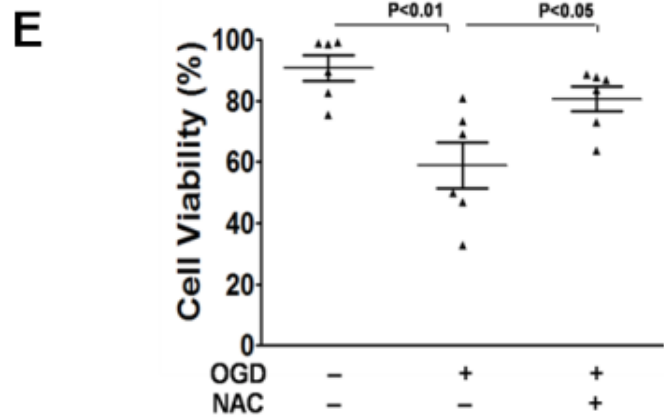
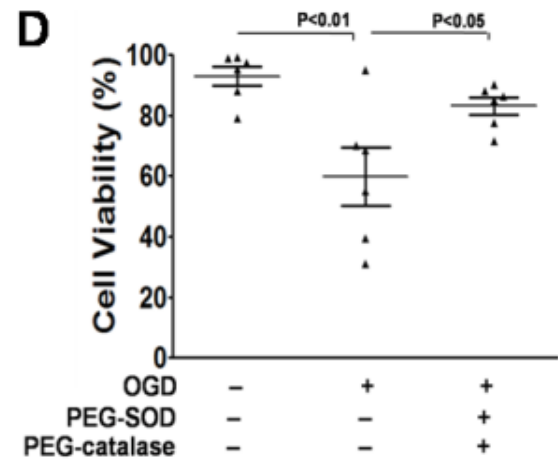
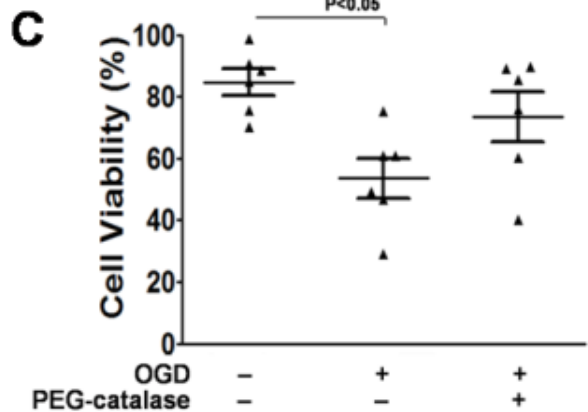
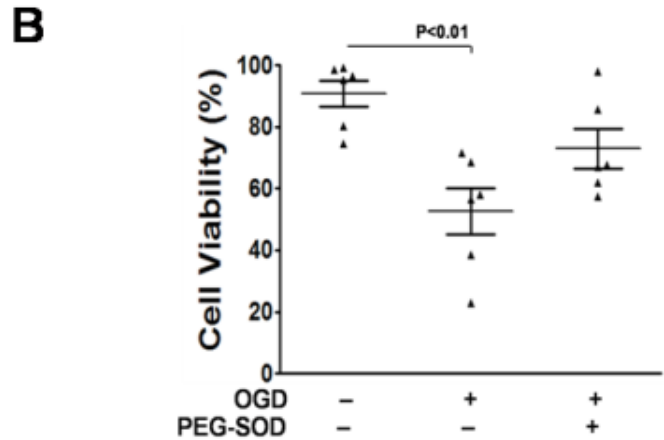
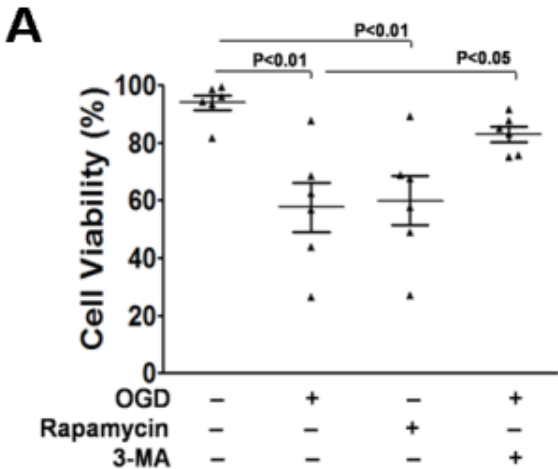


Fig. S7





Supplementary table 1. Chemicals List

S.No.	Chemical Name	Cat. No.	Company
SiRNAs			
1-	Ambra1	EHU067871	Sigma-Aldrich, Burlington, USA
2-	Beclin1	EHU061741	Sigma-Aldrich, Burlington, USA
3-	Scrambled siRNA	SIC005	Sigma-Aldrich, Burlington, USA
qRT-PCR reagents			
4-	Ambra1	Hs00387943	Applied Biosystems, Foster city, USA
5-	TaqMan gene expression assay kit	4331182	Applied Biosystems, Foster city, USA
6-	Beclin1	Hs00186838	Applied Biosystems, Foster city, USA
7-	GAPDH	Hs02758991	Applied Biosystems, Foster city, USA
8-	cDNA Revert Aid First Strand cDNA Synthesis Kit	K1622	Applied Biosystems, Foster city, USA
9-	TaqMan Universal Master Mix II with UNG	4440042	Applied Biosystems, Foster city, USA
Cell-culture reagents			
10-	Dulbecco's Modified Eagle Medium (DMEM)	AT006	Himedia, Mumbai, India
11-	Fetal Bovine Serum (FBS)	10438026	Gibco, Waltham, USA
12-	Penicillin	15240-062	Gibco, Waltham, USA
13-	Streptomycin	15240-062	Gibco, Waltham, USA
14-	DMEM without serum, glucose	AT186	Himedia, Mumbai, India
15-	Trypsin EDTA	25200072	Gibco, Waltham, USA
16-	Trypan Blue	6397D	LobaChemie, Mumbai, India
17-	DMSO	196055	MP Biomedicals, LLC, France
18-	Lipofectamine 3000	L3000008	Invitrogen, Waltham, USA
19-	Dihydroethidium (DHE)	D7008	Sigma-Aldrich, Burlington, USA

20-	Amplex Red	A22188	Invitrogen, Waltham, USA
21-	RIPA Buffer	R0278	Sigma-Aldrich, Burlington, USA
22-	Protease and Phosphatase Inhibitors	5871S	Cell Signaling Technology, Danvers, United States
23-	Pierce BCA Protein Assay Kit	23225	Thermo Fisher Scientific, Bangalore, India
Western blot reagents			
24-	PVDF Membrane	1620177	BioRad, Hercules, USA
25-	5% Non-Fat dry milk	1706404	BioRad, Hercules, USA
26-	Clarity™ Western ECL Substrate	1705061	BioRad, Hercules, USA
27-	Trizol	15596026	Thermo Fisher Scientific, Bangalore, India
Immunofluorescence reagents			
28-	4',6-diamidino-2-phenylindole (DAPI)	Ab104139	Abcam, Cambridge, UK
Plastic-wares			
29-	6-well cell culture plate	0030720113	eppendorf, North America, USA
30-	12- well cell culture plate	0030721110	eppendorf, North America, USA
31-	96- well cell culture plate	0030730119	eppendorf, North America, USA
32-	35 x 10 mm cell culture Dish	0030700112	eppendorf, North America, USA
33-	Slides	PIC-1	BLUE STAR, Mumbai, India

Supplementary table 2. Concentration, dilution and treatment duration of the activators and inhibitors used in this study

hDPSC Cells					
S. No.	Activators/ Inhibitors	Cat. No.	Company	Concentration	Treatment Duration
1.	Rapamycin	R0395	Sigma-Aldrich, Burlington, USA	10μM	1 h pre-OGD treatment
2.	3-Methyladenine (3-MA)	M9281	Sigma-Aldrich, Burlington, USA	10mM	1 h pre-OGD treatment
3.	Bafilomycin A1 (Baf.A1)	B1793	Sigma-Aldrich, Burlington, USA	75nM	12 h during OGD treatment
4.	Rotenone	R8875	Sigma-Aldrich, Burlington, USA	10μM	1h pre-OGD treatment
5.	H ₂ O ₂	194057	MP Biomedicals, LLC, France	500μM	4 h pre-OGD treatment
6.	N-acetyl-L-cysteine(NAC)	A7250	Sigma-Aldrich, Burlington, USA	10mM	45 min pre-OGD treatment
7.	PEG-SOD	S9549	Sigma-Aldrich, Burlington, USA	500U/ml	24 h pre-OGD treatment
8.	PEG-Catalase	C4963	Sigma-Aldrich, Burlington, USA	100U/ml	24 h pre-OGD treatment
9.	PD98059	P215	Sigma-Aldrich, Burlington, USA	20μM	30 min. pre-OGD treatment
10.	SB202190	S7067	Sigma-Aldrich, Burlington, USA	10μM	1 h pre-OGD treatment
hMSC Cells					
1.	Rapamycin	R0395	Sigma-Aldrich,	100nM	12 h pre and 12 h during OGD treatment

			Burlington, USA		
2.	3-Methyladenine (3 MA)	M9281	Sigma- Aldrich, Burlington, USA	10mM	1h pre-OGD treatment
3.	Rotenone	R8875	Sigma- Aldrich, Burlington, USA	2µM	2 h pre-OGD treatment
4.	H ₂ O ₂	194057	MP Biomedicals LLC, France	500µM	4 h pre-OGD treatment
5.	N-acetyl-L-cysteine (NAC)	A7250	Sigma- Aldrich, Burlington, USA	10mM	30 min pre-OGD treatment
6.	PEG-SOD	S9549	Sigma- Aldrich, Burlington, USA	500U/ml	24 h pre-OGD treatment
7.	PEG-Catalase	C4963	Sigma- Aldrich, Burlington, USA	100U/ml	24 h pre-OGD treatment

Supplementary table 3. Antibodies and their dilution in western blotting

S. No.	Antibody	Western Dilution	Sources	Cat. No.	Company
Primary Antibodies					
1.	Beclin-1	1:2000	Mouse	66665-1-Ig	Proteintech, Rosemont, USA
2.	Ambra-1	1:1000	Rabbit	13762-1-AP	Proteintech, Rosemont, USA
3.	LC3A/B	1:1000	Rabbit	4108S	Cell Signaling Technology, Danvers, USA
4.	Phospho-ERK1/2	1:2000	Rabbit	ITP01015	ImmunoTag, St. Louis, USA
5.	Total -ERK1/2	1:2000	Rabbit	ITT00155	ImmunoTag, St. Louis, USA
6.	Phospho-P38	1:2000	Rabbit	ITP0338	ImmunoTag, St. Louis, USA
7.	Total P38	1:2000	Rabbit	ITT3514	ImmunoTag, St. Louis, USA
8.	Phospho JNK	1:1000	Rabbit	AF1205	R&D Systems, Minneapolis, USA
9.	Total JNK	1:1000	Rabbit	AF1387	R&D Systems, Minneapolis, USA
10.	Beta Actin	1:3000	Rabbit	ITT07018	ImmunoTag, St. Louis, USA
11.	GAPDH	1:3000	Rabbit	ITT5052	ImmunoTag, St. Louis, USA
Secondary Antibodies					

1
2
3
4
5
6
7
8
9
10
11
12
13
14
15
16
17
18
19
20
21
22
23
24
25
26
27
28
29
30
31
32
33
34
35
36
37
38
39
40
41
42
43
44
45
46
47
48
49
50
51
52
53
54
55
56
57
58
59
60

1.	Anti-Rabbit IgG	1:10000	Donkey	711-035-152	Jackson Immuno Research Laboratories, West Baltimore USA
2.	Anti-mouse IgG	1:10000	Horse	7076S	Cell Signaling Technology, Danvers, USA

Supplementary table 4. Antibodies and their dilution in immunocytochemistry

S. No.	Antibody	ICC Dilution	Sources	Cat. No.	Company
Primary Antibody					
1.	Beclin-1	1:500	Mouse	66665-1-Ig	Proteintech, Rosemont, USA
2.	Ambra-1	1:100	Rabbit	13762-1-AP	Proteintech, Rosemont, USA
Secondary Antibody					
S. No.	Primary Antibody	ICC Dilution	Sources	Cat. No.	Company
1.	Alexa Flour 488 Anti-rabbit	1:1000	Goat	111-545-003/125266	Jackson Immuno Research Laboratories, West Baltimore USA
2.	Alexa Flour 488 Anti-mouse	1:1000	Goat	111-545-003/126409	Jackson Immuno Research Laboratories, West Baltimore USA
3.	Alexa Flour 555 IgG Anti-Rabbit	1:1000	Goat	4413S	Cell Signaling Technology, Danvers, USA
4.	Alexa Flour 555 IgG Anti-Mouse	1:1000	Goat	4409S	Cell Signaling Technology, Danvers, USA

1
2
3
4
5
6
7
8
9
10
11
12
13
14
15
16
17
18
19
20
21
22
23
24
25
26
27
28
29
30
31
32
33
34
35
36
37
38
39
40
41
42
43
44
45
46
47
48
49
50
51
52
53
54
55
56
57
58
59
60

Supplementary table 5. TaqMan reagents and their composition used in this study

Component	Volume per reaction	Final concentration
TaqMan® Fast Advanced Master Mix (2X)	10.0 µL	1X
TaqMan® Assay (20X)	1.0 µL	1X
Nuclease-Free Water[2]	7.0 µL	-
cDNA	2 µL	-
Total volume per reaction	20 µL	-



HiMedia Laboratories Pvt. Ltd.

CERTIFICATE OF ANALYSIS

CL008-0.5

HiFi™ Human Dental Pulp Stem Cells (HDP-SC) Isolated from human dental pulp
0.5million cells/vial

Lot Number : **0000408610**
QC Test Date : 02.11.2019
Expiry Date : NA
Store at : Liquid nitrogen
Vapour Phase

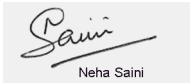
TEST	SPECIFICATIONS	RESULTS
Donor age (years)	1Year - 45Year	3Year
Donor sex	Male / Female	Male
Origin	Indian	Complies
Passage number	2	Complies
Number of viable cells per vial	NLT 500000	510000
Percentage viability	NLT 80%	100%
Morphology	Spindle shaped fibroblast-like adherent cells	Complies
No. of population doublings	NLT 15	20
CD90 (Flow Cytometry)	NLT 95%	98%
CD105 (Flow Cytometry)	NLT 95%	99.9%
CD146 (Flow Cytometry)	NLT 95%	98.3%
CD166(Flow Cytometry)	NLT 95%	98%
CD13 (Flow Cytometry)	NLT 95%	97.2%
CD34 (Flow Cytometry)	NMT 5%	0.3%
CD45 (Flow Cytometry)	NMT 5%	1%
Adipogenic differentiation	Positive	Complies
Osteogenic differentiation	Positive	Complies
Chondrogenic differentiation	Positive	Complies
Mycoplasma (PCR)	Not detected	Complies
Bacteria, Fungi, Anaerobes as per USP	Not detected	Complies
HIV (PCR)	Not detected	Complies
Hepatitis B virus (PCR)	Not detected	Complies

1
2
3
4
5
6
7
8
9
10
11
12
13
14
15
16
17
18
19
20
21
22
23
24
25
26
27
28
29
30
31
32
33
34
35
36
37
38
39
40
41
42
43
44
45
46
47
48
49
50
51
52
53
54
55
56
57
58
59
60

TEST	SPECIFICATIONS	RESULTS
Hepatitis C virus (PCR)	Not detected	Complies

Status of the material : **APPROVED**

For Peer Review



Neha Saini

Department, Quality Control
Animal Cell Culture



Reena Pius

Department, Quality Assurance
Animal Cell Culture

This is to certify that this lot passes and conforms to the above mentioned tests and specifications. User must ensure suitability of the product in their application prior to use.



HiMedia Laboratories Pvt. Ltd.

CERTIFICATE OF ANALYSIS

CL001-0.5

HiFi™ Human Wharton's Jelly Mesenchymal Stem Cells (HWJ-MSC)

Isolated from Wharton's Jelly of human umbilical cords

Lot Number : **0000164990**

QC Test Date : 30.03.2013

Expiry Date : NA

Store at : -196° C

TEST	SPECIFICATIONS	RESULTS
Donor age (years)	New Born	Complies
Donor sex	Male / Female	Male
Origin	Indian	Complies
Passage number	2	Complies
Number of viable cells per vial	NLT 500000	750000
Percentage viability	NLT 80%	96.77%
No. of population doublings	NLT 15	17
CD90 (Flow Cytometry)	NLT 95%	99.9%
CD105 (Flow Cytometry)	NLT 95%	99.9%
CD34 (Flow Cytometry)	NMT 5%	0.00%
CD45 (Flow Cytometry)	NMT 5%	0.07%
Adipogenic differentiation	Positive	Complies
Osteogenic differentiation	Positive	Complies
Chondrogenic differentiation	Positive	Complies
Mycoplasma (PCR)	Not detected	Complies
Bacteria, Fungi, Anaerobes as per USP	Not detected	Complies
HIV (PCR)	Not detected	Complies
Hepatitis B virus (PCR)	Not detected	Complies

1
2
3
4
5
6
7
8
9
10
11
12
13
14
15
16
17
18
19
20
21
22
23
24
25
26
27
28
29
30
31
32
33
34
35
36
37
38
39
40
41
42
43
44
45
46
47
48
49
50
51
52
53
54
55
56
57
58
59
60

TEST	SPECIFICATIONS	RESULTS
Hepatitis C virus (PCR)	Not detected	Complies

Status of the material : **APPROVED**

For Peer Review



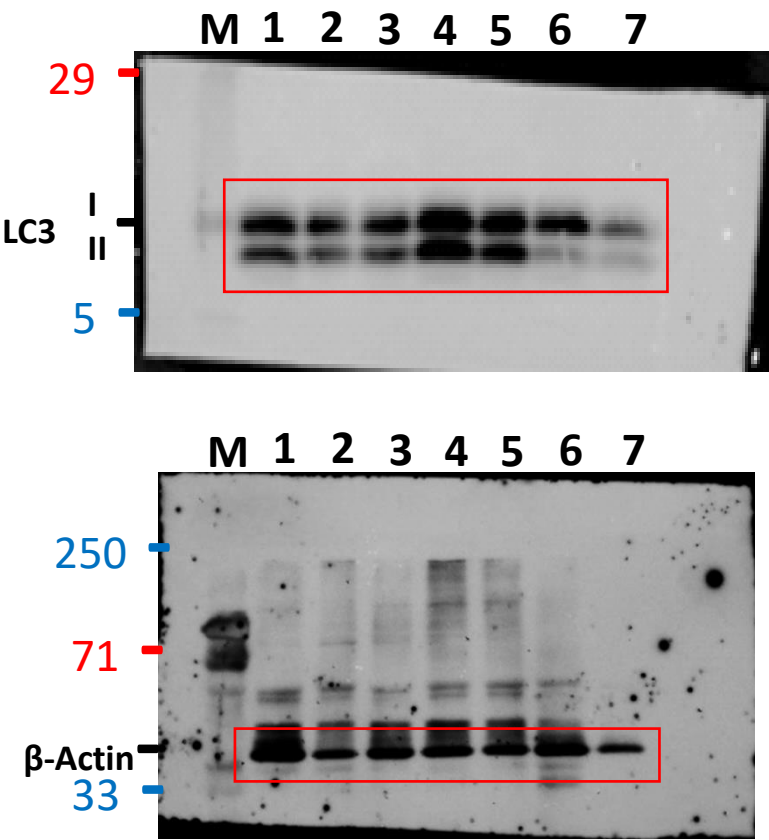
Department, Quality Control
Animal Cell Culture



Department, Quality Assurance
Animal Cell Culture

This is to certify that this lot passes and conforms to the above mentioned tests and specifications. User must ensure suitability of the product in their application prior to use.

This document has been produced electronically



1
2
3
4
5
6
7
8
9
10
11
12
13
14
15
16
17
18
19
20
21
22
23
24
25
26
27
28
29
30
31
32
33
34
35
36
37
38
39
40
41

M Marker
1 Control
2 3 hr OGD
3 6 hr OGD
4 12 hr OGD
5 24 hr OGD
6 48 hr OGD
7 72 hr OGD

FIG. 1D

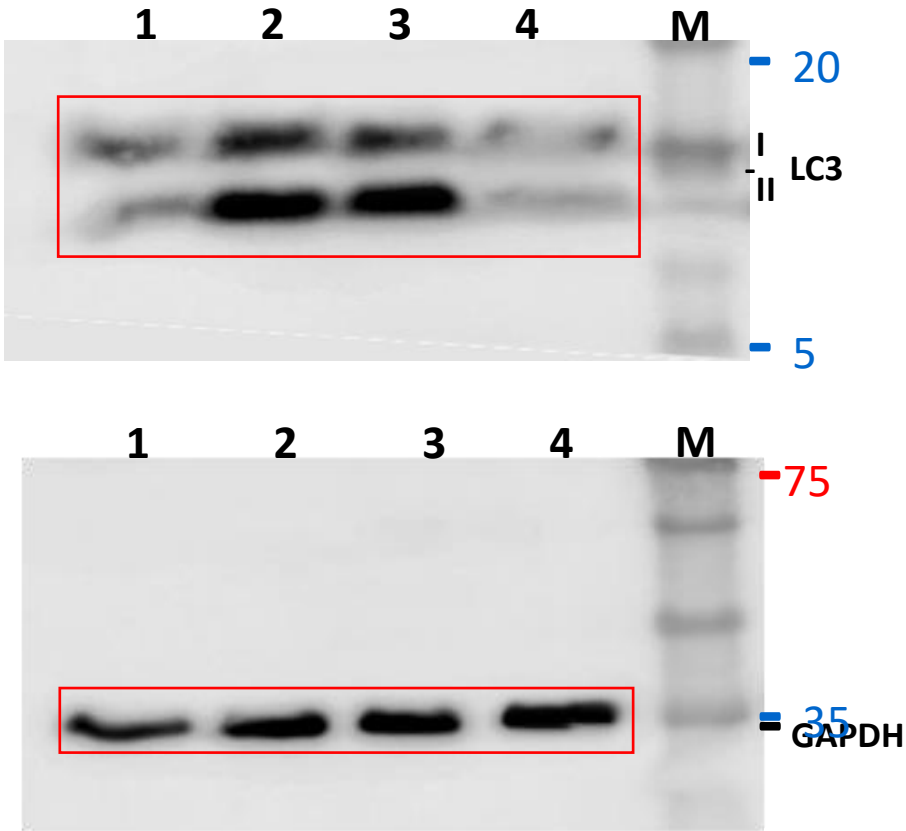
Stem Cells

Pairwise Comparisons of Treatment					
Sample 1-Sample 2	Test Statistic	Std. Error	Std. Test Statistic	Sig.	Adj. Sig. ^a
Control-48	-3.667	8.629	-0.425	0.671	1.000
Control-72	-5.444	8.629	-0.631	0.528	1.000
Control-3h	-13.111	8.629	-1.520	0.129	1.000
Control-6h	-13.222	8.629	-1.532	0.125	1.000
Control-24h	-15.111	8.629	-1.751	0.080	1.000
Control-12h	-26.444	8.629	-3.065	0.002	0.046
48-72	-1.778	8.629	-0.206	0.837	1.000
48-3h	9.444	8.629	1.095	0.274	1.000
48-6h	9.556	8.629	1.107	0.268	1.000
48-24h	11.444	8.629	1.326	0.185	1.000
48-12h	22.778	8.629	2.640	0.008	0.174
72-3h	7.667	8.629	0.889	0.374	1.000
72-6h	7.778	8.629	0.901	0.367	1.000
72-24h	9.667	8.629	1.120	0.263	1.000
72-12h	21.000	8.629	2.434	0.015	0.314
3h-6h	-0.111	8.629	-0.013	0.990	1.000
3h-24h	-2.000	8.629	-0.232	0.817	1.000
3h-12h	-13.333	8.629	-1.545	0.122	1.000
6h-24h	-1.889	8.629	-0.219	0.827	1.000
6h-12h	-13.222	8.629	-1.532	0.125	1.000
24h-12h	11.333	8.629	1.313	0.189	1.000

Each row tests the null hypothesis that the Sample 1 and Sample 2 distributions are the same.
Asymptotic significances (2-sided tests) are displayed. The significance level is .050.

a. Significance values have been adjusted by the Bonferroni correction for multiple tests.

FIG. 1G



M Marker
1 Control
2 OGD
3 Rapamycin+OGD
4 3-MA+OGD

FIG. 1G

Pairwise
Comparisons
of Treatment

Sample 1-Sample 2	Test Statistic	Std. Error	Std. Test Statistic	Sig.	Adj. Sig. ^a
Control-3- MA+OGD	0.000	4.051	0.000	1.000	1.000
Control- Rapamycin	-10.833	4.051	-2.674	0.007	0.045
Control-OGD	-13.167	4.051	-3.250	0.001	0.007
3-MA+OGD- Rapamycin	10.833	4.051	2.674	0.007	0.045
3-MA+OGD-OGD	13.167	4.051	3.250	0.001	0.007
Rapamycin-OGD	2.333	4.051	0.576	0.565	1.000

Fig 1H

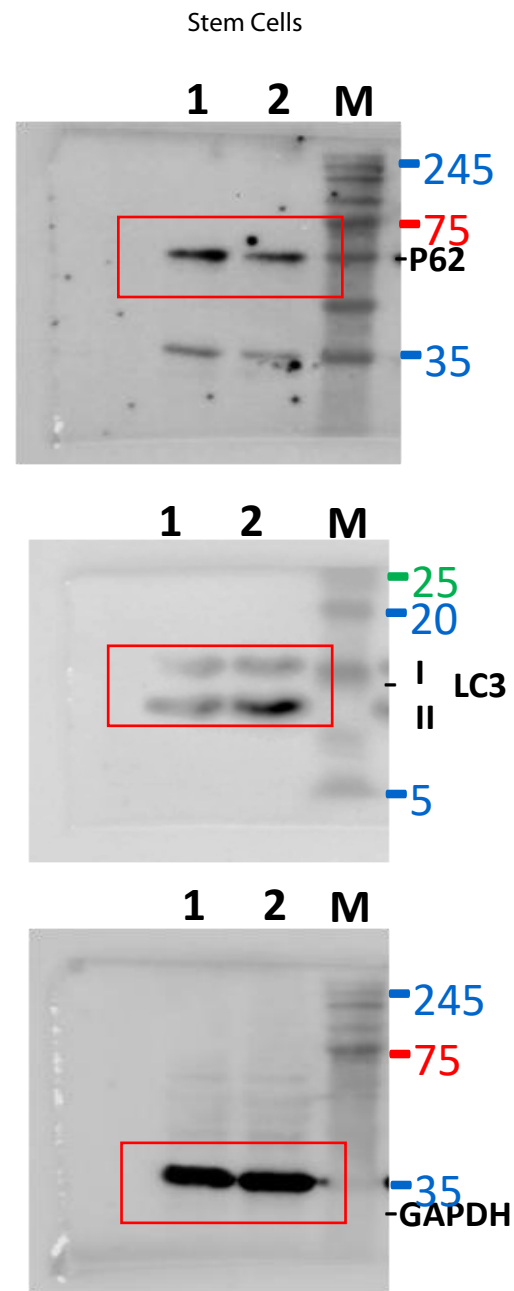


Fig 1H

P62

Hypothesis Test Summary				
	Null Hypothesis	Test	Sig. ^{a,b}	Decision
1	The distribution of Dependent is the same across categories of Treatment.	Independent-Samples Mann-Whitney U Test	.029 ^c	Reject the null hypothesis.

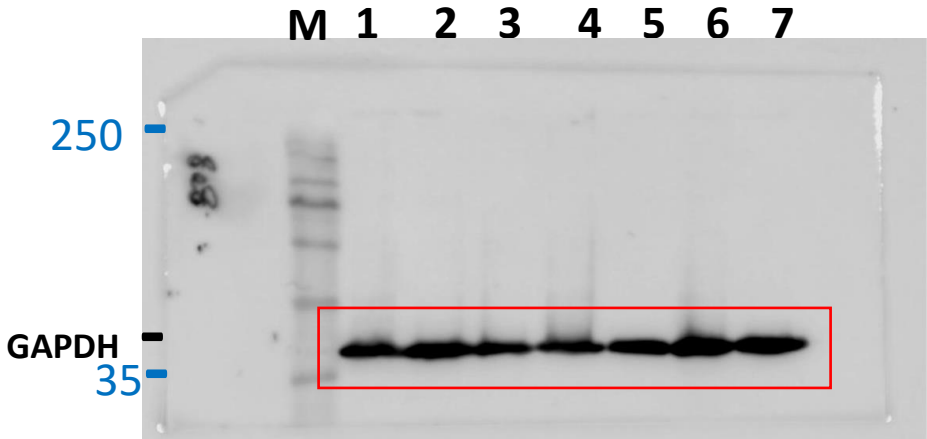
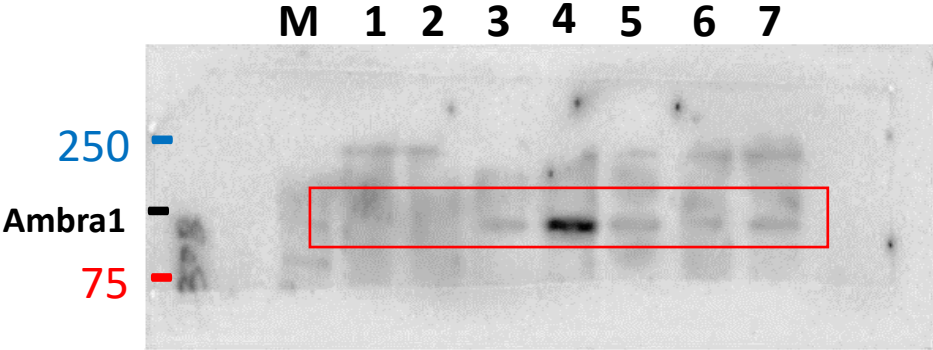
- a. The significance level is .050.
- b. Asymptotic significance is displayed.
- c. Exact significance is displayed for this test.

LC3 II/I

Hypothesis Test Summary				
	Null Hypothesis	Test	Sig. ^{a,b}	Decision
1	The distribution of Dependent is the same across categories of Treatment.	Independent-Samples Mann-Whitney U Test	.029 ^c	Reject the null hypothesis.

- a. The significance level is .050.
- b. Asymptotic significance is displayed.
- c. Exact significance is displayed for this test.

Fig 2C

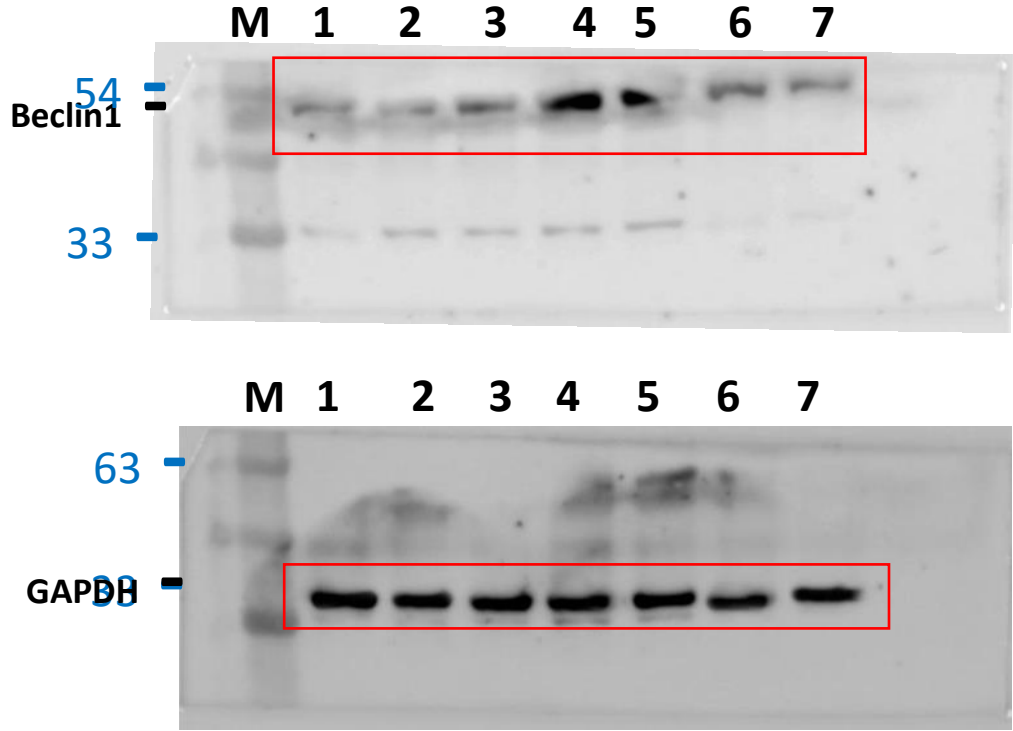


Pairwise Comparisons of Treatment					
Sample 1-Sample 2	Test Statistic	Std. Error	Std. Test Statistic	Sig.	Adj. Sig. ^a
Control-24H	-4.900	9.088	-0.539	0.590	1.000
Control-6H	-6.600	9.088	-0.726	0.468	1.000
Control-72H	-12.700	9.088	-1.397	0.162	1.000
Control-3H	-13.700	9.088	-1.507	0.132	1.000
Control-48	-16.400	9.088	-1.805	0.071	1.000
Control-12H	-29.700	9.088	-3.268	0.001	0.023
24H-6H	1.700	9.088	0.187	0.852	1.000
24H-72H	-7.800	9.088	-0.858	0.391	1.000
24H-3H	8.800	9.088	0.968	0.333	1.000
24H-48	-11.500	9.088	-1.265	0.206	1.000
24H-12H	24.800	9.088	2.729	0.006	0.133
6H-72H	-6.100	9.088	-0.671	0.502	1.000
6H-3H	7.100	9.088	0.781	0.435	1.000
6H-48	-9.800	9.088	-1.078	0.281	1.000
6H-12H	-23.100	9.088	-2.542	0.011	0.232
72H-3H	1.000	9.088	0.110	0.912	1.000
72H-48	3.700	9.088	0.407	0.684	1.000
72H-12H	17.000	9.088	1.871	0.061	1.000
3H-48	-2.700	9.088	-0.297	0.766	1.000
3H-12H	-16.000	9.088	-1.761	0.078	1.000
48-12H	13.300	9.088	1.463	0.143	1.000

Each row tests the null hypothesis that the Sample 1 and Sample 2 distributions are the same. Asymptotic significances (2-sided tests) are displayed. The significance level is .050.

a. Significance values have been adjusted by the Bonferroni correction for multiple tests.

Fig 2D



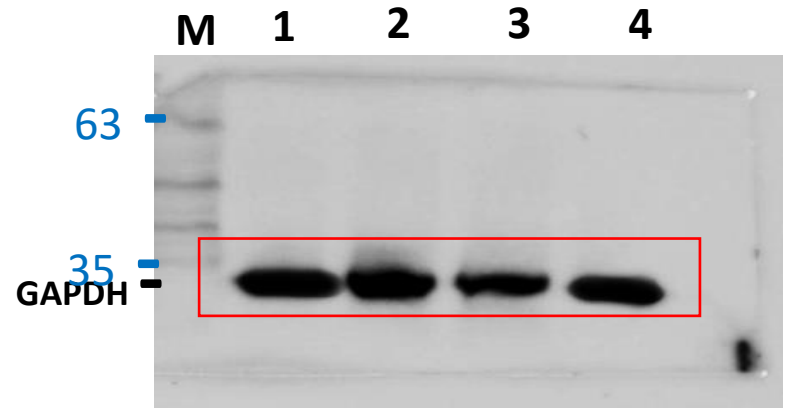
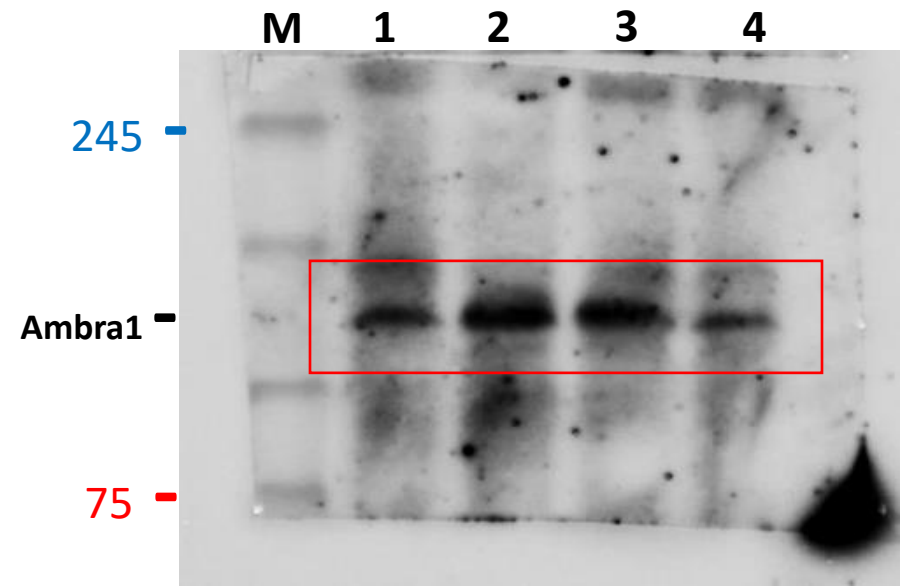
M Marker
1 Control
2 3 hr OGD
3 6 hr OGD
4 12 hr OGD
5 24 hr OGD
6 48 hr OGD
7 72 hr OGD

Pairwise Comparisons of Treatment						
Sample 1-Sample 2	Test Statistic	Std. Error	Std. Test Statistic	Sig.	Adj. Sig. ^a	
Control-24h	-3.222	8.629	-0.373	0.709	1.000	
Control-72h	-7.333	8.629	-0.850	0.395	1.000	
Control-48h	-15.889	8.629	-1.841	0.066	1.000	
Control-6h	-16.333	8.629	-1.893	0.058	1.000	
Control-3h	-19.000	8.629	-2.202	0.028	0.581	
Control-12h	-29.222	8.629	-3.387	0.001	0.015	
24h-72h	-4.111	8.629	-0.476	0.634	1.000	
24h-48h	-12.667	8.629	-1.468	0.142	1.000	
24h-6h	13.111	8.629	1.520	0.129	1.000	
24h-3h	15.778	8.629	1.829	0.067	1.000	
24h-12h	26.000	8.629	3.013	0.003	0.054	
72h-48h	8.556	8.629	0.992	0.321	1.000	
72h-6h	9.000	8.629	1.043	0.297	1.000	
72h-3h	11.667	8.629	1.352	0.176	1.000	
72h-12h	21.889	8.629	2.537	0.011	0.235	
48h-6h	0.444	8.629	0.052	0.959	1.000	
48h-3h	3.111	8.629	0.361	0.718	1.000	
48h-12h	13.333	8.629	1.545	0.122	1.000	
6h-3h	2.667	8.629	0.309	0.757	1.000	
6h-12h	-12.889	8.629	-1.494	0.135	1.000	
3h-12h	-10.222	8.629	-1.185	0.236	1.000	

Each row tests the null hypothesis that the Sample 1 and Sample 2 distributions are the same.
Asymptotic significances (2-sided tests) are displayed. The significance level is .050.

a. Significance values have been adjusted by the Bonferroni correction for multiple tests.

FIG 2G



M Marker
1 Control
2 OGD
3 siCont.+OGD
4 siAmbra1+OGD

FIG 2G

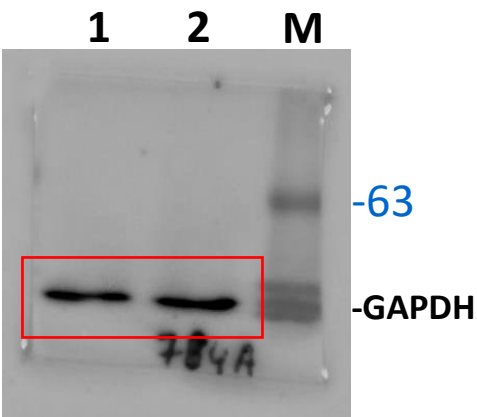
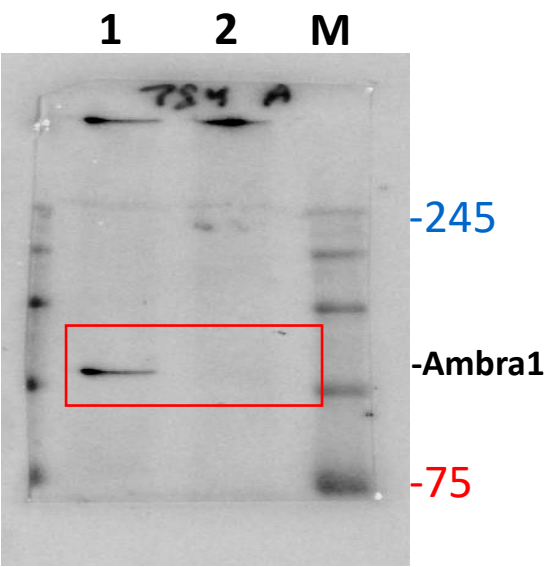
Pairwise Comparisons of Treatment

Sample 1- Sample 2	Test Statistic	Std. Error	Std. Test Statistic	Sig.	Adj. Sig. ^a
Control- siAmbra1+OG D	-2.750	4.654	-0.591	0.555	1.000
Control- SiCont.+OGD	-13.625	4.654	-2.927	0.003	0.021
Control-OGD	-15.625	4.654	-3.357	0.001	0.005
siAmbra1+OG D- SiCont.+OGD	10.875	4.654	2.337	0.019	0.117
siAmbra1+OG D-OGD	12.875	4.654	2.766	0.006	0.034
SiCont.+OGD- OGD	2.000	4.654	0.430	0.667	1.000

Each row tests the null hypothesis that the Sample 1 and Sample 2 distributions are the same. Asymptotic significances (2-sided tests) are displayed. The significance level is .050.

a. Significance values have been adjusted by the Bonferroni correction for multiple tests.

FIG 2G



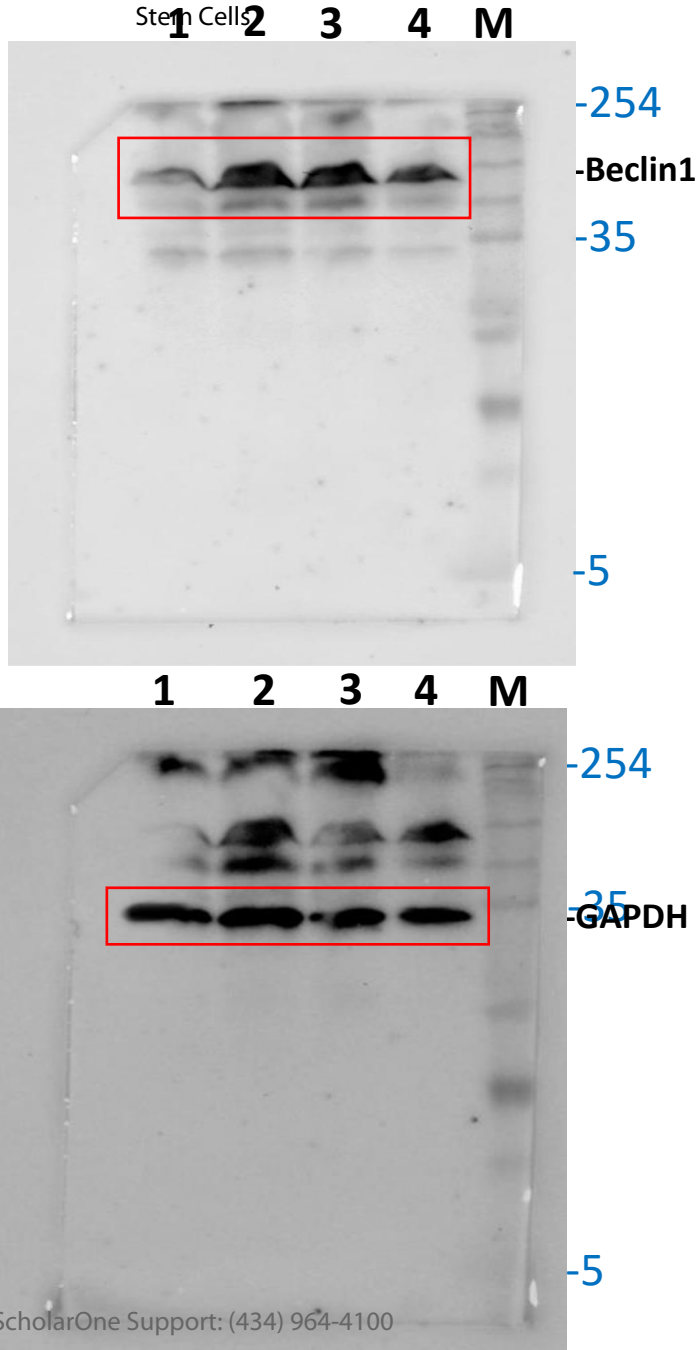
M Marker
1 SiAmbra1
2 Si Ambra+OGD

FIG 2G

Hypothesis Test Summary				
	Null Hypothesis	Test	Sig. ^{a,b}	Decision
1	The distribution of Dependent is the same across categories of Treatment.	Independent-Samples Mann-Whitney U Test	.029 ^c	Reject the null hypothesis.

- a. The significance level is .050.
- b. Asymptotic significance is displayed.
- c. Exact significance is displayed for this test.

FIG 2H



M Marker

1 Control

2 OGD

3 siCont.+OGD

4 siBeclin1+OGD

FIG 2H

Pairwise Comparisons of Treatment

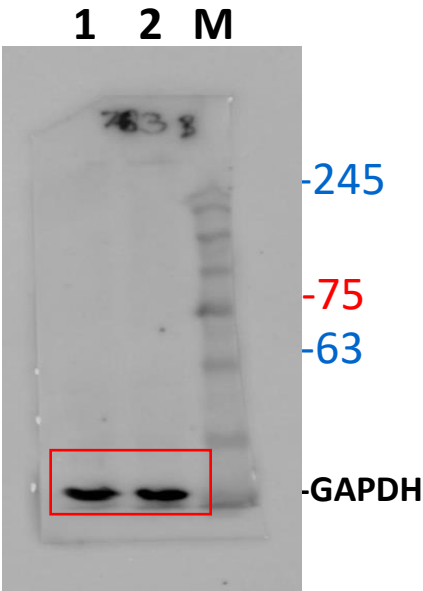
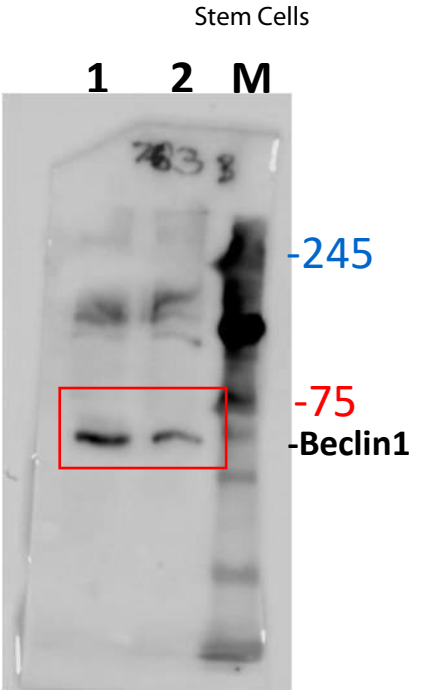
Sample 1- Sample 2	Test Statistic	Std. Error	Std. Test Statistic	Sig.	Adj. Sig. ^a
Control- siBeclin1+OG D	-3.000	4.363	-0.688	0.492	1.000
Control- SiCont.+OGD	-15.286	4.363	-3.503	0.000	0.003
Control-OGD	-15.714	4.363	-3.602	0.000	0.002
siBeclin1+OG D- SiCont.+OGD	12.286	4.363	2.816	0.005	0.029
siBeclin1+OG D-OGD	12.714	4.363	2.914	0.004	0.021
SiCont.+OGD- OGD	0.429	4.363	0.098	0.922	1.000

Each row tests the null hypothesis that the Sample 1 and Sample 2 distributions are the same.

Asymptotic significances (2-sided tests) are displayed. The significance level is .050.

a. Significance values have been adjusted by the Bonferroni correction for multiple tests.

FIG 2H



ScholarOne Support: (434) 964-4100

M Marker
1 SiBeclin1
2 Si Beclin1+OGD

FIG 2H

1
2
3
4
5
6
7
8
9
10
11
12
13
14
15
16
17
18
19
20
21
22
23
24
25
26
27
28
29
30
31
32
33
34
35
36
37
38
39
40
41

Hypothesis Test Summary				
	Null Hypothesis	Test	Sig. ^{a,b}	Decision
1	The distribution of Dependent is the same across categories of Treatment.	Independent-Samples Mann-Whitney U Test	.029 ^c	Reject the null hypothesis.

a. The significance level is .050.

b. Asymptotic significance is displayed.

c. Exact significance is displayed for this test.

Fig 3 A

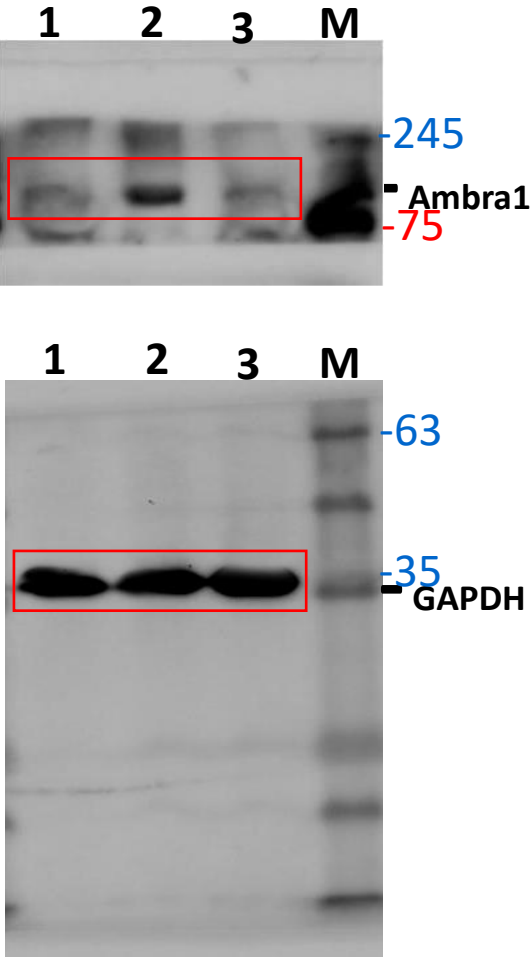


Fig 3 A

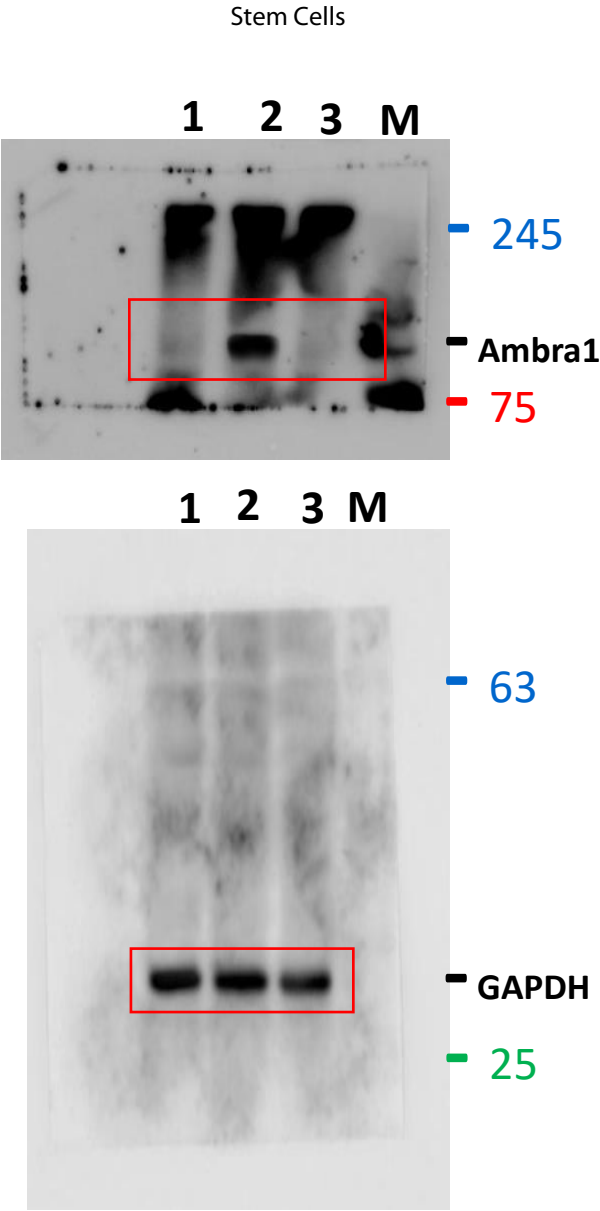
Pairwise Comparisons of Treatment

Sample 1- Sample 2	Test Statistic	Std. Error	Std. Test Statistic	Sig.	Adj. Sig. ^a
Control-PEG- SOD+OGD	0.000	2.505	0.000	1.000	1.000
Control-OGD	-6.000	2.505	-2.396	0.017	0.050
PEG- SOD+OGD- OGD	6.000	2.505	2.396	0.017	0.050

Each row tests the null hypothesis that the Sample 1 and Sample 2 distributions are the same. Asymptotic significances (2-sided tests) are displayed. The significance level is .050.

a. Significance values have been adjusted by the Bonferroni correction for multiple tests.

Fig 3 B



M Marker

1 Control

2 OGD

3 PEG-Catalase+OGD

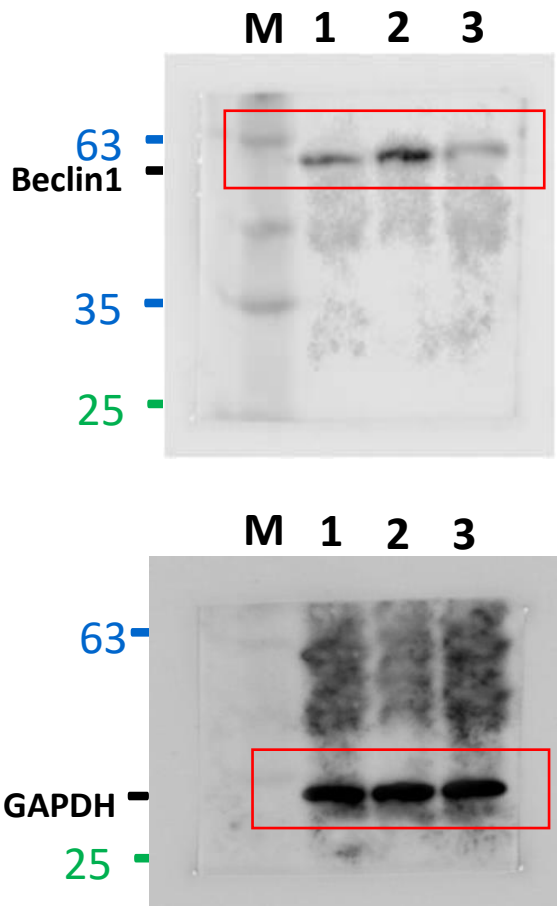
Fig 3 B

Pairwise Comparisons of Treatment					
Sample 1- Sample 2	Test Statistic	Std. Error	Std. Test Statistic	Sig.	Adj. Sig. ^a
Control-PEG- Catalase+OGD	0.000	2.505	0.000	1.000	1.000
Control-OGD	-6.000	2.505	-2.396	0.017	0.050
PEG- Catalase+OGD- OGD	6.000	2.505	2.396	0.017	0.050

Each row tests the null hypothesis that the Sample 1 and Sample 2 distributions are the same.
Asymptotic significances (2-sided tests) are displayed. The significance level is .050.

a. Significance values have been adjusted by the Bonferroni correction for multiple tests.

Fig 3 C



M Marker
1 Control
2 OGD
3 PEG-SOD+OGD

Fig 3 C

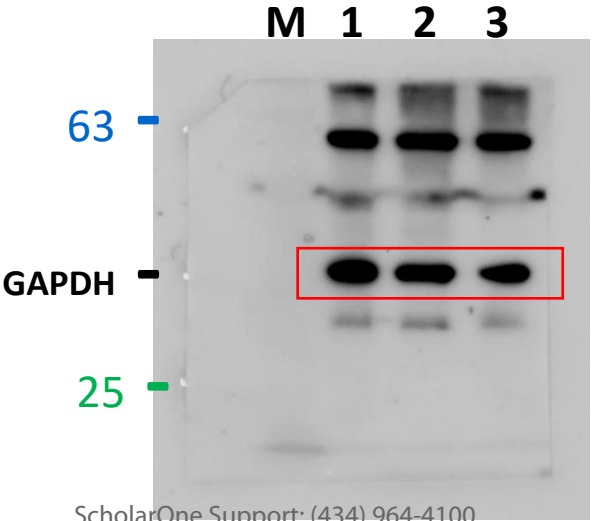
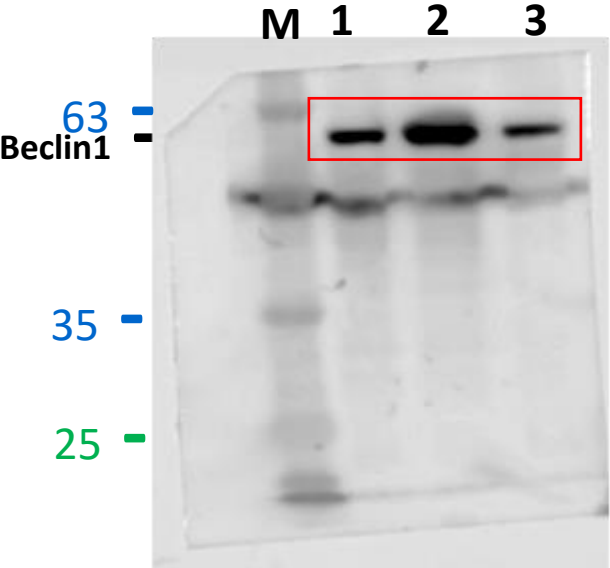
Pairwise Comparisons of Treatment

Sample 1- Sample 2	Test Statistic	Std. Error	Std. Test Statistic	Sig.	Adj. Sig. ^a
Control-PEG- SOD+OGD	0.000	2.505	0.000	1.000	1.000
Control-OGD	-6.000	2.505	-2.396	0.017	0.050
PEG- SOD+OGD- OGD	6.000	2.505	2.396	0.017	0.050

Each row tests the null hypothesis that the Sample 1 and Sample 2 distributions are the same.
Asymptotic significances (2-sided tests) are displayed. The significance level is .050.

a. Significance values have been adjusted by the Bonferroni correction for multiple tests.

Fig 3 D



M Marker
1 Control
2 OGD
3 PEG-Catalase+OGD

Fig 3 D

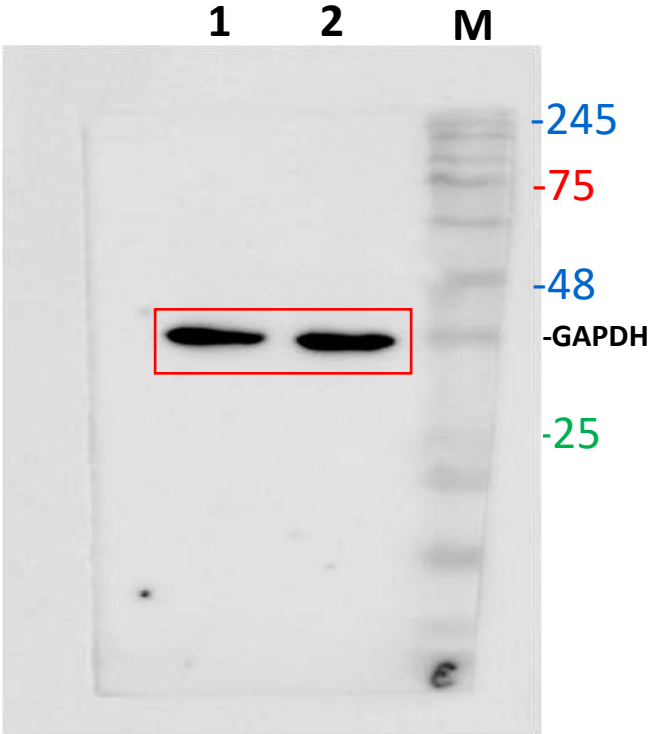
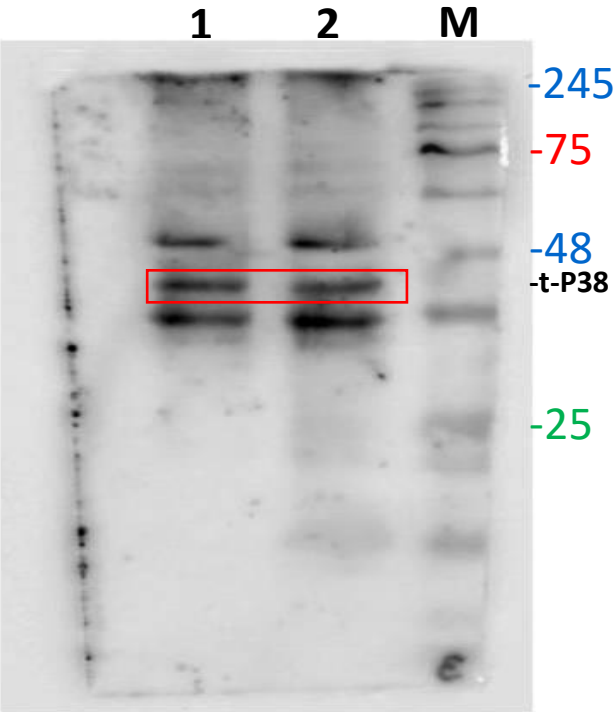
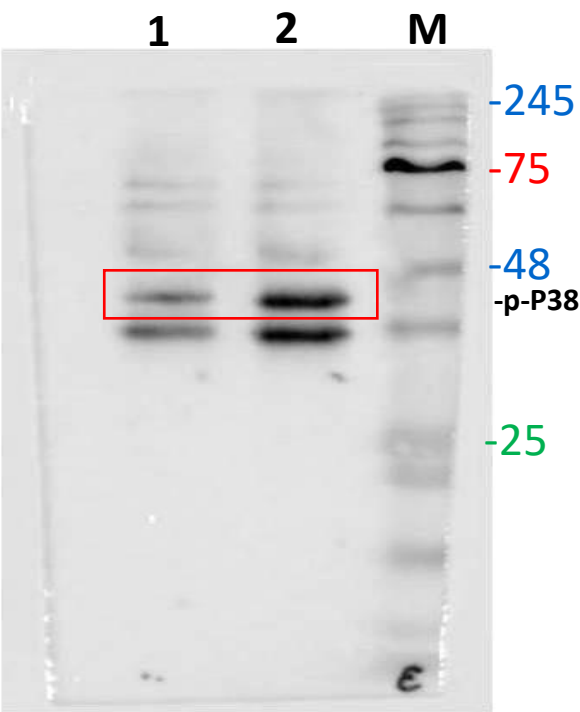
Pairwise Comparisons of Treatment

Sample 1- Sample 2	Test Statistic	Std. Error	Std. Test Statistic	Sig.	Adj. Sig. ^a
PEG- Catalase+OG D-Control	1.000	2.777	0.360	0.719	1.000
PEG- Catalase+OG D-OGD	8.000	2.777	2.880	0.004	0.012
Control-OGD	-7.000	2.777	-2.520	0.012	0.035

Each row tests the null hypothesis that the Sample 1 and Sample 2 distributions are the same.
Asymptotic significances (2-sided tests) are displayed. The significance level is .050.

a. Significance values have been adjusted by the Bonferroni correction for multiple tests.

Fig 4A

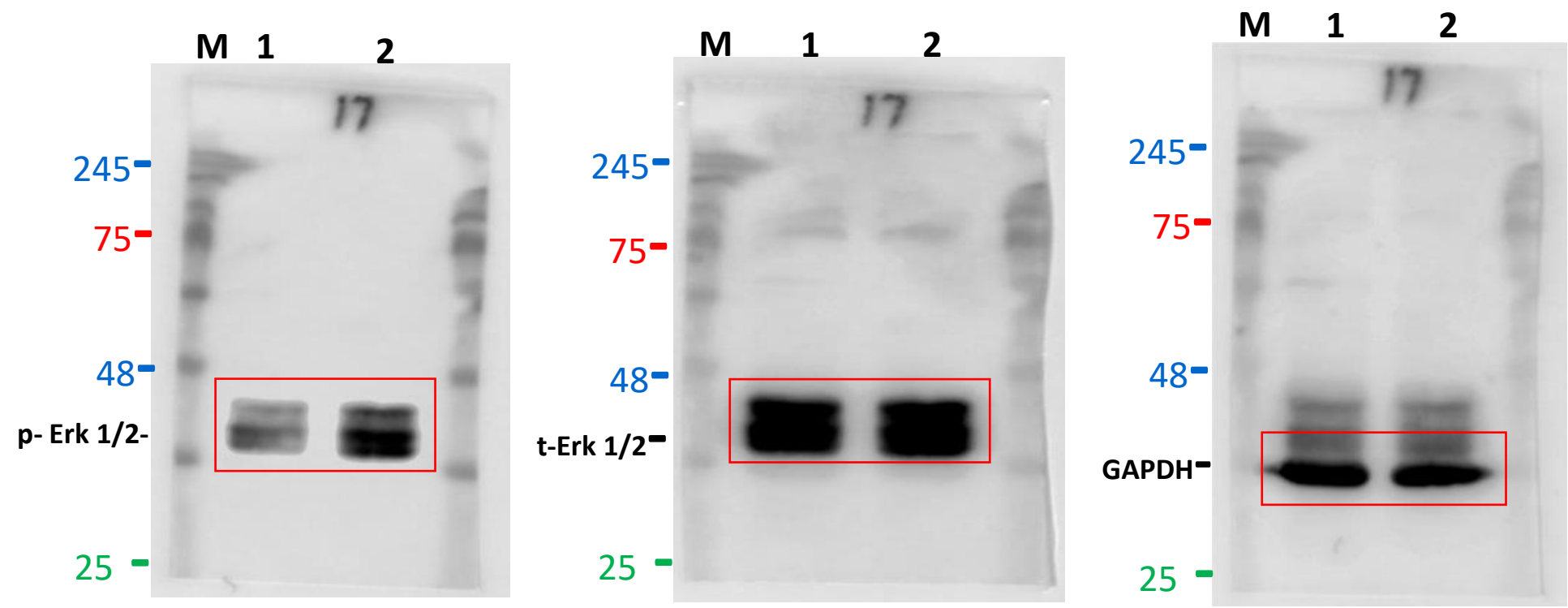


M Marker
1 Cont.
2 OGD

Fig 4A

Independent-Samples Mann-Whitney U Test Summary	
Total N	8
Mann-Whitney U	16.000
Wilcoxon W	26.000
Test Statistic	16.000
Standard Error	3.251
Standardized Test Statistic	2.460
Asymptotic Sig.(2-sided test)	0.014
Exact Sig.(2-sided test)	0.029

Fig 4B

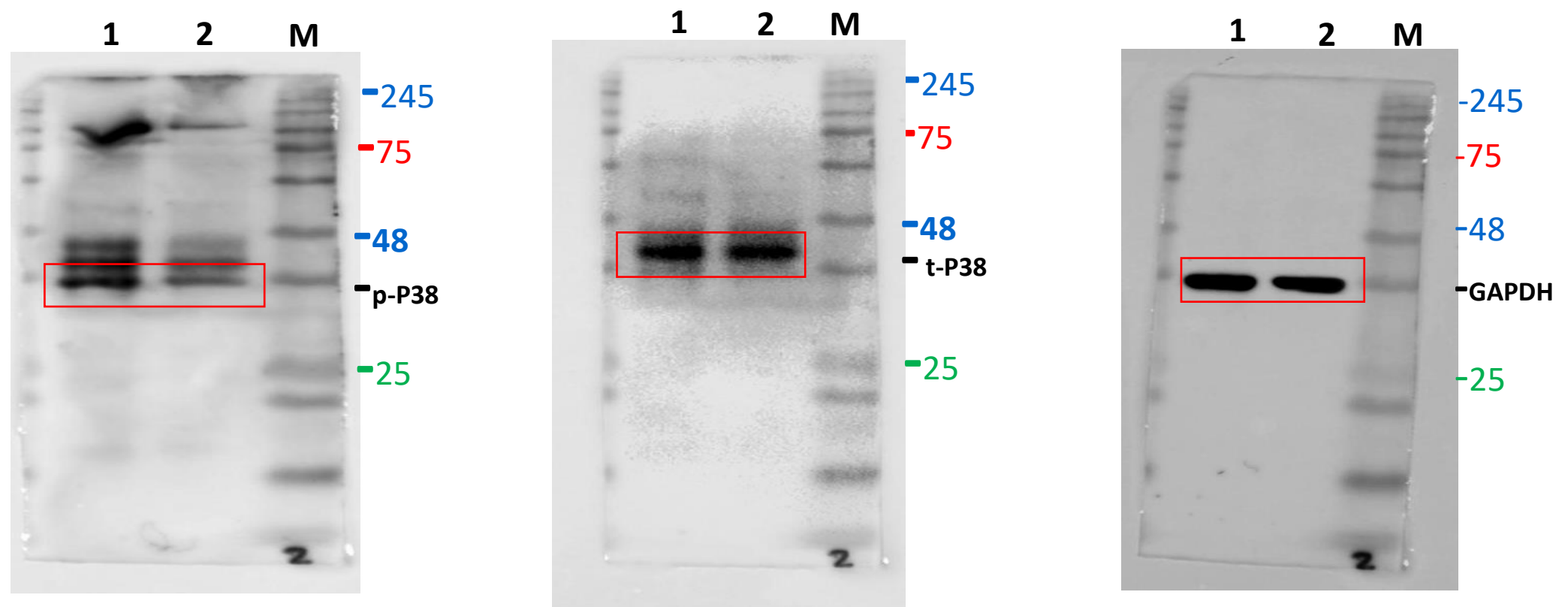


M Marker
1 Cont.
2 OGD

Fig 4B

Independent-Samples Mann-Whitney U Test Summary		
Total N		8
Mann-Whitney U		16.000
Wilcoxon W		26.000
Test Statistic		16.000
Standard Error		3.251
Standardized Test Statistic		2.460
Asymptotic Sig.(2-sided test)		0.014
Exact Sig.(2-sided test)		0.029

Fig 4C

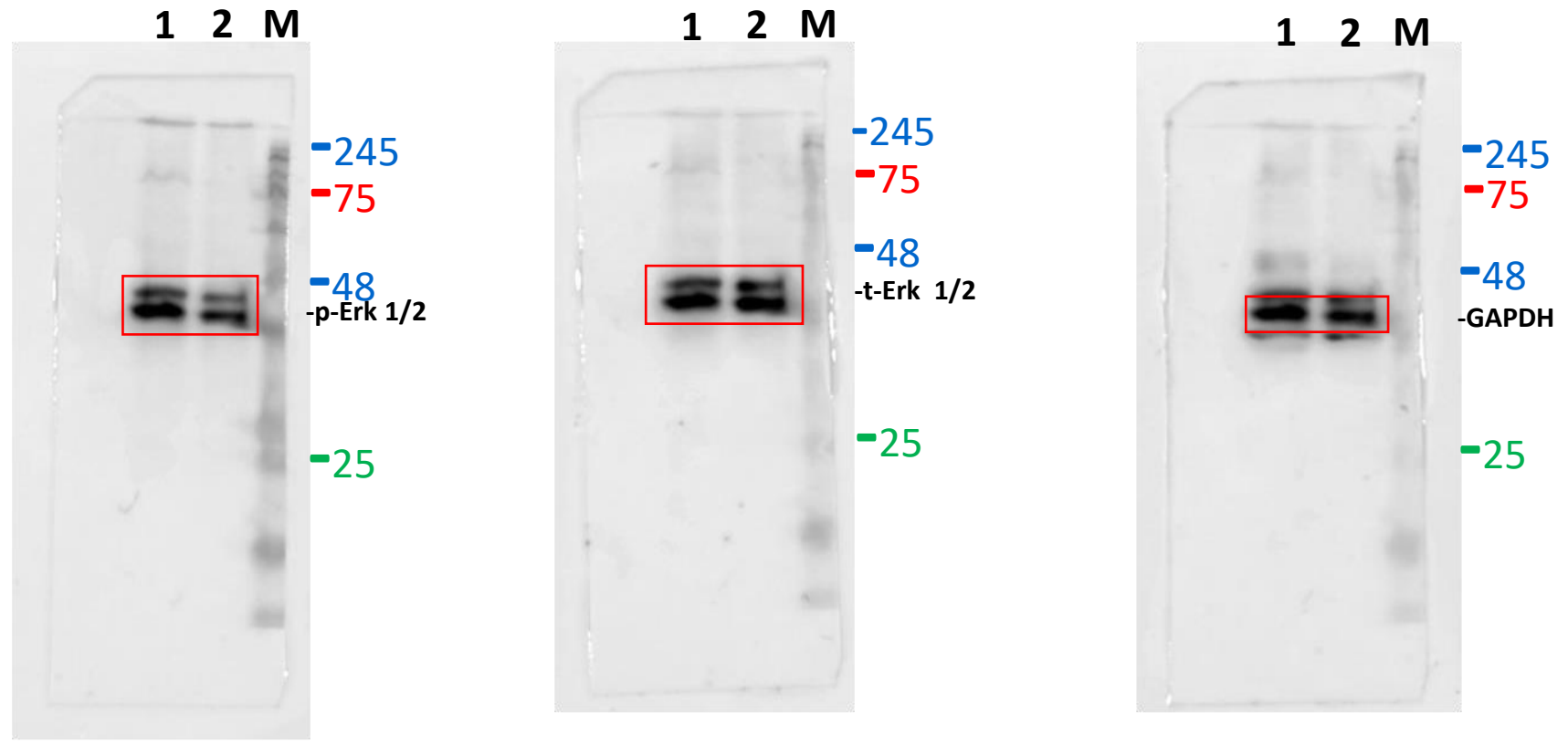


M Marker
1 OGD
2 SB202190+OGD

Fig 4C

Independent-Samples Mann-Whitney U Test Summary	
Total N	8
Mann-Whitney U	0.000
Wilcoxon W	10.000
Test Statistic	0.000
Standard Error	3.251
Standardized Test Statistic	-2.460
Asymptotic Sig.(2-sided test)	0.014
Exact Sig.(2-sided test)	0.029

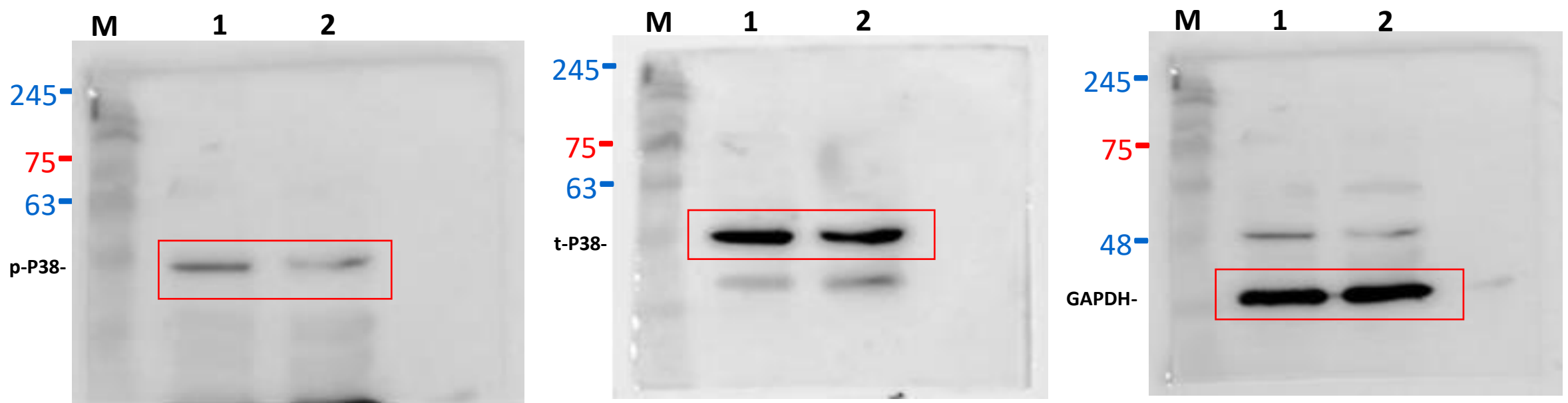
Fig 4D



M Marker
1 OGD
2 PD98059+OGD

Independent-Samples Mann-Whitney U Test Summary		
Total N		8
Mann-Whitney U		0.000
Wilcoxon W		10.000
Test Statistic		0.000
Standard Error		3.251
Standardized Test Statistic		-2.460
Asymptotic Sig.(2-sided test)		0.014
Exact Sig.(2-sided test)		0.029

1
2
3
4
5
6
7
8
9
10
11
12
13
14
15
16
17
18
19
20
21
22
23
24
25
26
27
28
29
30
31
32
33
34
35
36
37
38
39
40
41



M Marker
1 OGD
2 PEG-SOD+OGD

Fig 4E

1

2

3

4

5

6

7

8

9

10

11

12

13

14

15

16

17

18

19

20

21

22

23

24

25

26

27

28

29

30

31

32

33

34

35

36

37

38

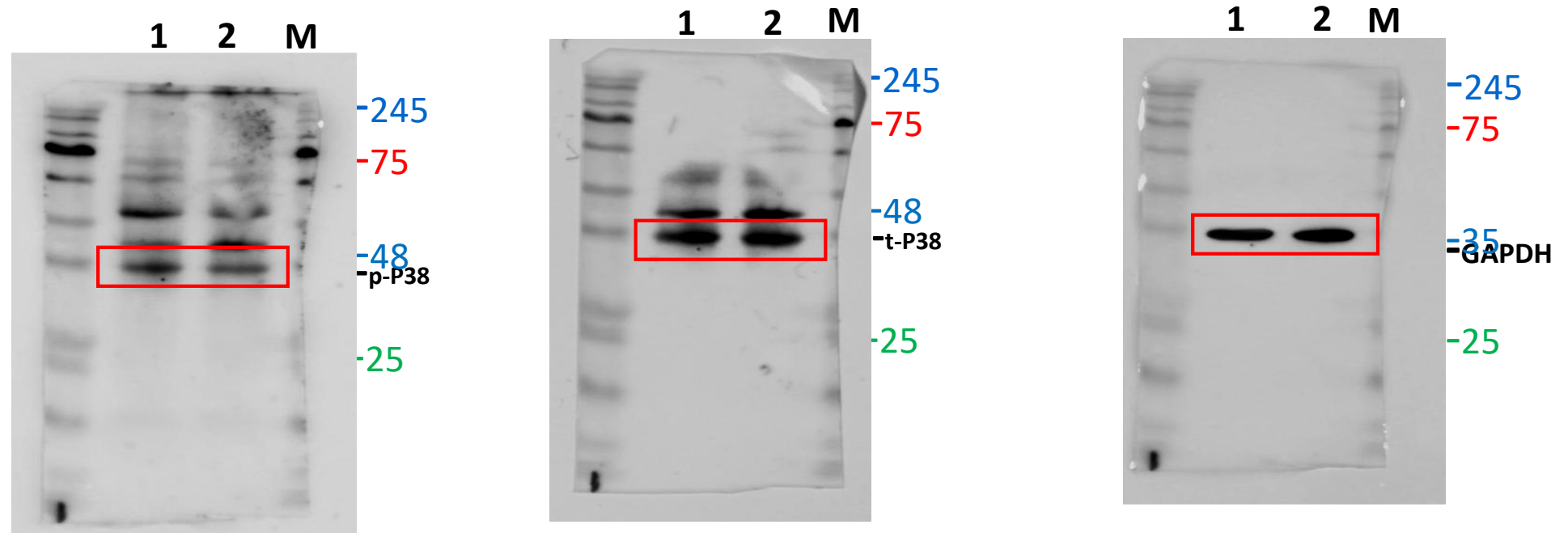
39

40

41

Independent-Samples Mann-Whitney U Test Summary		
Total N		8
Mann-Whitney U		0.000
Wilcoxon W		10.000
Test Statistic		0.000
Standard Error		3.251
Standardized Test Statistic		-2.460
Asymptotic Sig.(2-sided test)		0.014
Exact Sig.(2-sided test)		0.029

Fig 4F



M Marker
1 OGD
2 PEG-Catalase+OGD

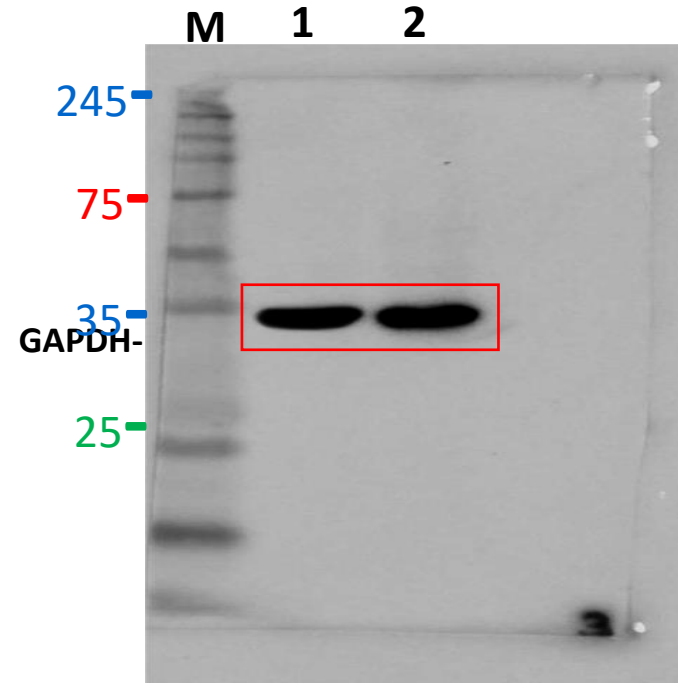
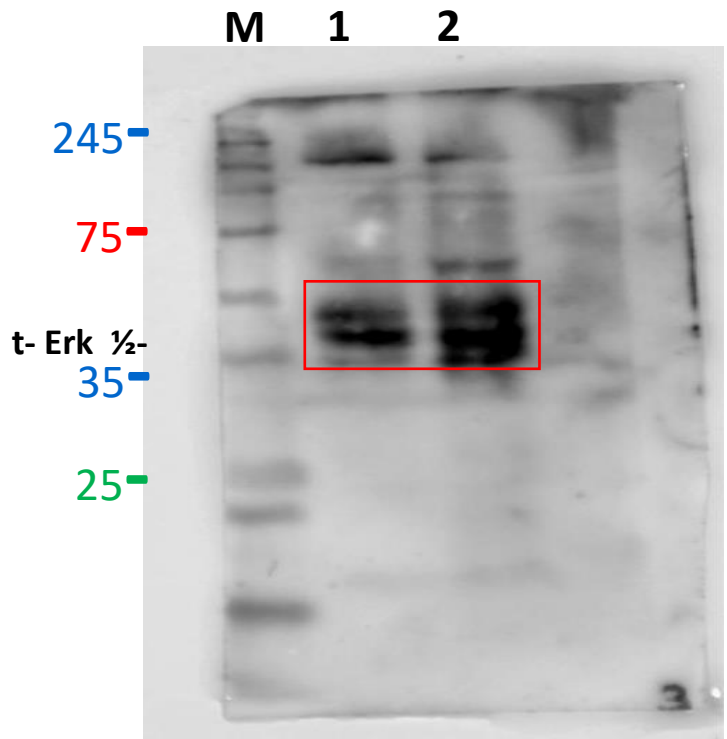
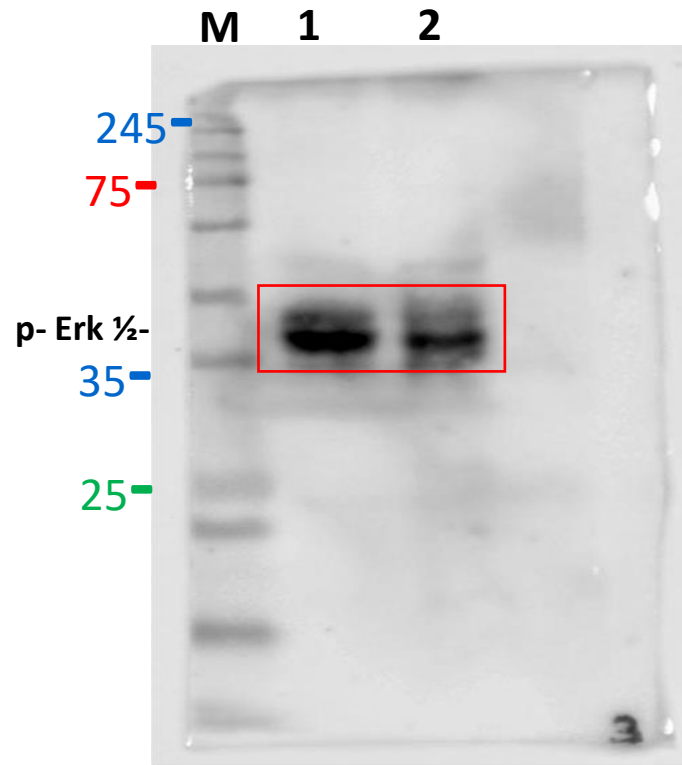
Fig 4F

1
2
3
4
5
6
7
8
9
10
11
12
13
14
15
16
17
18
19
20
21
22
23
24
25
26
27
28
29
30
31
32
33
34
35
36
37
38
39
40
41

Independent-Samples Mann-Whitney U Test Summary		
Total N		8
Mann-Whitney U		0.000
Wilcoxon W		10.000
Test Statistic		0.000
Standard Error		3.251
Standardized Test Statistic		-2.460
Asymptotic Sig.(2-sided test)		0.014
Exact Sig.(2-sided test)		0.029

Fig 4G

1
2
3
4
5
6
7
8
9
10
11
12
13
14
15
16
17
18
19
20
21
22
23
24
25
26
27
28
29
30
31
32
33
34
35
36
37
38
39
40
41



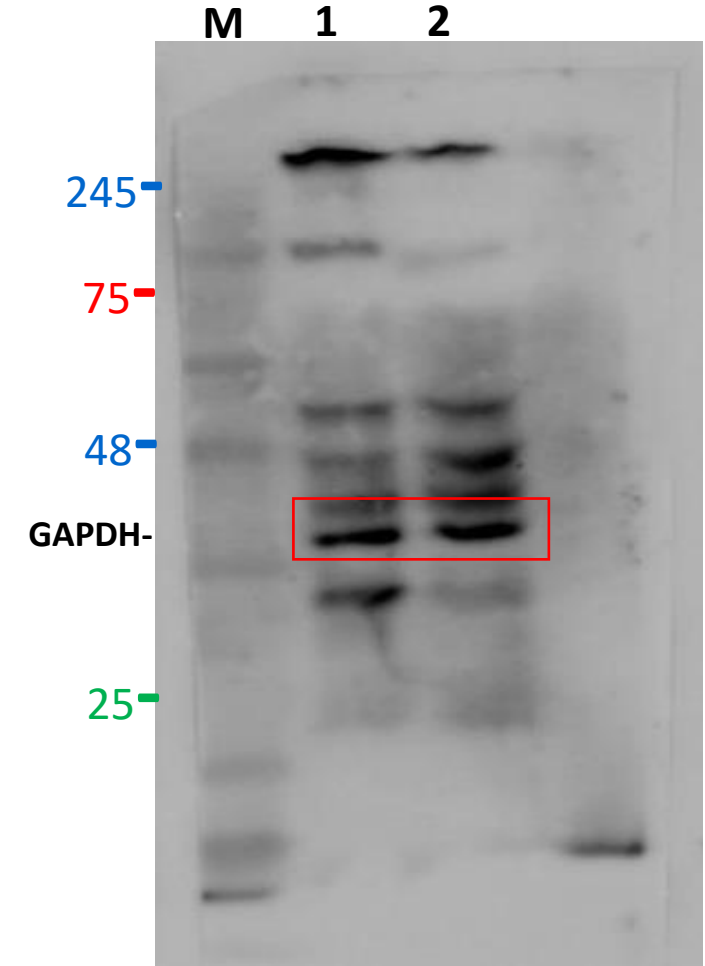
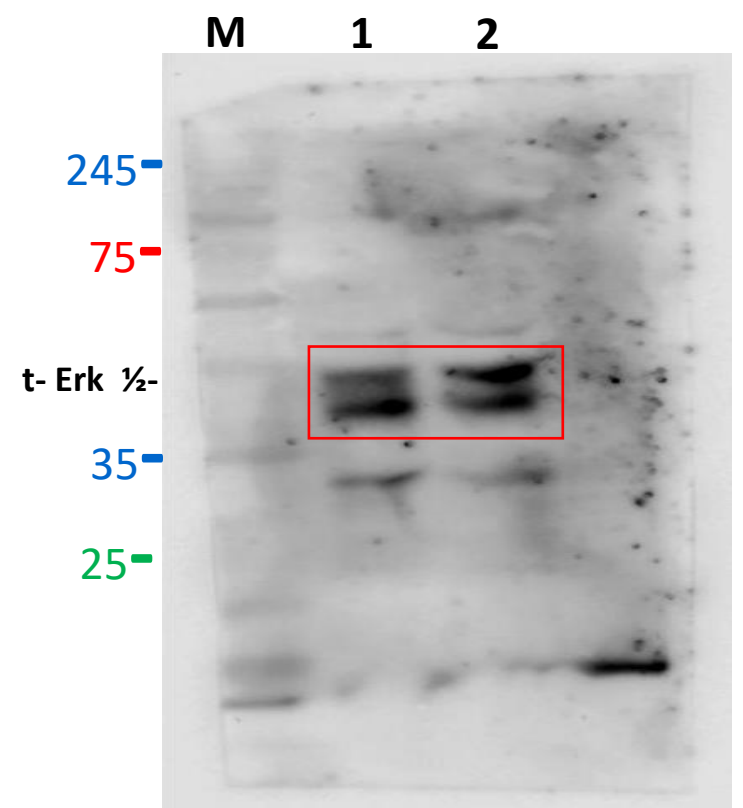
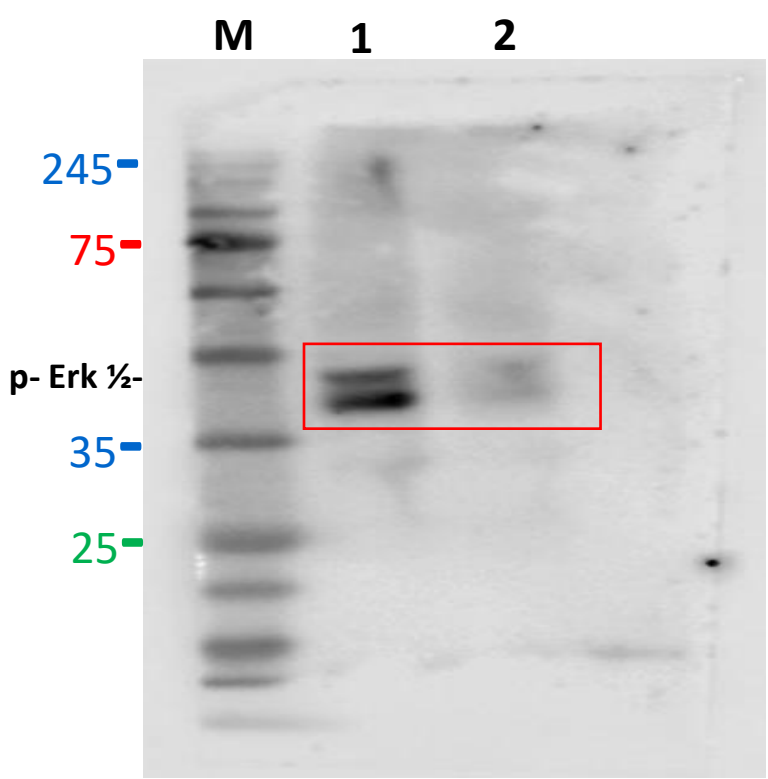
M Marker
1 OGD
2 PEG-SOD+OGD

Fig 4G

Independent-Samples Mann-Whitney U Test Summary	
Total N	8
Mann-Whitney U	0.000
Wilcoxon W	10.000
Test Statistic	0.000
Standard Error	3.251
Standardized Test Statistic	-2.460
Asymptotic Sig.(2-sided test)	0.014
Exact Sig.(2-sided test)	0.029

Fig 4H

1
2
3
4
5
6
7
8
9
10
11
12
13
14
15
16
17
18
19
20
21
22
23
24
25
26
27
28
29
30
31
32
33
34
35
36
37
38
39
40
41

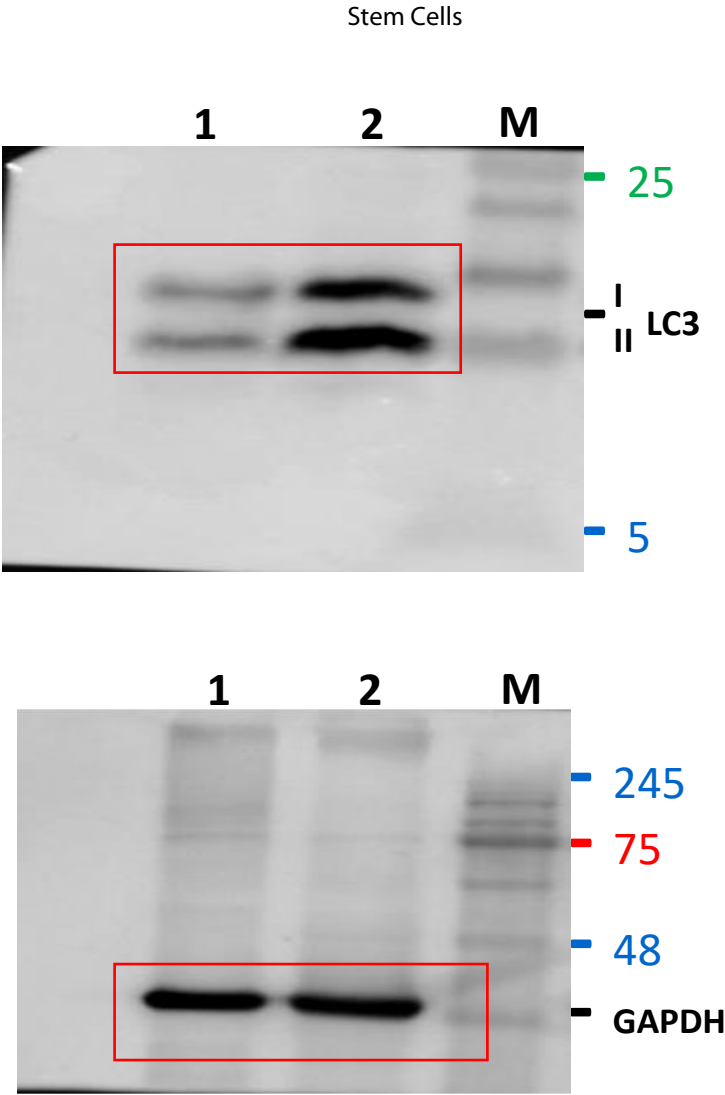


M Marker
1 OGD
2 PEG-Catalase+ OGD

Fig 4H

Independent-Samples Mann-Whitney U Test Summary	
Total N	8
Mann-Whitney U	0.000
Wilcoxon W	10.000
Test Statistic	0.000
Standard Error	3.251
Standardized Test Statistic	-2.460
Asymptotic Sig.(2-sided test)	0.014
Exact Sig.(2-sided test)	0.029

FIG. S2D

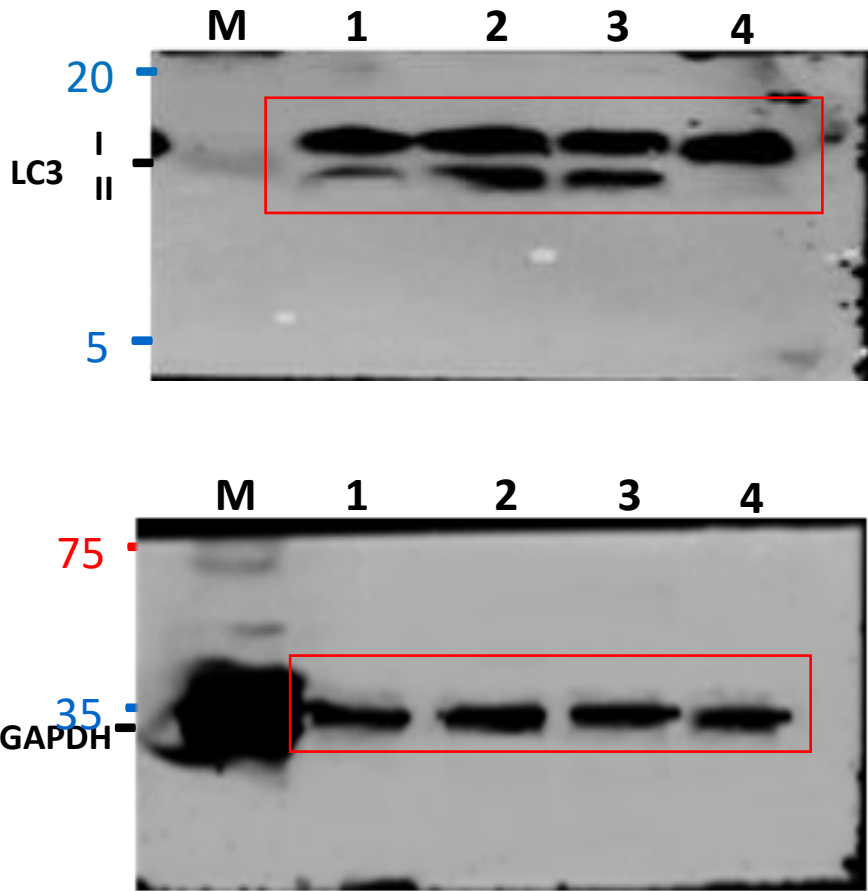


M Marker
1 Control
2 OGD

FIG. S2D

Independent-Samples Mann-Whitney U Test Summary	
Total N	8
Mann-Whitney U	16.000
Wilcoxon W	26.000
Test Statistic	16.000
Standard Error	3.251
Standardized Test Statistic	2.460
Asymptotic Sig.(2-sided test)	0.014
Exact Sig.(2-sided test)	0.029

FIG. S2E



M Marker
1 Control
2 OGD
3 Rapamycin+OGD
4 3-MA+OGD

FIG. S2E

Pairwise Comparisons of Treatment

Sample 1- Sample 2	Test Statistic	Std. Error	Std. Test Statistic	Sig.	Adj. Sig. ^a
Cont- 3MA+OGD	-4.750	4.654	-1.021	0.307	1.000
Cont-OGD	-17.125	4.654	-3.679	0.000	0.001
Cont- Rapamycin	-18.125	4.654	-3.894	0.000	0.01
3MA+OGD- OGD	12.375	4.654	2.659	0.008	0.047
3MA+OGD- Rapamycin	13.375	4.654	2.874	0.004	0.024
OGD- Rapamycin	-1.000	4.654	-0.215	0.830	1.000

Each row tests the null hypothesis that the Sample 1 and Sample 2 distributions are the same.
Asymptotic significances (2-sided tests) are displayed. The significance level is .050.
a. Significance values have been adjusted by the Bonferroni correction for multiple tests.

FIG. S2F

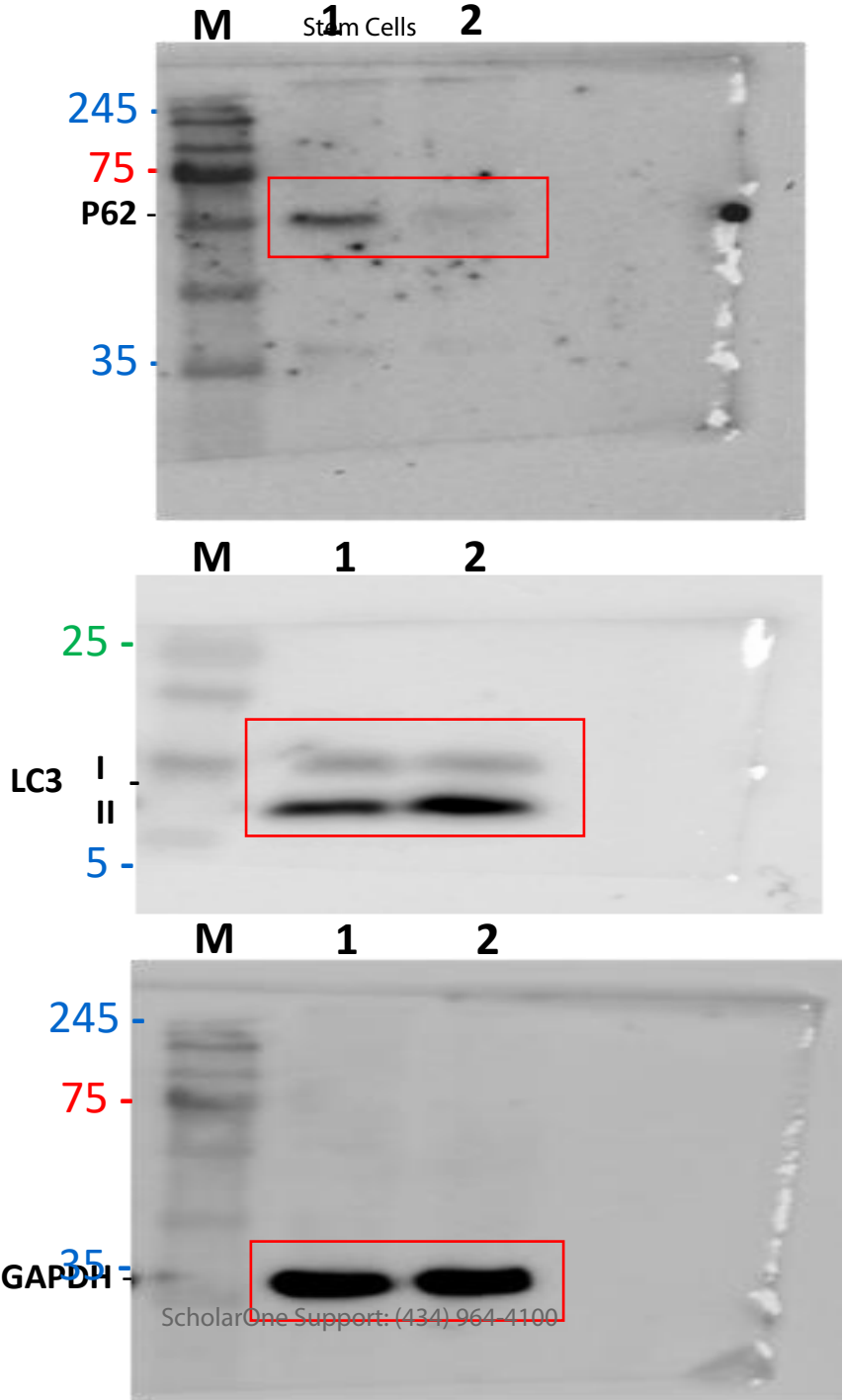


FIG. S2F

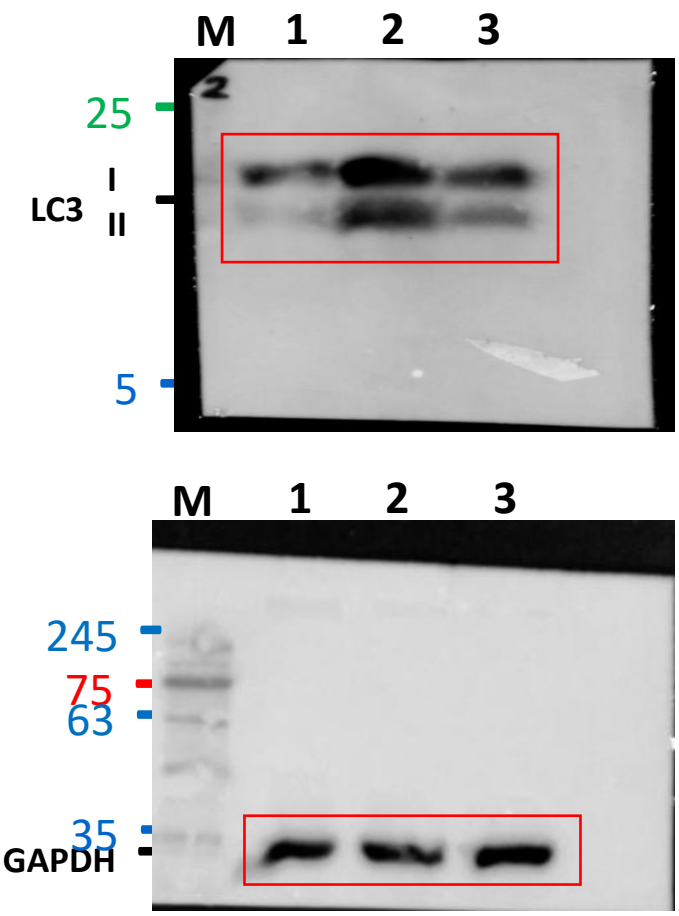
P62

Independent-Samples Mann-Whitney U Test Summary		
Total N		8
Mann-Whitney U		0.000
Wilcoxon W		10.000
Test Statistic		0.000
Standard Error		3.251
Standardized Test Statistic		-2.460
Asymptotic Sig.(2-sided test)		0.014
Exact Sig.(2-sided test)		0.029

LC3 II/I

Independent-Samples Mann-Whitney U Test Summary		
Total N		8
Mann-Whitney U		16.000
Wilcoxon W		26.000
Test Statistic		16.000
Standard Error		3.251
Standardized Test Statistic		2.460
Asymptotic Sig.(2-sided test)		0.014
Exact Sig.(2-sided test)		0.029

FIG. S3A

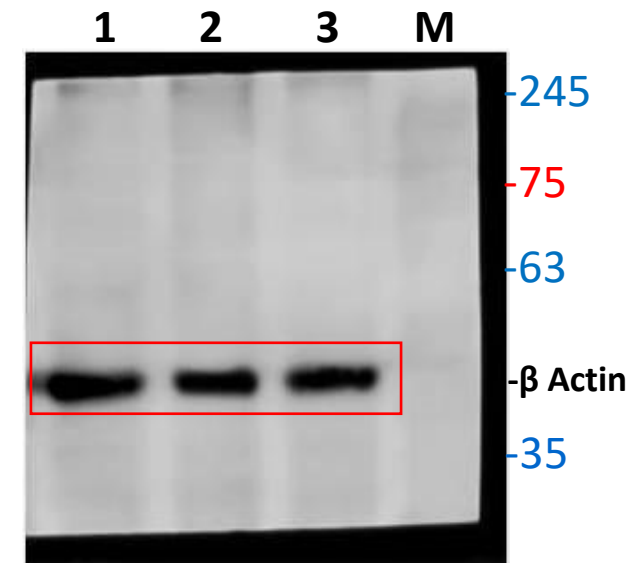
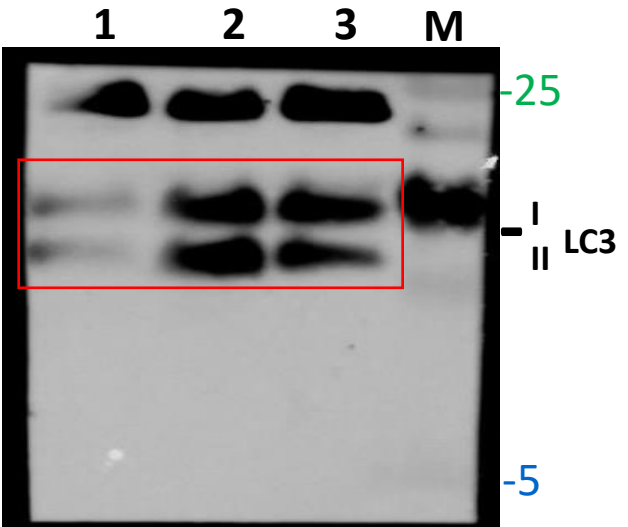


M Marker
1 Control
2 OGD
3 PEG-SOD+OGD

FIG. S3A

Pairwise Comparisons of Treatment					
Sample 1- Sample 2	Test Statistic	Std. Error	Std. Test Statistic	Sig.	Adj. Sig. ^a
Peg- SOD+OGD- Cont	1.000	2.777	0.360	0.719	1.000
Peg- SOD+OGD- OGD	8.000	2.777	2.880	0.004	0.012
Cont-OGD	-7.000	2.777	-2.520	0.012	0.035
Each row tests the null hypothesis that the Sample 1 and Sample 2 distributions are the same. Asymptotic significances (2-sided tests) are displayed. The significance level is .050.					
a. Significance values have been adjusted by the Bonferroni correction for multiple tests.					

FIG. S3B



ScholarOne Support: (434) 964-4100

M Marker
1 Control
2 OGD
3 PEG CATALASE+OGD

FIG. S3B

Pairwise Comparisons of Treatment

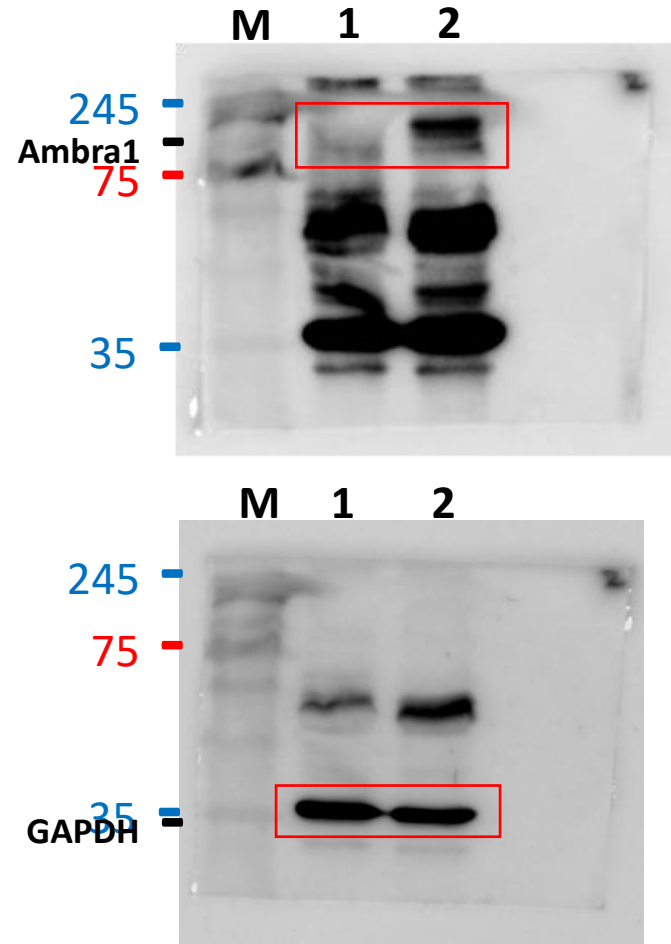
Sample 1- Sample 2	Test Statistic	Std. Error	Std. Test Statistic	Sig.	Adj. Sig. ^a
Cont-Peg- SOD+OGD	0.000	2.505	0.000	1.000	1.000
Cont-OGD	-6.000	2.505	-2.396	0.017	0.050
Peg- SOD+OGD- OGD	6.000	2.505	2.396	0.017	0.050

Each row tests the null hypothesis that the Sample 1 and Sample 2 distributions are the same. Asymptotic significances (2-sided tests) are displayed. The significance level is .050.

a. Significance values have been adjusted by the Bonferroni correction for multiple tests.

FIG. S3C

Stem Cells

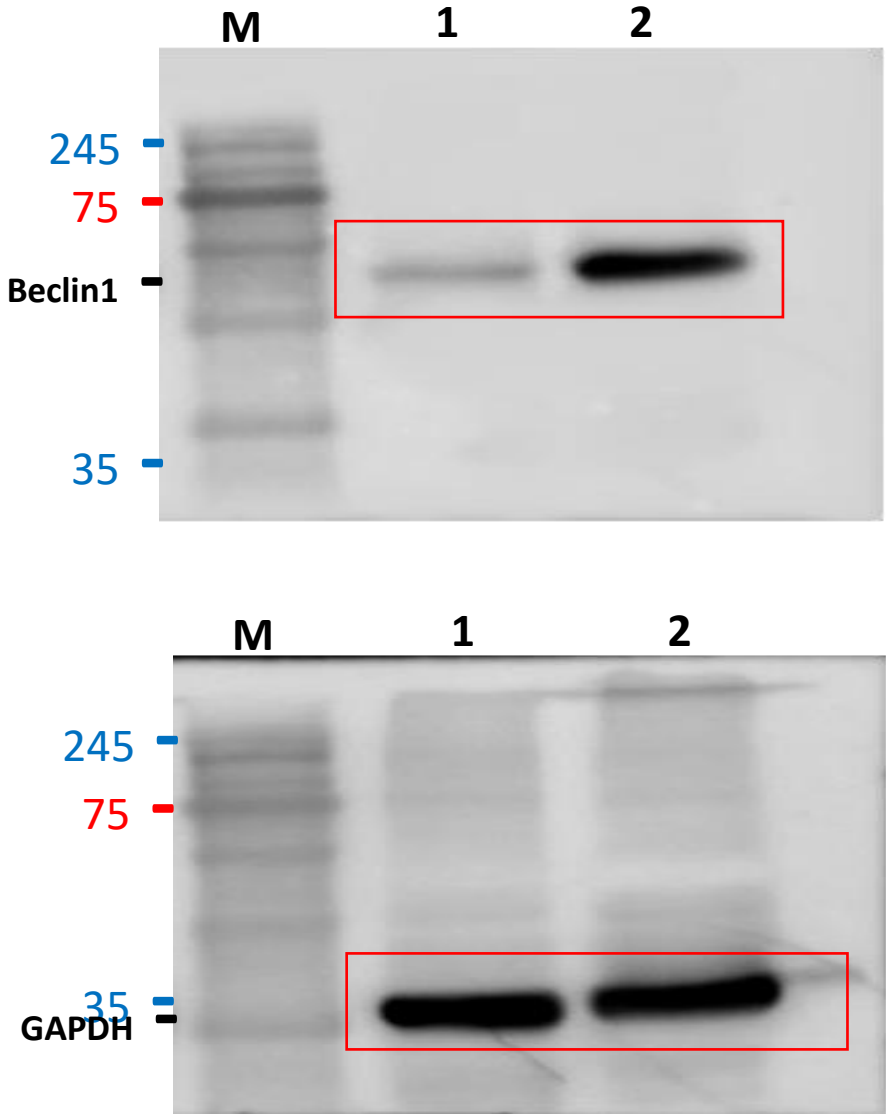


M Marker
1 Control
2 OGD

FIG. S3C

Independent-Samples Mann-Whitney U Test Summary	
Total N	8
Mann-Whitney U	16.000
Wilcoxon W	26.000
Test Statistic	16.000
Standard Error	3.251
Standardized Test Statistic	2.460
Asymptotic Sig.(2-sided test)	0.014
Exact Sig.(2-sided test)	0.029

FIG. S3D

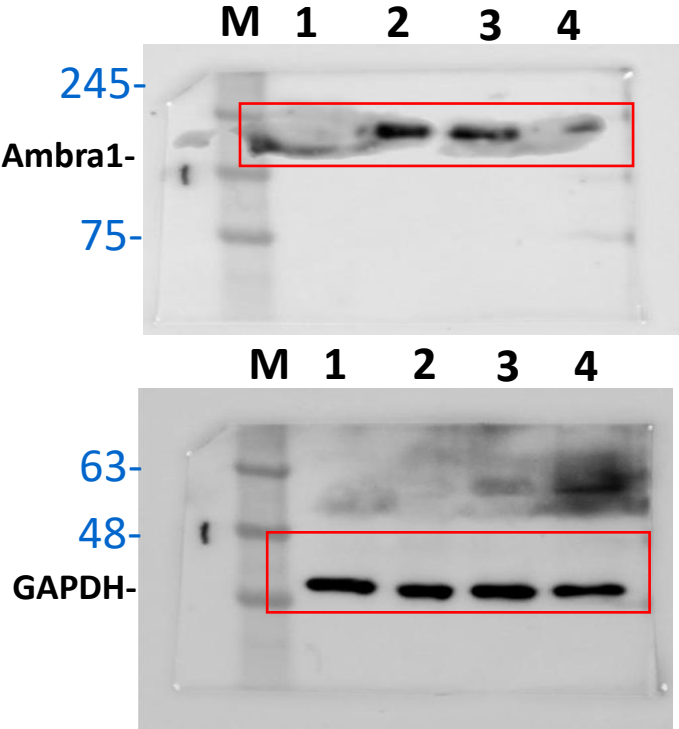


M Marker
1 Control
2 OGD

FIG. S3D

Independent-Samples Mann-Whitney U Test Summary	
Total N	8
Mann-Whitney U	16.000
Wilcoxon W	26.000
Test Statistic	16.000
Standard Error	3.251
Standardized Test Statistic	2.460
Asymptotic Sig.(2-sided test)	0.014
Exact Sig.(2-sided test)	0.029

FIG. S3E



M Marker
1 Control
2 OGD
3 siCont.+ OGD
4 siAmbra1 + OGD

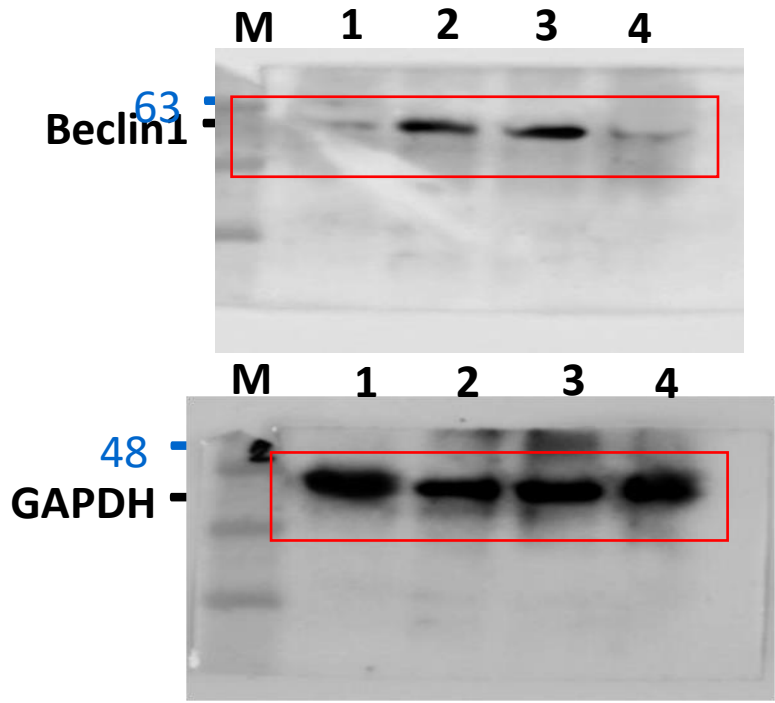
FIG. S3E

Pairwise Comparisons of Treatment

Sample 1- Sample 2	Test Statistic	Std. Error	Std. Test Statistic	Sig.	Adj. Sig. ^a
siAmbra1+O GD-Cont	0.143	4.363	0.033	0.974	1.000
siAmbra1+O GD-OGD	12.000	4.363	2.750	0.006	0.036
siAmbra1+O GD-siCont	14.429	4.363	3.307	0.001	0.006
Cont-OGD	-11.857	4.363	-2.718	0.007	0.039
Cont-siCont	-14.286	4.363	-3.274	0.001	0.006
OGD-siCont	-2.429	4.363	-0.557	0.578	1.000

Each row tests the null hypothesis that the Sample 1 and Sample 2 distributions are the same. Asymptotic significances (2-sided tests) are displayed. The significance level is .050.

a. Significance values have been adjusted by the Bonferroni correction for multiple tests.



M Marker
1 Control
2 OGD
3 siCont.+ OGD
4 siBeclin1 + OGD

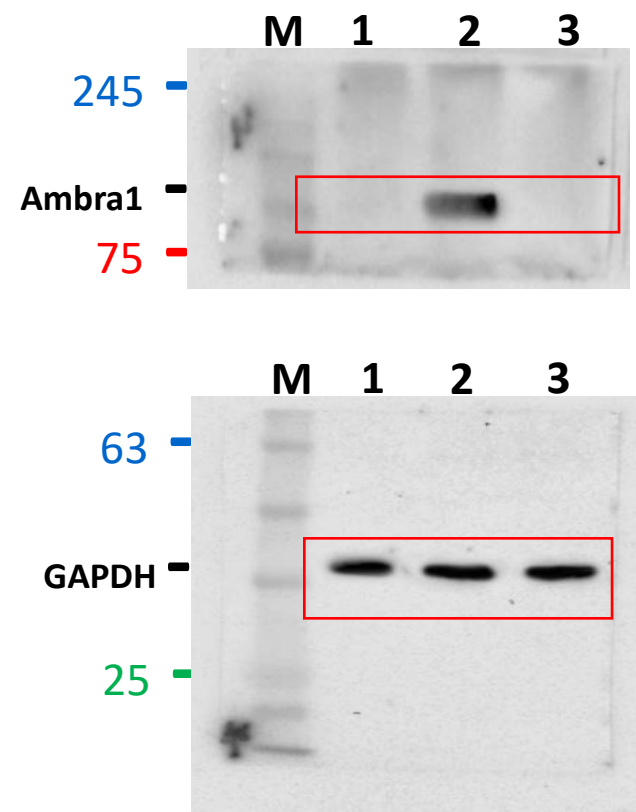
FIG. S3F

Pairwise Comparisons of Treatment					
Sample 1- Sample 2	Test Statistic	Std. Error	Std. Test Statistic	Sig.	Adj. Sig. ^a
Cont- siAmbra1+OG D	-0.667	4.051	-0.165	0.869	1.000
Cont-siCont	-11.333	4.051	-2.797	0.005	0.031
Cont-OGD	-12.000	4.051	-2.962	0.003	0.018
siAmbra1+OG D-siCont	10.667	4.051	2.633	0.008	0.051
siAmbra1+OG D-OGD	11.333	4.051	2.797	0.005	0.031
siCont-OGD	0.667	4.051	0.165	0.869	1.000

Each row tests the null hypothesis that the Sample 1 and Sample 2 distributions are the same. Asymptotic significances (2-sided tests) are displayed. The significance level is .050.

a. Significance values have been adjusted by the Bonferroni correction for multiple tests.

Fig S4A



M Marker
1 Control
2 OGD
3 PEG-SOD+OGD

Fig S4A

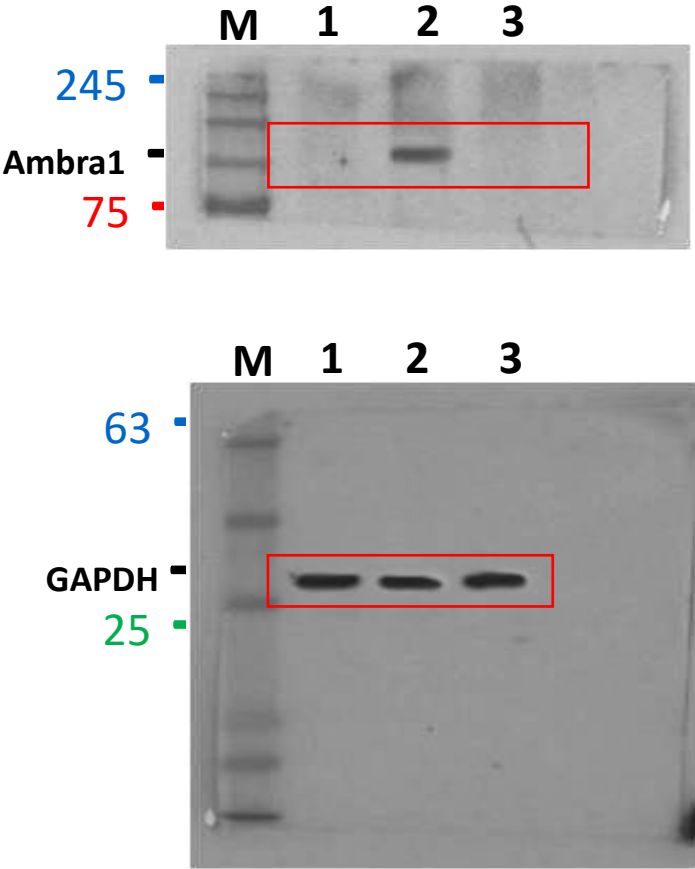
Pairwise Comparisons of Treatment

Sample 1- Sample 2	Test Statistic	Std. Error	Std. Test Statistic	Sig.	Adj. Sig. ^a
Cont-Peg- SOD+OGD	0.000	2.505	0.000	1.000	1.000
Cont-OGD	-6.000	2.505	-2.396	0.017	0.050
Peg- SOD+OGD- OGD	6.000	2.505	2.396	0.017	0.050

Each row tests the null hypothesis that the Sample 1 and Sample 2 distributions are the same.
Asymptotic significances (2-sided tests) are displayed. The significance level is .050.

a. Significance values have been adjusted by the Bonferroni correction for multiple tests.

Fig S4B



M Marker
1 Control
2 OGD
3 PEG-Catalase+OGD

Fig S4B

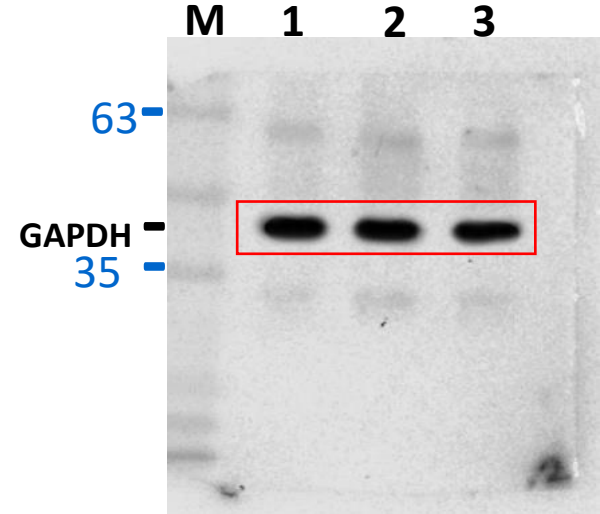
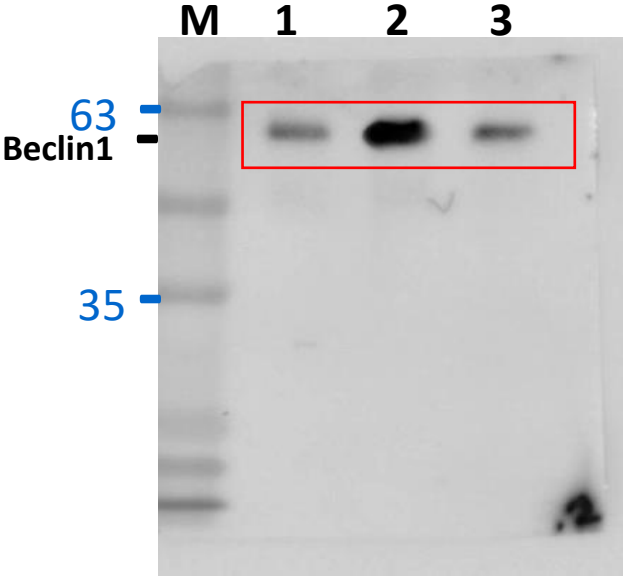
Pairwise Comparisons of Treatment

Sample 1- Sample 2	Test Statistic	Std. Error	Std. Test Statistic	Sig.	Adj. Sig. ^a
Cont-Peg- Catalase+OGD	0.000	2.505	0.000	1.000	1.000
Cont-OGD	-6.000	2.505	-2.396	0.017	0.050
Peg- Catalase+OGD -OGD	6.000	2.505	2.396	0.017	0.050

Each row tests the null hypothesis that the Sample 1 and Sample 2 distributions are the same. Asymptotic significances (2-sided tests) are displayed. The significance level is .050.

a. Significance values have been adjusted by the Bonferroni correction for multiple tests.

Fig S4C



M Marker
1 Control
2 OGD
3 PEG-SOD+OGD

Fig S4C

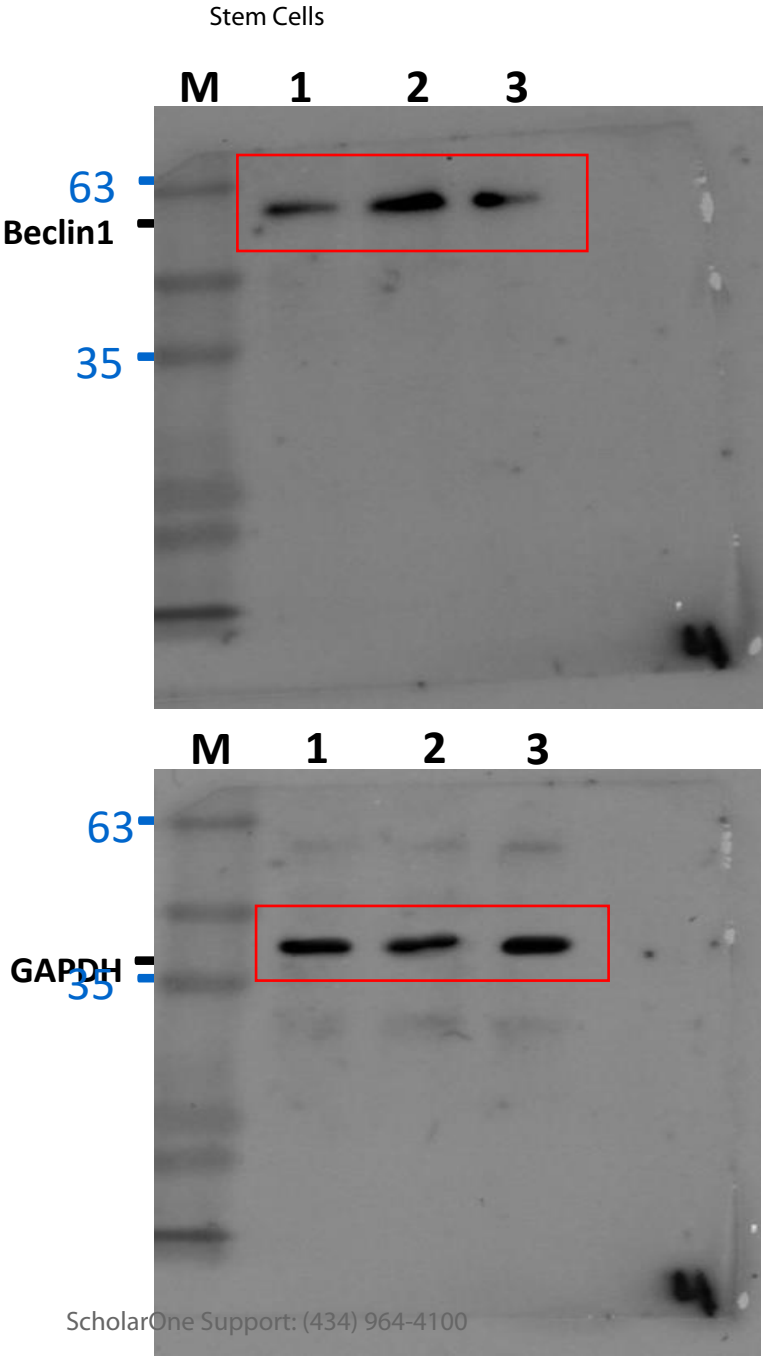
Pairwise Comparisons of Treatment

Sample 1- Sample 2	Test Statistic	Std. Error	Std. Test Statistic	Sig.	Adj. Sig. ^a
Cont-Peg- SOD+OGD	-1.000	2.777	-0.360	0.719	1.000
Cont-OGD	-8.000	2.777	-2.880	0.004	0.012
Peg- SOD+OGD- OGD	7.000	2.777	2.520	0.012	0.035

Each row tests the null hypothesis that the Sample 1 and Sample 2 distributions are the same.
Asymptotic significances (2-sided tests) are displayed. The significance level is .050.

a. Significance values have been adjusted by the Bonferroni correction for multiple tests.

Fig S4D



M Marker
1 Control
2 OGD
3 PEG-Catalase+OGD

Fig S4D

Pairwise Comparisons of Treatment

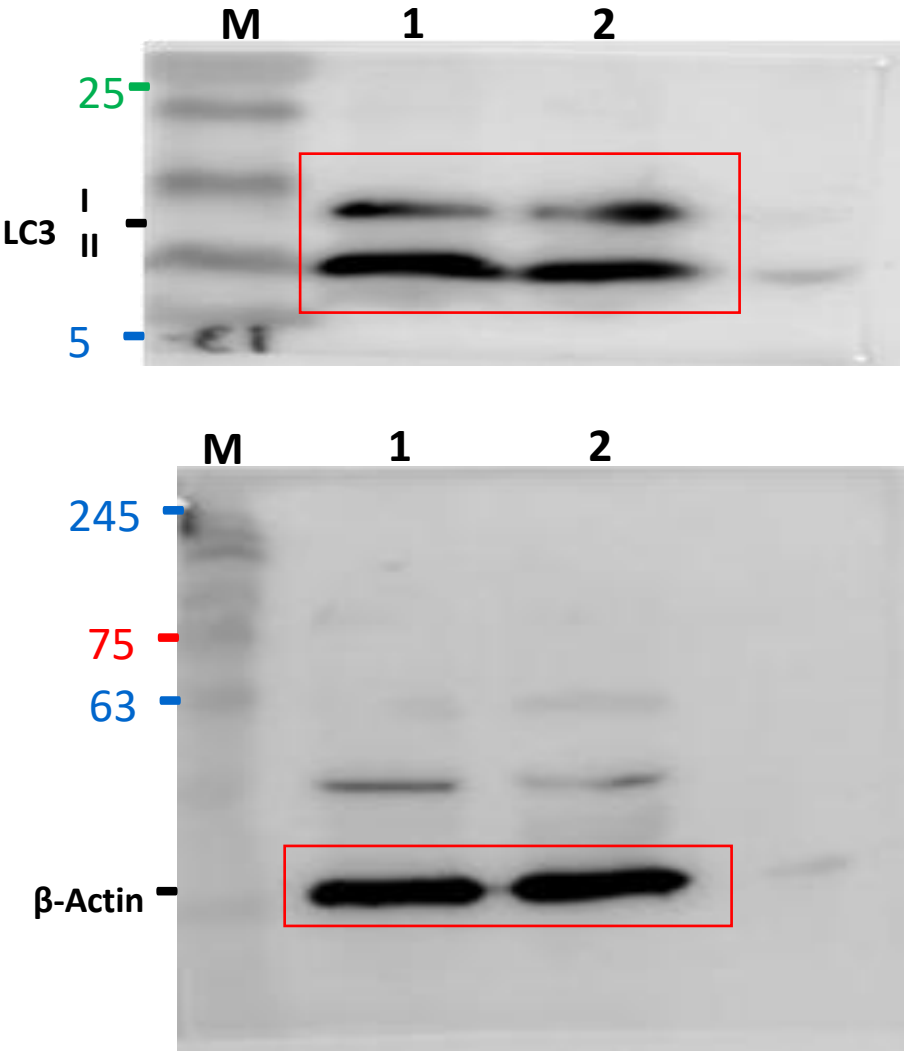
Sample 1- Sample 2	Test Statistic	Std. Error	Std. Test Statistic	Sig.	Adj. Sig. ^a
Cont-Peg- Catalase+OGD	0.000	2.505	0.000	1.000	1.000
Cont-OGD	-6.000	2.505	-2.396	0.017	0.050
Peg- Catalase+OGD -OGD	6.000	2.505	2.396	0.017	0.050

Each row tests the null hypothesis that the Sample 1 and Sample 2 distributions are the same. Asymptotic significances (2-sided tests) are displayed. The significance level is .050.

a. Significance values have been adjusted by the Bonferroni correction for multiple tests.

Fig S5A

Stem Cells



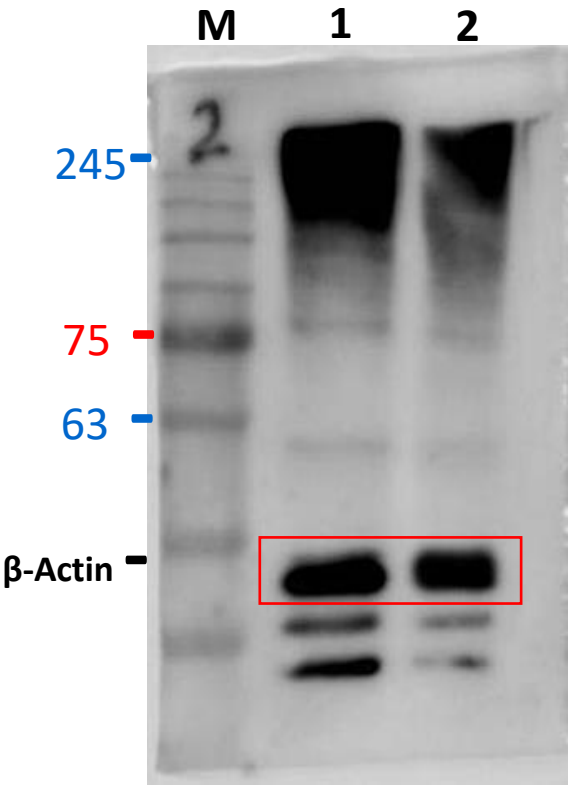
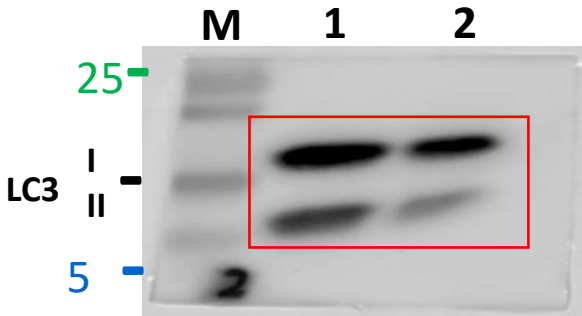
M Marker
1 OGD
2 SB202190+OGD

Fig S5A

Independent-Samples Mann-Whitney U Test Summary		
Total N		8
Mann-Whitney U		0.000
Wilcoxon W		10.000
Test Statistic		0.000
Standard Error		3.251
Standardized Test Statistic		-2.460
Asymptotic Sig.(2-sided test)		0.014
Exact Sig.(2-sided test)		0.029

Fig S5B

Stem Cells

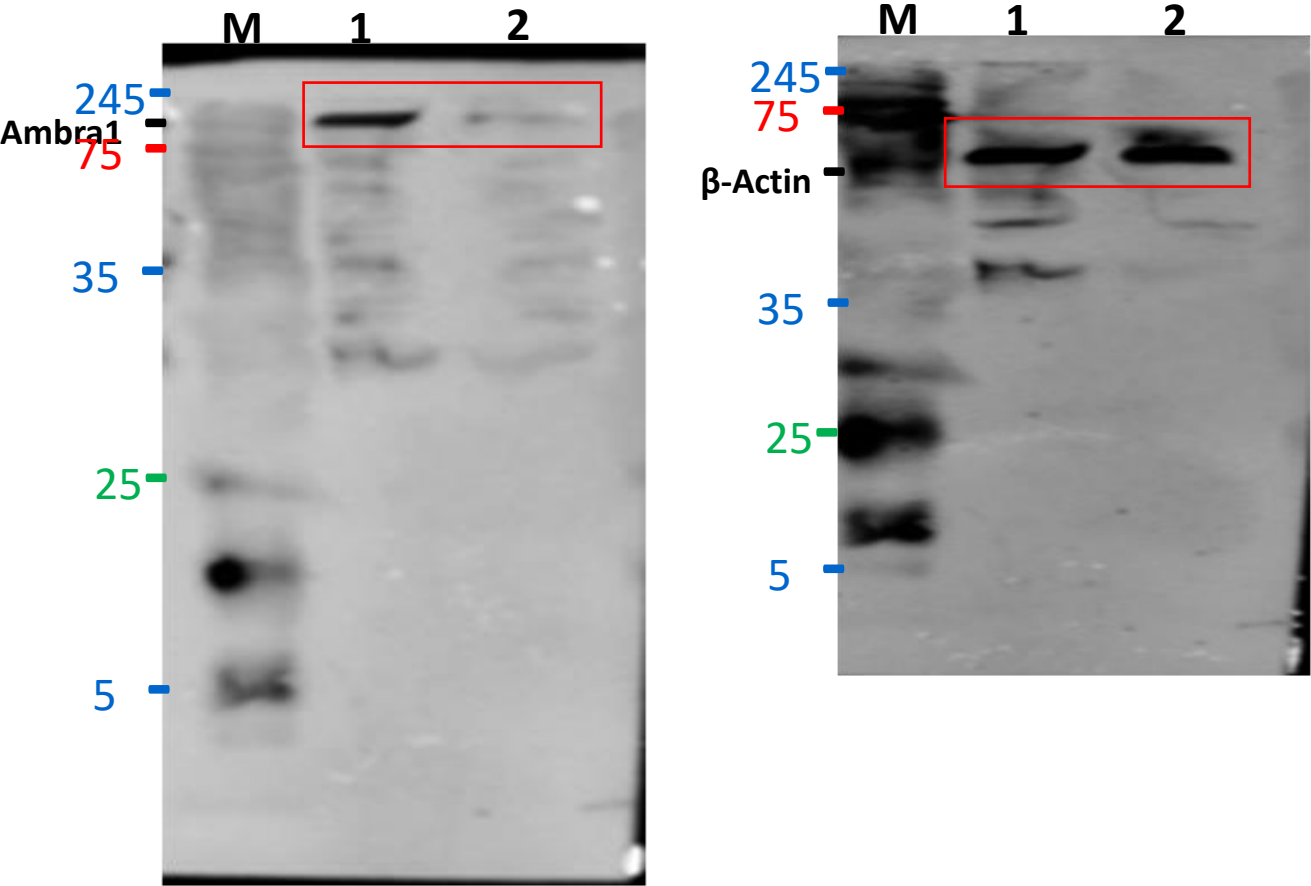


M Marker
1 OGD
2 PD98059+OGD

Fig S5B

Independent-Samples Mann-Whitney U Test Summary	
Total N	8
Mann-Whitney U	0.000
Wilcoxon W	10.000
Test Statistic	0.000
Standard Error	3.251
Standardized Test Statistic	-2.460
Asymptotic Sig.(2-sided test)	0.014
Exact Sig.(2-sided test)	0.029

Fig S5C



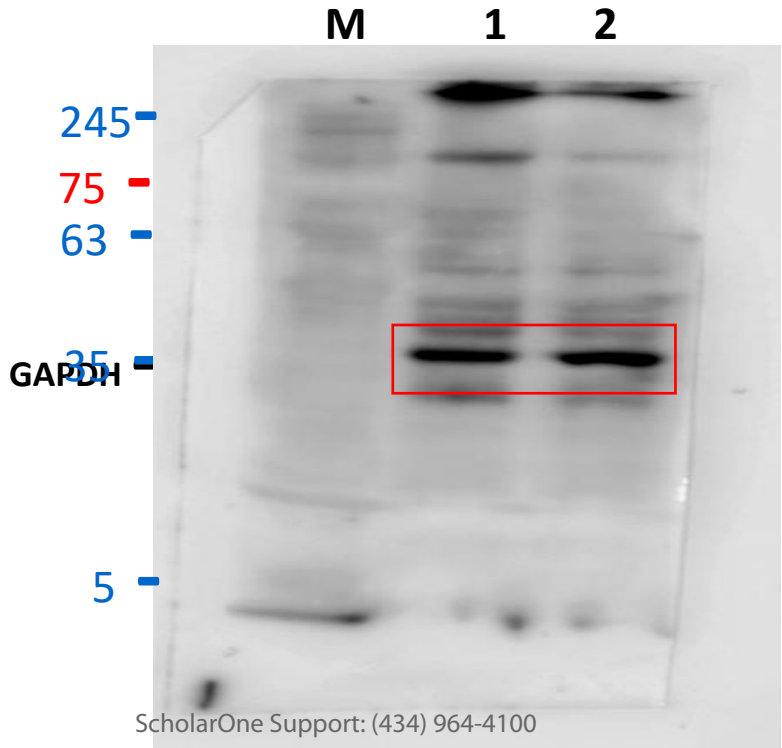
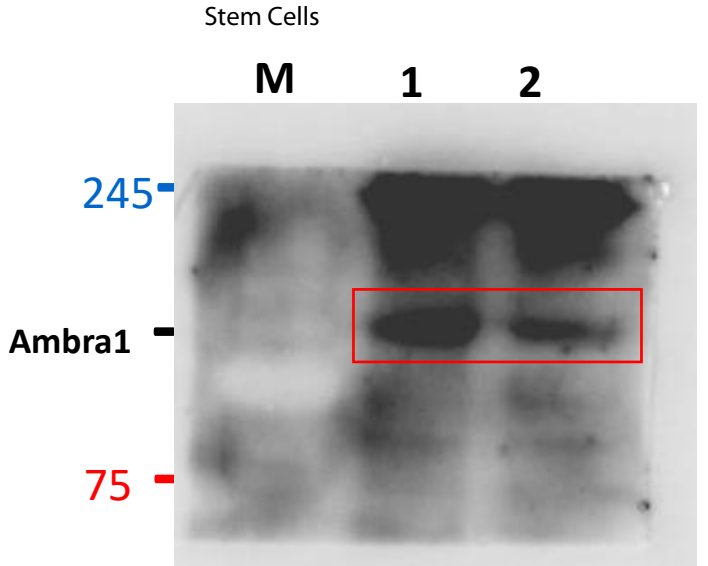
M Marker
1 OGD
2 SB202190+OGD

Fig S5C

Independent-Samples Mann-Whitney U Test Summary

Total N	8
Mann-Whitney U	0.000
Wilcoxon W	10.000
Test Statistic	0.000
Standard Error	3.251
Standardized Test Statistic	-2.460
Asymptotic Sig.(2-sided test)	0.014
Exact Sig.(2-sided test)	0.029

Fig S5D



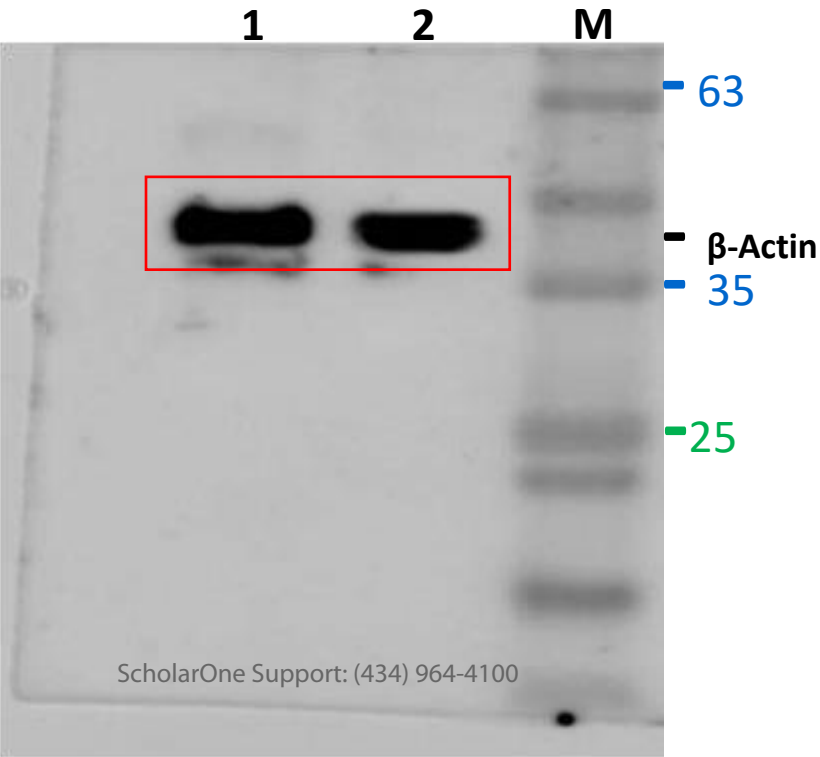
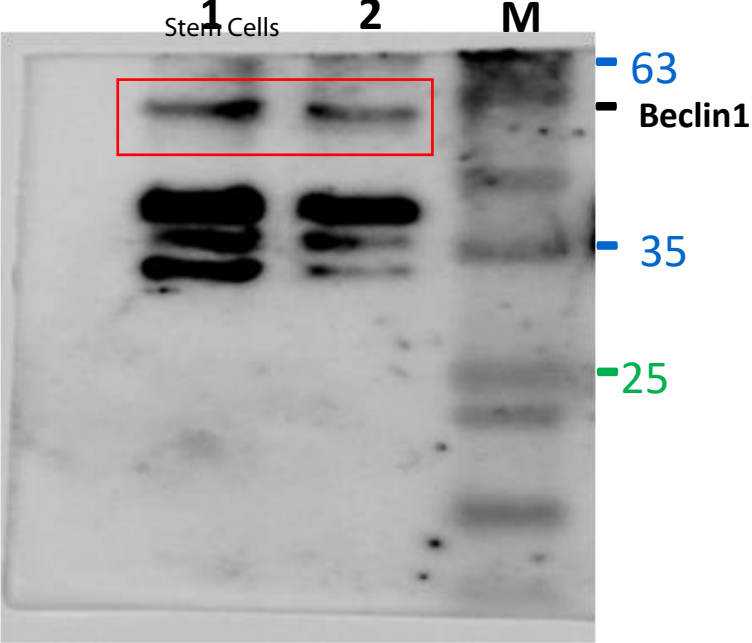
M Marker
1 OGD
2 PD98059+OGD

Fig S5D

Independent-Samples Mann-Whitney U Test Summary

Total N	8
Mann-Whitney U	0.000
Wilcoxon W	10.000
Test Statistic	0.000
Standard Error	3.251
Standardized Test Statistic	-2.460
Asymptotic Sig.(2-sided test)	0.014
Exact Sig.(2-sided test)	0.029

Fig S5E



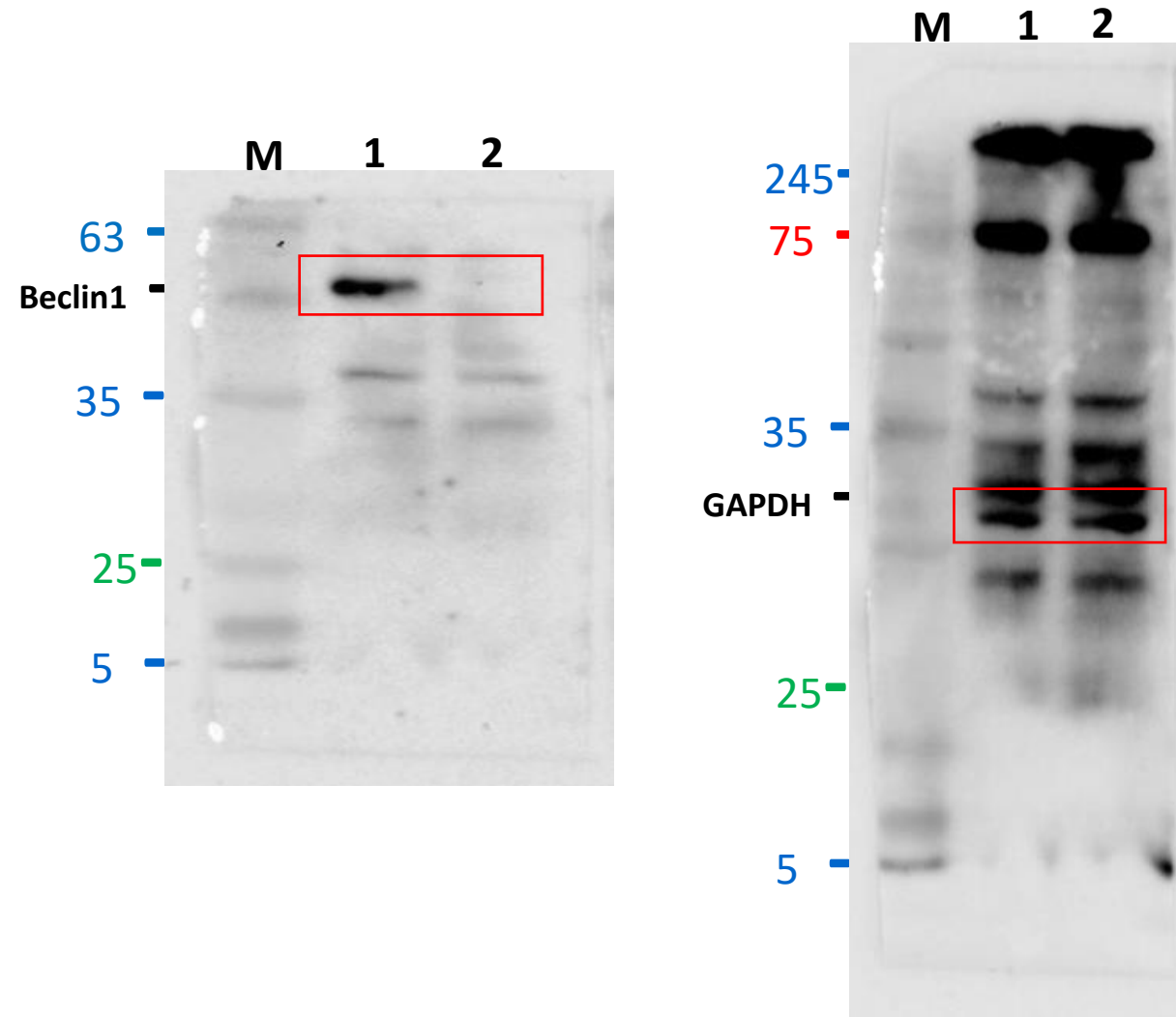
Marker
OGD
SB202190+OGD

Fig S5E

Independent-Samples Mann-Whitney U Test Summary

Total N	8
Mann-Whitney U	0.000
Wilcoxon W	10.000
Test Statistic	0.000
Standard Error	3.251
Standardized Test Statistic	-2.460
Asymptotic Sig.(2-sided test)	0.014
Exact Sig.(2-sided test)	0.029

Fig S5F

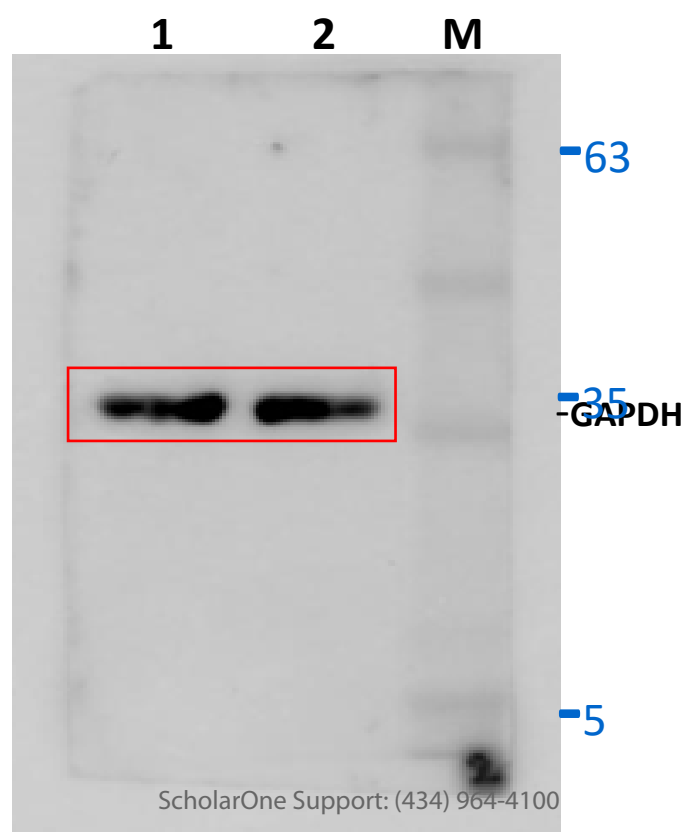
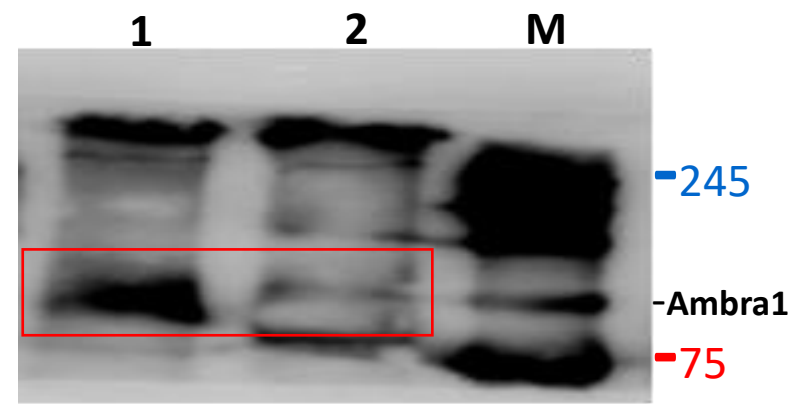


M Marker
1 OGD
2 PD98059+OGD

Fig S5F

Independent-Samples Mann-Whitney U Test Summary	
Total N	8
Mann-Whitney U	0.000
Wilcoxon W	10.000
Test Statistic	0.000
Standard Error	3.251
Standardized Test Statistic	-2.460
Asymptotic Sig.(2-sided test)	0.014
Exact Sig.(2-sided test)	0.029

Fig S5G



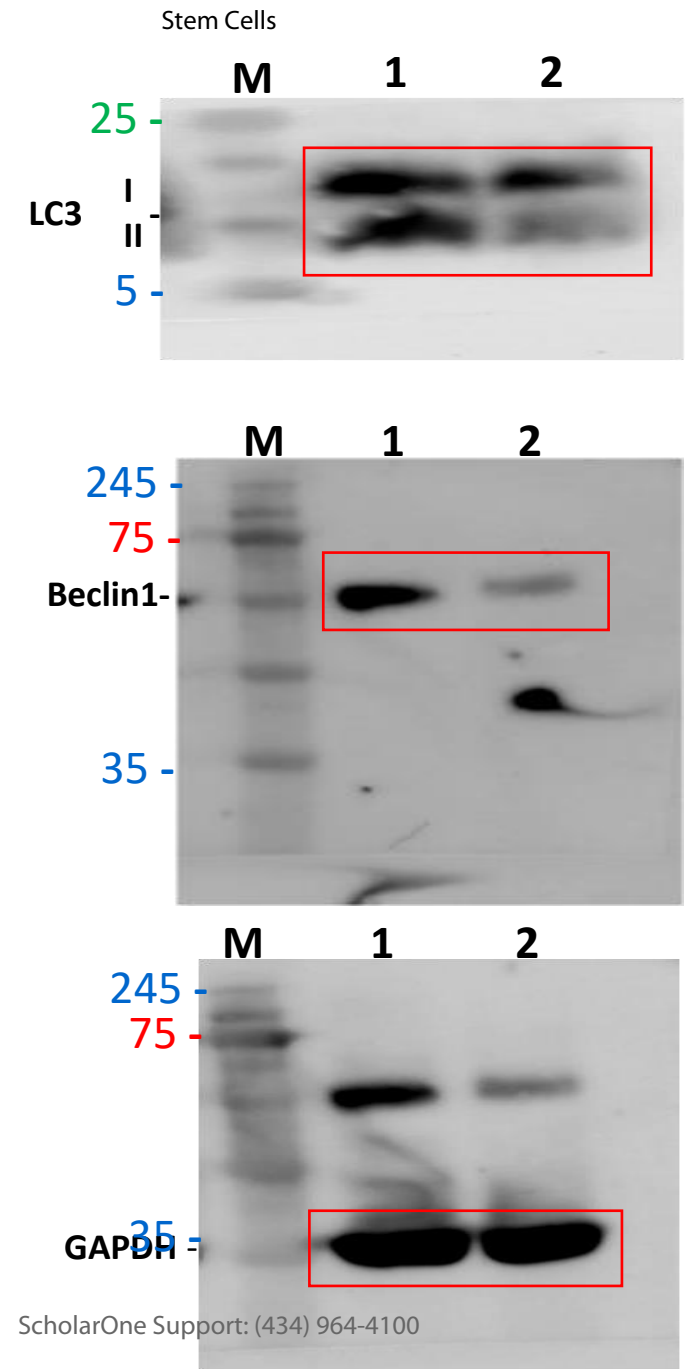
M Marker
1 Control
2 OGD+SB202190+PD98059

Fig S5G

Independent-Samples Mann-Whitney U Test Summary

Total N	8
Mann-Whitney U	0.000
Wilcoxon W	10.000
Test Statistic	0.000
Standard Error	3.251
Standardized Test Statistic	-2.460
Asymptotic Sig.(2-sided test)	0.014
Exact Sig.(2-sided test)	0.029

Fig S5H



M Marker
1 Control
2 OGD+SB202190+PD98059

Fig S5H

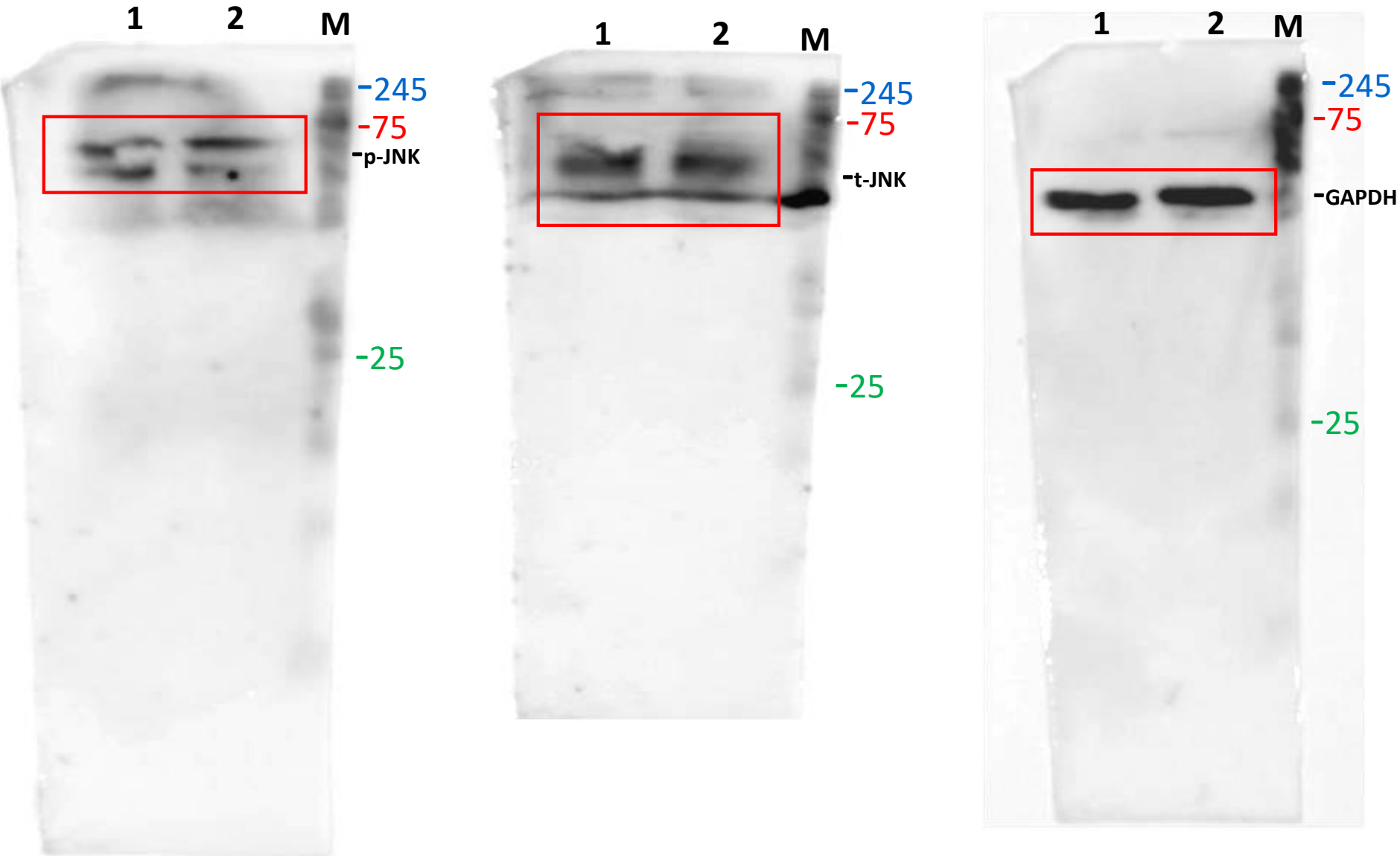
LC3 II/I

Independent-Samples Mann-Whitney U Test Summary		
Total N		8
Mann-Whitney U		0.000
Wilcoxon W		10.000
Test Statistic		0.000
Standard Error		3.251
Standardized Test Statistic		-2.460
Asymptotic Sig.(2-sided test)		0.014
Exact Sig.(2-sided test)		0.029

Beclin1

Independent-Samples Mann-Whitney U Test Summary		
Total N		8
Mann-Whitney U		0.000
Wilcoxon W		10.000
Test Statistic		0.000
Standard Error		3.251
Standardized Test Statistic		-2.460
Asymptotic Sig.(2-sided test)		0.014
Exact Sig.(2-sided test)		0.029

1
2
3
4
5
6
7
8
9
10
11
12
13
14
15
16
17
18
19
20
21
22
23
24
25
26
27
28
29
30
31
32
33
34
35
36
37
38
39
40
41



M Marker
1 Control
2 OGD

Fig S6

Independent-Samples Mann-Whitney U Test Summary

Total N	8
Mann-Whitney U	8.000
Wilcoxon W	18.000
Test Statistic	8.000
Standard Error	3.251
Standardized Test Statistic	0.000
Asymptotic Sig.(2-sided test)	1.000
Exact Sig.(2-sided test)	1.000

